Carbon Fiber Reinforced Polymer Cavity for Vehicular Antennas

Ing. Dipl.-Ing. Gerald Artner BSc

Dissertation

Submitted in partial fulfillment of the requirements for the degree of
Doktor der technischen Wissenschaften
to the
Technische Universität Wien
Fakultät für Elektrotechnik und Informationstechnik

Vienna, 2017

advised by

Univ.-Prof. Dr.-Ing. Christoph F. Mecklenbräuker
Technische Universität Wien
Institute of Telecommunications

First Examiner

Prof. Dr.-Ing.Thomas Zwick
Karlsruher Institut für Technologie
Institut für Hochfrequenztechnik und Elektronik

Second Examiner

Dr.-Ing. Wim Kotterman
Technische Universität Ilmenau
Institut für Informationstechnik

Abstract

Vehicles increasingly communicate with their surrounding environment. They are no longer mere receptors of radio broadcasts, but actively exchange information with their surroundings. These communicative vehicles will radically change our view on transportation. They enable cooperative driving and are used as mobile access nodes for telecommunication networks – no longer just moving combustion engines. Extended radio frequency hardware is the technical basis for this increase in wireless vehicular communication. The critical part of the communication system are the antennas, as they have to be placed outside the vehicles hull and therefore become interdependent with vehicle design. This dissertation examines the influence of carbon fiber reinforced polymer on vehicular antennas and the development of an antenna cavity for vehicles. Together these findings secure enough construction space for antennas in future light-weight constructed vehicles.

Electric cars are increasingly constructed with chassis made from Carbon Fiber Reinforced Polymer (CFRP). This requires the characterization of these materials for vehicular antennas. Material samples are measured inside rectangular waveguides and the material parameters are estimated with the Nicolson-Ross-Weir method. Measurement results show, that the electric conductivity of CFRP with twill-weave and CFRP with fiber shreds on the surface are approximately isotropic in the investigated frequency range around 6 GHz. This motivates the use of recycled CFRP. Sustainable materials are in this case also optimal for antenna applications. The transition from metal to CFRP chassis influences monopole antennas, which are currently widely used in automotive applications, as these antennas use chassis parts as ground plane. Both narrowband and wideband monopole antennas are measured on ground planes manufactured from different CFRP.

A cavity for vehicular antennas is designed, manufactured, measured and evaluated. The cavity is larger than currently used roof-mounted shark-fin antenna modules and can be manufactured as part of the chassis and hidden therein. As proof that the production of such a cavity is realizable for electric cars, a prototype is built from CFRP. To show feasibility for

antennas, several antennas are measured and evaluated inside the cavity. Investigated antennas include a monopole antenna and an inverted-F antenna, both manufactured as laser-structured injection molded parts; a broadband conical monopole antenna and intelligent antennas with reconfigurable radiation patterns. Detailed measurement based evaluations of the antennas inside the cavity show that the cavity concept is feasible. Influences of the cavity on the functionality of the antennas inside are also analyzed by measurement. Strong influences on the antennas occur at frequencies in the high single-digit gigahertz range, where the cavity is electrically large.

Kurzfassung

Fahrzeuge kommunizieren zunehmend mit ihrer Umgebung. Sie sind nicht länger bloße Empfänger für Rundfunk, sondern tauschen aktiv Informationen mit ihrer Umgebung aus. Diese kommunikativen Vehikel, werden unsere Sichtweise von Fahrzeugen radikal ändern. Sie werden kooperatives Fahren ermöglichen und mobile Kommunikationsknoten für Telefonnetze werden; nicht länger sind sie bloß rollende Verbrennungsmotoren. Als technische Grundlage dafür wird Hardware zur mobilen, drahtlosen Kommunikation am Fahrzeug benötigt. Die kritischen Bauteile beim Entwurf dieser Funksysteme sind die Antennen, da diese an der Außenhaut des Fahrzeugs angebracht werden müssen und damit in Wechselwirkung mit dem Fahrzeugdesign treten. Diese Dissertation behandelt den Einfluss von kohlefaserverstärktem Kunststoff auf Fahrzeugantennen und die Entwicklung einer Antennenvertiefung für Fahrzeuge. Gemeinsam sichern diese beiden Untersuchungen ausreichend Bauraum für Antennen in kommunikativen Fahrzeugen in Leichtbauweise.

Da elektrisch betriebene Fahrzeuge zunehmend mit Karosserien aus Kohlefaser verstärktem Kunststoff (CFK) hergestellt werden, muss der Einfluss solcher Materialien auf Fahrzeugantennen untersucht werden. Materialproben werden in Rechteckhohlleitern gemessen und die Materialeigenschaften mit der Nicolson-Ross-Weir Methode geschätzt. Die Messergebnisse zeigen, dass die elektrischen Leitfähigkeiten von CFK mit Köperbindung und CFK mit Faserschnipseln auf der Oberfläche im untersuchten Frequenzbereich um die 6 GHz annähernd isotrop sind. Das motiviert den Einsatz von, aus Wiederverwertungsprozessen gewonnen, Kohlenstofffasern. Nachhaltige Materialien sind im vorliegenden Fall auch für Antennenanwendungen optimal. Der Wechsel von Metall- zu CFK-Karosserien beeinflusst vor allem die derzeit in der Automobilbranche verwendeten Monopolantennen, da diese Karosserieteile als Masseflächen nutzen. Sowohl schmalbandige als auch breitbandige Monopolantennen werden auf unterschiedlich ausgeführten Masseflächen aus CFK gemessen.

Eine Vertiefung für Fahrzeugantennen wird entworfen, gefertigt, gemessen und evaluiert. Die Vertiefung ist größer als derzeit verwendete Haifisch-

flossenantennenmodule, kann als Teil der Karosserie gefertigt und in dieser verdeckt werden. Als Beweis für die fertigungstechnische Realisierbarkeit für elektrische Autos wird ein Prototyp aus kohlefaserverstärktem Kunststoff hergestellt. Um die antennentechnische Umsetzbarkeit zu prüfen, werden mehrere Antennen in der Vertiefung gemessen und evaluiert. Darunter sind eine Monopolantenne und eine invertierte-F Antenne, welche als laserstrukturierte Spritzgussbauteile gefertigt sind, eine breitbandige konische Monopolantenne und intelligente Antennen mit rekonfigurierbaren Richtcharakteristiken. Detaillierte messtechnische Untersuchungen der Antennen in der Vertiefung zeigen, dass das Konzept funktioniert. Einflüsse der Vertiefung auf die Funktionsweise der Antennen werden ebenfalls mit Messungen untersucht. Vor allem bei Frequenzen im hohen einstelligen Gigahertzbereich, wo die Vertiefung elektrisch groß ist, zeigen sich starke Beeinflussungen der Antennen.

Acknowledgment

Ich danke meiner Mutter Lydia Artner, meinem Vater Richard Artner und meiner Schwester Cornelia Pecavar. Ohne ihre Liebe und Unterstützung hätte ich nicht an einer Universität studieren können.

The funding from the Christian Doppler Laboratory for Wireless Technologies for Sustainable Mobility is gratefully acknowledged.

Two actions of the European Cooperation in Science and Technology (COST) framework were vital in connecting me with other scientists and provided the platform where several research collaborations started: COST IC1004 for Cooperative Radio Communications for Green Smart Environments and COST CA15104 for Inclusive Radio Communication Networks for 5G and Beyond (IRACON). I thank COST IRACON for funding my collaboration with Karlsruhe Institute of Technology (KIT) with a Short Term Scientific Mission (STSM) grant.

The Arbeitsgemeinschaft Hochfrequenztechnik (ARGE HF) program of the Österreichische Forschungsgemeinschaft (ÖFG) allowed me to exchange with other scientists in Austria.

I thank my supervisor Christoph Mecklenbräuker for enabling me to do self-reliant, scientific research and for providing funding and guidance along the way. I thank Robert Langwieser for teaching me advanced, high frequency engineering and contributing to several of my research projects, which resulted in numerous publications. It is a pleasure to work with you. I thank Philipp Gentner for our collaboration on the measurements with the NRW-method in Chapter 2.1.1. Philipp also contributed simulations in the early stages of the project.

My colleagues at the Institute of Telecommunications created a fruitful and fun work environment, that ultimately makes scientific excellence thrive. Some important names in alphabetic order: Taulant Berisha, Sebastian Caban, Agnes Fastenbauer, Philipp Gentner, Gabor Hannak, Gregor Lasser, Martin Lerch, Martin Mayer, Ronald Nissel, Stefan Pratschner, Shrief Magdy

Rizkalla, Veronika Shivaldova and Erich Zöchmann.
I had the pleasure to contribute to the Vienna young Scientists Symposium (VSS), where I helped in the organizing committee in 2016 and chaired the symposium in 2017. I want to thank the vice rector for research and innovation Johannes Fröhlich for funding and the VSS team, who made this an unique experience: Bianka Ullmann, Richard Zemann, Heinz Krebs, Philipp Hans, Taraneh Rouhi, Irene Hahn and Antonija Bogadi.
I acknowledge that Stefan Pratschner knows a lot more about antenna mast construction time management than I do.

Contents

Abbreviations

AM	Amplitude Modulation
ARGE HF	Arbeitsgemeinschaft Hochfrequenztechnik
AUT	Antenna Under Test
CAN	Controller Area Network
C2C	Car-to-Car
C2X	Car-to-Any
CFRP	Carbon Fiber Reinforced Polymer
COST	European Cooperation in Science and Technology
DAB	Digital Audio Broadcasting
DARS	Digital Audio Radio Service
DSRC	Dedicated Short-Range Communications
ETSI	European Telecommunications Standards Institute
FM	Frequency Modulation
FR4	Flame Retardant 4
GLONASS	Globalnaya Navigatsionnaya Sputnikovaya Sistema
GNSS	Global Navigation Satellite System
GPS	Global Positioning System
GSM	Global System for Mobile Communications
HFSS	High Frequency Structural Simulator
IEEE	Institute of Electrical and Electronics Engineers
IFA	Inverted-F Antenna
IoT	Internet of Things
IRACON	Inclusive Radio Communication Networks for 5G and Beyond
ISM	Industrial, Scientific and Medical
ITS	Intelligent Transport System
KIT	Karlsruhe Institute of Technology
LDS	Laser Direct Structuring
LIN	Local Interconnect Network
LoS	Line-of-Sight
LTE	Long-Term Evolution

MEMS	Microelectromechanical Systems
MID	Molded Interconnect Device
MIMO	Multiple-Input and Multiple-Output
MUT	Material Under Test
NRW	Nicolson-Ross-Weir
ÖFG	Österreichische Forschungsgemeinschaft
PEC	Perfect Electric Conductor
PCB	Printed Circuit Board
RFID	Radio Frequency Identification
SAR	Synthetic Aperture Radar
SDARS	Satellite Digital Audio Radio Service
SMA	SubMiniature version A
STSM	Short Term Scientific Mission
UAV	Unmanned Aerial Vehicle
UHF	Ultra High Frequency
UMTS	Universal Mobile Telecommunications System
V2V	Vehicle-to-Vehicle
V2I	Vehicle-to-Infrastructure
V2X	Vehicle-to-Any
VHF	Very High Frequency
VSS	Vienna young Scientists Symposium
WLAN	Wireless Local Area Network

List of Figures

Chapter 1

Introduction

1.1 About this Dissertation

In this dissertation a cavity for vehicular antennas is developed, simulated, manufactured and evaluated. Carbon Fiber Reinforced Polymer (CFRP) is used for the construction of a prototype, as these composites are now increasingly used for the light-weight construction of vehicles.

After an introduction to vehicular communication and antennas Chapter 2 investigates CFRP for automotive antennas. Material properties are measured and CFRP is evaluated as antenna ground plane material with measurements of narrowband monopole antennas, wideband monopole antennas and measurement of an automotive antenna module on a CFRP car roof.

Chapter 3 starts with general remarks on mounting positions and modules for automotive antennas. Then simulations of antenna cavities are discussed and compared to measured results. A prototype of a vehicular antenna cavity made from CFRP and its production are shown. Several antennas are measured inside the cavity prototype, to quantify the influence of the antenna cavity onto automotive antennas. These antennas include a conical monopole antenna, a monopole antenna for Vehicle-to-Any (V2X) communication and an Inverted-F Antenna (IFA) in Laser Direct Structuring (LDS) technology and a pattern reconfigurable antenna. Furthermore, a variation of the cavity for the roof edge is prototyped and evaluated and multiple antennas inside the cavity are measured.

Several conclusions are drawn in Chapter 4.

1.2 Publications

As part of my doctoral studies I have published several peer-reviewed scientific articles. Large parts of this dissertation are based on previously published work listed below. As first author I have been the main contributor and was responsible for handling the manuscript. Scientific papers, where I am not first author, are not listed. My publications without peer-review are not listed. Several manuscripts are currently under peer-review and are not listed.

Publications in peer-reviewed journals:

[1] G. Artner, R. Langwieser, and C. F. Mecklenbräuker, "Concealed CFRP Vehicle Chassis Antenna Cavity", *IEEE Antennas and Wireless Propagation Letters*, vol. 16, no. 1, pp. 1415–1418, 2017. DOI: 10.1109/LAWP.2016.2637560

[2] G. Artner, P. K. Gentner, J. Nicolics, and C. F. Mecklenbräuker, "Carbon Fiber Reinforced Polymer With Shredded Fibers: Quasi-Isotropic Material Properties and Antenna Performance", *International Journal of Antennas and Propagation*, vol. 2017, no. Article ID 6152651, 2017. DOI: 10.1155/2017/6152651

Publications in international peer-reviewed conferences:

[3] G. Artner, R. Langwieser, G. Lasser, and C. F. Mecklenbräuker, "Effect of Carbon-Fiber Composites as Ground Plane Material on Antenna Performance", in *IEEE-APS Topical Conference on Antennas and Propagation in Wireless Communications (APWC)*, Palm Beach, Aruba, 2014, pp. 711–714. DOI: 10.1109/APWC.2014.6905580

[4] G. Artner, R. Langwieser, and C. F. Mecklenbräuker, "Material Induced Changes of Antenna Performance in Vehicular Applications", in *IEEE International Conference on Microwaves, Communications, Antennas and Electronic Systems (COMCAS)*, Tel Aviv, Israel, 2015. DOI: 10.1109/COMCAS.2015.7360442

[5] G. Artner and R. Langwieser, "Performance of an Automotive Antenna Module on a Carbon-Fiber Composite Car Roof", in *10th European Conference on Antennas and Propagation (EuCAP)*, Davos, Switzerland, 2016. DOI: 10.1109/EuCAP.2016.7481852

[6] G. Artner, R. Langwieser, R. Zemann, and C. F. Mecklenbräuker, "Carbon Fiber Reinforced Polymer Integrated Antenna Module", in *IEEE-APS Topical Conference on Antennas and Propagation in Wireless Communications (APWC)*, Cairns, Australia, 2016. DOI: 10.1109/APWC.2016.7738118

[7] G. Artner, R. Langwieser, and C. F. Mecklenbräuker, "A MID Dipole Antenna in LDS Technology", in *24th Telecommunications Forum (TELFOR)*, Belgrade, Serbia, 2016. DOI: 10.1109/TELFOR.2016.7818832

[8] G. Artner, J. Kowalewski, C. F. Mecklenbräuker, and T. Zwick, "Pattern Reconfigurable Antenna With Four Directions Hidden in the Vehicle Roof", in *International Workshop on Antenna Technology (iWAT)*, Athens, Greece, 2017, pp. 84–87. DOI: 10.1109/IWAT.2017.7915323

[9] G. Artner, R. Langwieser, and C. F. Mecklenbräuker, "Carbon Fiber Reinforced Polymer as Antenna Ground Plane Material Up to 10 GHz", in *European Conference on Antennas and Propagation (EuCAP)*, Paris, France, 2017, pp. 3612–3616. DOI: 10.23919/EuCAP.2017.7928128

[10] G. Artner, R. Langwieser, and C. F. Mecklenbräuker, "Vehicular Roof Antenna Cavity for Coverage at Low Elevation Angles", in *IEEE AP-S Symposium on Antennas and Propagation and USNC-URSI Radio Science Meeting*, San Diego, USA, 2017

[11] G. Artner and C. F. Mecklenbräuker, "Exchangeable Bases for Rapid Prototyping of Carbon Fiber Reinforced Polymer Antenna Cavities", in *IEEE-APS Topical Conference on Antennas and Propagation in Wireless Communications (APWC)*, Verona, Italy, 2017

[12] G. Artner, "The Communicative Vehicle: Multiple Antennas in a Chassis Antenna Cavity", in *IEEE Vehicular Technology Conference Fall (VTC)*, Toronto, Canada, 2017

Publications in national peer-reviewed conferences:

[13] G. Artner and C. Mecklenbräuker, "Carbon-Fiber Composites in Antenna Applications", in *Vienna young Scientists Symposium (VSS)*, Vienna, Austria: Book-of-Abstracts.com, Heinz A. Krebs, 2015, pp. 108–109, ISBN: 978-3-9504017-0-7

[14] G. Artner and R. Langwieser, "Lightweight Antenna Materials For The Internet Of Things", in *Vienna young Scientists Symposium (VSS)*, Vienna, Austria: Book-of-Abstracts.com, Heinz A. Krebs, 2016, pp. 80–81, ISBN: 978-3-9504017-2-1

1.3 Wireless Vehicular Communication

Vehicles are per definition mobile, which makes wired communication only possible in rare cases, e.g. with trains via the metal rails and overhead lines. Vehicular communication is therefore almost exclusively wireless communications. Audiovisual communication has been the de facto standard for vehicular communication since the invention of vehicles. Early communication with hand gestures and shouts was replaced by technical equipment. The early 1900s saw the introduction of trafficators, which were soon replaced by turn signals [15] and brake lights. Traffic signs and traffic lights convey information to vehicles. They are used to communicate regulatory traffic limitations to the driver, such as speed limits, important destinations, or to warn of dangerous areas. Signal-horns warn of imminent danger. The main drawback of these systems is the extremely low information throughput and, in the case of visual communication, the required Line-of-Sight (LoS). Vehicular communication systems based on electromagnetic waves offer a tremendous increase in transferable information and work beyond a LoS between transmitter and receiver. Modern cars already use a wide variety of radio frequency communication systems, which are briefly discussed in this section.

1.3.1 Broadcast Reception

Several services on vehicles receive information, but do not actively transmit. Reception of audio radio signals was the first vehicular service that used radio frequency systems (Amplitude Modulation (AM), Frequency Modulation (FM)). The focus is infotainment - Radio stations introduced traffic reporting in the 1970s to broadcast important traffic information to vehicles. Currently audio services are transmitted as Digital Audio Radio Service (DARS), typical standards are Digital Audio Broadcasting (DAB) and Satellite Digital Audio Radio Service (SDARS). Television is also available on many modern cars.

Global Navigation Satellite System (GNSS) are used to locate vehicles on road maps, which enables a large variety of services. Vehicles can dynamically plan their journeys. Traffic jams and roadblocks are avoided by updating maps via the internet. Automated driving and lane-keeping are supported by GNSS. Regulatory traffic limitation (e.g. speed limits) can be conveyed to the driver based on the vehicle's position, until sufficient coverage with smart road signs is achieved, or image recognition software is able to extract this information from the filmed environment. Current GNSS systems are the American Global Positioning System (GPS) and the Russian Globalnaya

Navigatsionnaya Sputnikovaya Sistema (GLONASS). The European Galileo and Chinese Beidou2 systems are still in development. Sensor fusion is in development to combine the data from GNSS, accelerometers, cameras, radar and lidar to increase the precision of vehicle location estimators.

1.3.2 Mobile Communication

Mobile telephony was immediately popular with drivers and passengers. Vehicular telephony became so widespread and frequently used, that distraction of drivers due to mobile phones became an issue. Hands-free equipment is now required in Austria according to §102 Abs. 3 Kraftfahrgesetz. Physically, mobile telephony inside cars is impaired, as the vehicles' chassis acts as a Faraday cage – electromagnetic waves can only propagate through the windows. As car windows are now metalized to insulate heat, these vehicles then use external antennas for mobile telephony. As is described in Sec. 1.4.1 automotive antenna modules increase 2G, 3G and 4G coverage for passengers. Mobile telephony and Wifi, or similar technologies such as bluetooth, provide infotainment services to passengers via screens in the seat and console, or to mobile devices like tablets and smart phones. Electronic toll collection systems are now mandatory in many countries.

1.3.3 Automotive Sensor Networks

Proper operation of most functional units of a vehicle can be monitored via wires. Electronic components are then connected with a vehicle bus. Commonly used protocols are Controller Area Network (CAN) and Local Interconnect Network (LIN). Wireless sensor networks are increasingly used to shrink the vehicles' cable harness where necessary.

But not all components can be connected with wires. Tire monitoring systems use sensors in the vehicle to measure air pressure and tire wear [16]. Tires are hard to monitor because they rotate. Rotary joints are expensive and difficult to implement. Tire pressure monitoring systems currently use sensors located on the rim or built directly into the tire. Radio Frequency Identification (RFID) can be used to read data from most automotive sensors, including sensors in the tire [17]. Typically the sensor information is read with one reader module per tire located in the wheel arch. A single reader antenna can be placed in the center of a cars' base plate with the use of metasurfaces [18]. Tire pressure monitoring systems are mandatory in the USA since 2007 [19], in the European Union they were introduced with regulation Nr. 661/2009 [20]. In Austria the transitional period on tire pressure monitoring systems is expected to end November 2017.

Vehicles use radar, lidar and cameras to map the surrounding area. The driver typically gets vision around the car on a display in the console. Knowledge of their surroundings helps vehicles to avoid traffic accidents and allows automated driving and parking. Automated driving is currently researched by most major car manufacturers. Ethical implications are still being discussed by society and legislators slowly adapt the law to technical progress.

1.3.4 Vehicles in the Internet of Things

The concept of the Internet of Things (IoT) changed the perception of cars. Vehicles are now perceived as connected devices in the IoT. They are seen as moving sensor networks and their data is invaluable to numerous applications. Vehicle owners benefit from information gathered by other vehicles and transmitted over the internet. Real-time traffic data is combined with the vehicles' positions obtained from GNSS and to plan the vehicle's route towards their destinations such, that the vehicle avoids roadblocks and traffic congestion. More than that it becomes feasible to forecast traffic, as the number of connected vehicles increases. These forecasts then allow to dynamically route traffic such that congestion don't appear in the first place. An important feature is that connected vehicles can drive in unity. Cooperative driving is predicted to tremendously increase the efficiency of vehicles driving in groups. It can eliminate stop-and-go traffic and speed up the start up process of standing vehicle groups at intersections.

As another example data from sensors, which monitor the proper functionality of vehicles' units, can be combined for a large number of vehicles. The combined data can then be used to more accurately forecast necessary vehicle maintenance. Measurement data from vehicle sensors can be pooled. For example data from tire monitoring can be fused on the internet to obtain a more precise forecast on the next required service. The vehicle's software can now be updated via the internet, just as it is already possible for most other computers. These updates can be performed via the owners Wireless Local Area Network (WLAN) or data services in cellular networks. The car no longer needs to be driven to a service station for that purpose. Seeing vehicles as part of the IoT allows owners to customize their vehicle with software applications, that they can chose and buy according to their own preferences. This is already done with great success for smart phones, where an influx of specialized software has become available for individual desires. Workers can install office applications, amateur radio operators can enhance the vehicles communication systems, scientists can more easily access vehicle functions for their research, etc.

1.3.5 Cooperative Driving

Realtime information from vehicular sensor networks already enables automated driving and information accessed through the IoT supports the vehicle in the long-term, but there is a large gap between these two information sources. Sensors are limited to the vehicles' own viewpoints and are obstructed by buildings and other vehicles. Information relayed through the IoT might be too slow for some applications, especially during safety related events.

For cooperative driving, vehicles need to communicate directly with each other. They exchange information from their sensor networks and relay this information to vehicles who did not get the original message, e.g. with tall vehicle relaying [21]. Vehicles share their large-scale paths (e.g. driving from Vienna to Graz) in the IoT to forecast congestion and they exchange their current trajectories (e.g. lane changes) directly with surrounding road users. Cooperative vehicles actively coordinate to protect vulnerable road users, such as pedestrians and cyclists. Activating an airbag prior to an accident is possible with cooperative driving, when other parties transmit warning signals before impact. The radio frequency communication solutions that enable cooperative driving are researched under the labels Vehicle-to-Vehicle (V2V), Vehicle-to-Infrastructure (V2I), V2I and more specifically as Car-to-Any (C2X) communication [22]. For this purpose a frequency band at 5.9 GHz was reserved for Intelligent Transport Systems (ITSs) by the European Telecommunications Standards Institute (ETSI) [23]. Future vehicles will cooperate, and communicative vehicles are needed as a technical basis for cooperation.

1.4 Automotive Antennas

In this dissertation antennas are defined as passive devices which transform electromagnetic waves propagating along a waveguide into free-space propagating electromagnetic waves and vice versa.

This definition distinguishes antennas from devices that either only transmit electromagnetic waves (e.g. lasers, light-emitting diodes) or only receive electromagnetic waves (e.g. photosensors) The definition implies that a wave is transformed and not received and then generated in a different form (i.e. phase information is preserved). This also means that complex systems, which receive and and subsequently transmit electromagnetic waves are not considered to be antennas (e.g. repeaters, mobile phones). It also excludes antenna definitions with added functionality such as filtennas, rectennas, active antennas etc. The components that add functionality are then not considered part of the antenna.

It is assumed that the reader is familiar with antennas. Several excellent books on antennas are available and a general introduction to antennas is not given as part of this dissertation. Without claim of completeness, the following books are widely considered to be standard literature for varying degrees of prior education [24–26]. Vehicular antennas are almost exclusively electrically small antennas. An overview of small antennas and small antenna design techniques is given in [27]. Automotive antennas are discussed in [28], but vehicular and automotive antennas are discussed throughout this dissertation because of the relevance and proximity to the dissertation's topic.

1.4.1 Automotive Antenna Design

The antennas of the transmitter and the receiver are an essential part of any wireless communication system. Identical to antenna design for other applications, the goal of automotive antenna design is to develop antennas suitable for the proper functionality of the communication system, i.e. design an antenna that maximizes the channel capacity. This is done by designing an antenna with the required antenna gain, radiation pattern, polarization, bandwidth and input impedance. But while other telecommunication components like amplifiers, filters, mixers, etc. can be designed mostly independent from their specific applications, two problems occur when designing antennas for vehicles.

Firstly, the antenna influences the car. Car chassis are made from metal, or electric conductive materials in general. Antennas therefore must be placed on the outside of the vehicle, as electromagnetic waves do not penetrate electric conductors of sufficient thickness. Most antennas even protrude

from the vehicle, which influences the vehicles' drag coefficients. Antennas are connected to electromagnetic waveguides, as they transform guided electromagnetic waves into free space propagating waves. This requires holes in the hull, which influence mechanical stability. For mass produced vehicles the most important factor might be that antennas influence the aesthetic design of the vehicle, which is a major selling point. At large wavelengths even antennas that are electrically small (relative to wavelength) are physically large.

Secondly, the car influences the antenna. It follows from the first point that automotive antennas can not be designed without limitations. Vehicular antennas are influenced by the geometry and materials of the vehicle. Depending on the mounting position, radiation is shadowed by the vehicle itself, e.g. an antenna in the rear bumper does not radiate towards the front. Several antennas are often collected and confined within an antenna module of limited space. This is a necessary limitation, as the antennas are developed by suppliers and not the car manufacturers themselves.

The goal of vehicular antenna design is to design antennas in accordance with the communication system's requirements, while minimizing the influence of the antenna on the vehicle and compensating the influence of the vehicle on the antenna. This motivates vehicular antenna design as a scientific endeavor. The goal of scientific, vehicular antenna design is to characterize the influence of vehicles on antennas, assess antenna concepts for vehicles, develop simulation models for vehicular antennas and develop design processes that reduce the interdependency of vehicle and antenna.

1.4.2 Historical Development and State of the Art

A good overview of automotive antenna designs is given in [28]. Early vehicular antennas were used for the reception of radio broadcasts in the high kilohertz and low megahertz range. Whip antennas allowed the reception of these radio signals with AM and FM [29] and they are still in use.

The number of vehicular antennas has increased steadily since then. Antennas for GNSS were added for navigation systems. AM and FM antennas were replaced by antennas for DAB and SDARS. For infotainment antennas for television reception and data transfer to the internet are available. Mobile telephony is supported with antennas connecting to cellular networks. Short range communication antennas are used for remote keyless entry, tire pressure monitoring, electronic toll collection and V2X communication.

In modern vehicles AM/FM antennas are integrated into the windows [30]. The physical size of antennas operating at a few megahertz is still a challenging task today for military vehicles [31]. The possibility to excite

characteristic modes of the vehicles themselves is currently being investigated [32]. It is also possible to excite a part of the vehicle, such as the rearview mirror [33].

In the 2000s antennas were gathered in antenna modules mounted at the rear end of the vehicle roof, which have become the de facto standard for most automotive antennas [34–51]. These antenna modules are referred to as *shark-fins*, due to the appearance of their aerodynamic covering. The modules currently contain antennas for GNSS (GPS and GLONASS), mobile telephony (Global System for Mobile Communications (GSM), Universal Mobile Telecommunications System (UMTS) and Long-Term Evolution (LTE)), DARS (SDARS and DAB), remote keyless entry, C2X for ITS (Dedicated Short-Range Communications (DSRC), IEEE 802.11p) and WLAN. Also in the 2000s automotive multi-antenna systems were investigated [52–64]. Around the 2010s automotive antenna modules contain diversity antennas for C2X and/or LTE to support Multiple-Input and Multiple-Output (MIMO) communication [65–75].

Also around 2010 frequency- and pattern-reconfigurable antennas are investigated for the automotive sector. Large antenna arrays for beam-steering are currently not economically feasible in automotive applications [76]. Pattern-reconfigurable antennas can improve capacity in static MIMO scenarios [77]. Several pattern reconfigurable antennas have been developed by Kowalewski et al. [78–83]. Simulations suggest, that single pattern reconfigurable antennas increase capacity over antennas with static patterns in vehicular scenarios [84]. Other concepts exploit spatial diversity by switching between antennas at different locations [85]. Measurements in Sec. 3.4.3 show that pattern reconfigurable antennas are feasible in a chassis cavity.

Radio frequency hardware and electronics are moved close to shark-fin modules to form intelligent antenna systems and save cost on coaxial cables [86, 87].

1.4.3 Future Requirements

The number of antennas on vehicles is expected to grow further. The LTE Advanced standard already allows 8×8 MIMO communication. Cooperative driving will further increase the demand in reliability for safety critical communication and in throughput for infotainment communication. To increase reliability *different* antennas will be mounted on vehicles and use spatial, frequency, polarization and pattern diversity. Shark-fin antenna modules can not significantly grow in size and mounting several protruding antenna modules on cars severely influences their aesthetic appearance.

One solution is to let go of aesthetic and aerodynamic requirements. Such

systems are already in use for prototypes of self-driving cars, where radar and lidar are mounted one meter above the vehicle roofs with support structures. Antenna radiation is then no longer influenced or shadowed by the vehicle. Omnidirectional radiation is easily possible. These antenna systems might become feasible under the condition that dedicated city-cars appear, which are not suitable for high speeds, and that the customers accept the changed appearance of vehicles.

Another solution is to find mounting positions, where antennas no longer influence the aesthetics and aerodynamics of vehicles. This means hiding the antenna in already present car parts. Several concealed antenna positions have already been investigated including bumpers, rearview mirrors, sideview mirrors, spoilers, trunk lids and small cavities for single antennas. All these positions share the problem, that the space is already occupied by other functional units. Antennas can then not be developed independently. In Chapter 3 an antenna cavity is presented, which can be manufactured as part of vehicle chassis. The chassis antenna cavity is larger than shark-fin modules, dedicated antenna space and can be fully concealed.

The current understanding of antenna optimization is that the antenna should maximize channel capacity. Radiation patterns can be synthesized, which maximize capacity for each channel. As vehicular channels change very fast, it is in practice not possible to adapt to the channel in every transmission. Advanced techniques such as beam steering with large arrays are also currently not economically feasible for automotive applications.

In live networks it is difficult to estimate radio frequency channels and channel capacity for vehicles, because the vehicle moves between estimation and transmission. Communication schemes that require accurate knowledge of channel capacity or channel state information at the transmitter are therefore difficult to use for vehicular communication. In [88] it is proposed to use predictor antennas to estimate channel and capacity and wait for data transmission until a second antenna is moved to the location of the predictor antenna. For multiple-antenna systems it is proposed to arrange the antennas in a line and let every antenna act as predictor for the antenna behind it. Although it can be expected that implementing such a scheme would cause problems, it is evident, that estimating communication channels and their capacity for several antennas will become a challenging task in the future.

1.4.4 Vehicle Influences on Antennas

As discussed in Sec. 1.4.1, a task of vehicular antenna research is to characterize influences of the vehicle on antennas. Early investigations for example measured the influence of sirens mounted on police cars and compared six

different mounting positions for whip antennas in the megahertz range [89]. The influence of body gaps is measured on a car model in [90]. Simulations of roof curvature and roof rack crossbars show influences on gain patterns up to 7 dB [91]. Different positions on a roof ground plane are simulated in [92]. In [93] the influence of bumpers, paint and saltwater on an automotive antenna array are measured. Protective covers of shark-fin modules are investigated in [94].

An experiment conducted by Kwoczek et al. drew much interest in the automotive antenna community [95]. Measurements of Car-to-Car (C2C) antennas together with a panorama glass roof showed a gain reduction of $15 - 20$ dB, essentially preventing C2C communication in driving direction. Measurements at 800 MHz and 2.6 GHz showed that this does not happen for mobile telephony antennas [96]. On the contrary, because the dielectric glass is placed in the near field, wave propagation is even slightly stronger in the direction of the panorama window. Simulations suggest that a wave is guided inside the glass for 5.9 GHz C2C [97]. The paper also puts heavy emphasis on precise simulation models, the proper modeling of the roof-to-window transition region shows 6 dB difference in gain pattern depending on the metal-to-glass transition used. A solution to the problem is to metallize the panorama window [98].

Although material properties are sometimes already well known before their application in vehicular antennas, such as aluminum, stainless steel or Flame Retardant 4 (FR4), sometimes vehicular antenna researchers have to characterize these materials and their influence on vehicular antennas. Pell et al. measured the influence of automotive paints on antennas [99]. The surprising finding was, that metallic paints behave like dielectrics and only cause a small gain reduction of 0.5 dB. The use of an electrostatic primer during painting however causes a gain reduction of 1.5 dB. A shark-fin antenna module manufactured as Molded Interconnect Device (MID) with the LDS process is presented and measured in [71, 100]. Previously, several LDS substrate materials' properties were measured [101]. The influence of resin covers on automotive millimeter-wave radar is discussed in [102]. Carbon Fiber Reinforced Polymer are used for the lightweight construction of planes, boats and cars. CFRP are increasingly used as chassis material for electric cars. The antenna cavity presented in this dissertation in Sec. 3 is built from CFRP to demonstrate the applicability for future vehicles. Several experiments and measurements are presented in Chapter 2 that estimate the material properties of CFRP used in the automotive industry and the influence of CFRP onto automotive antennas. Detailed summaries of CFRP properties and their influences on antennas are given in Sec. 2.1 and Sec. 2.2.

Simulation models for cars are mainly limited in their geometric complexity by the calculation speed of commercial software. Simple wire grid models [90] transitioned to coarse meshes [103, 104]. For antennas close to or on windows it is essential to model the cars' interior [105, 106]. For intra-vehicular communication and antennas on the windows it is also necessary to consider passengers in the simulation [107]. Simulations are especially important as automotive antenna development follows strict time-lines and the final vehicle is unavailable during development [108].

Discussions of antenna performance throughout this dissertation are based on the uncertainties stemming from imprecise vehicular antenna simulation, uncharacterized materials and vehicle parts which change between car models, or might even be optional add-ons. While a gain-reduction of smaller than a decibel due to a CFRP reflector would be considered a significant influence for space applications and would lead to the reflector being metalized; changes of a few decibel in gain patterns would not be considered to be significant in automotive applications, as they would be within simulation precision, be in the same order of magnitude as currently unknown material properties and be overshadowed by the influence of optional add-ons such as roof racks.

1.5 Evaluation and Measurement of Vehicular Antennas

Antenna performance is classically quantified by the measures input impedance, bandwidth, polarization, radiation efficiency and the gain pattern. Automotive antennas typically use waveguides with a $50\,\Omega$ impedance and antenna impedance should then be matched to the cable impedance as well as possible to minimize the return loss. Antenna impedance matching to $50\,\Omega$ is depicted in this dissertation as return loss or as scattering parameters (S-parameters) over frequency. Visualization of antenna matching with smith charts is more useful during antenna design, but the bandwidth of the matching is not immediately visible.

This dissertation uses realized gain, as this quantity is obtained from measurements in the anechoic chamber. The Institute of Electrical and Electronics Engineers (IEEE) defines antenna gain on the basis of power accepted by the antenna, whereas the realized gain includes the antenna mismatch [109]. Antenna gain after the IEEE definition can be calculated from realized gain and S-parameters, but with good antenna matching the realized gain is practically identical to the IEEE gain definition. Antenna gain after the IEEE definition is only calculated for the conical monopole antenna on a CFRP ground plane in Sec. 2.2.2, as the matching is poor below 1 GHz. Antenna gain is given in dBi in reference to an isotropic radiator, as in the IEEE definition.

For single antenna systems these quantities accurately reflect the performance of an antenna. Return loss, gain pattern and radiation efficiency are used as the primary measures for antenna performance in this dissertation to quantify the influence of CFRP onto antennas in Chapter 2 and the antenna cavity in Chapter 3. Methods that link antenna design choices to influences of these key performance indicators are well known in the literature.

Multiple antenna systems are now increasingly used on vehicles, but the performance evaluation of multiple antenna systems is still debated among scientists. In addition to regular performance measures for MIMO antennas (e.g. multiplexing efficiency of MIMO antennas [110]), evaluation of vehicular MIMO has to take into account effects specific to vehicular communication. Multiple antenna systems can be used for different purposes like Multiple-Input and Multiple-Output (MIMO) transmission schemes or antenna selection as diversity in case the active antenna is shadowed. The evaluation also needs to be based on the application, i.e. high data-rate for infotainment, but high reliability for safety relevant communication. Repeatable performance measurements in live networks are currently not possible. Although

such measurement procedures are being researched at the time of writing this dissertation, none of the state-of-the-art procedures are both meaningful and repeatable in a scientific sense. Measurements are influenced by a large variety of parameters, which the researcher currently has little control over and often can't even access. Examples are data-rate limitations, cell-load, scheduling algorithms, vendor specific implementations of standards, street layout, architecture, etc. Nevertheless, several procedures exist to evaluate vehicular MIMO antennas.

In [111] it is found that simple propagation models like random line-of-sight and rich isotropic multipath are not suitable to evaluate vehicular antennas, as they do not accurately reflect vehicular scenarios (see Chapter 2 in [111]). It is proposed in [111] to limit the angles of arrival either based on simulations or measurement and then evaluate antennas based on received power.

Assessment of MIMO antennas on the system level is investigated by Ekiz in [112]. Ekiz performs measurements in live networks and separates measurements into active and passive. [112] defines condition number and mutual information as key performance indicators for passive measurements. Received signal strength indicator, signal-to-interference-plus-noise-ratio and throughput are used as key performance indicators for active measurements.

Reichardt inserts simulated or measured gain patterns into ray-tracing simulations and evaluates them based on channel capacity [113–115]. Moreover, [115] presents a methodology to synthesize radiation patterns from ray-tracing simulations, which are near-optimum in some average sense. A more limited methodology is also presented, where such gain patterns can be synthesized from measurements in live networks. The possibility to synthesize near-optimum gain patterns further motivates the use of gain patterns to evaluate antennas in this dissertation.

Over-the-air testing in virtual electromagnetic environments is investigated in [116]. Over-the-air testing can be used to measure whole vehicles [117–119] and it has already been used to evaluate a GNSS antenna [120].

1.5.1 Antenna Measurements in an Anechoic Chamber

All antenna gain measurements in this dissertation are performed inside anechoic chambers. Anechoic chambers serve two purposes: They shield the measurement from outside radiation, and they prevent reflections on the inside which would otherwise interfere with waves radiated directly from the antenna.

The anechoic chamber at the Institute of Telecommunications of the Technische Universität Wien uses a spherical near-field measurement sys-

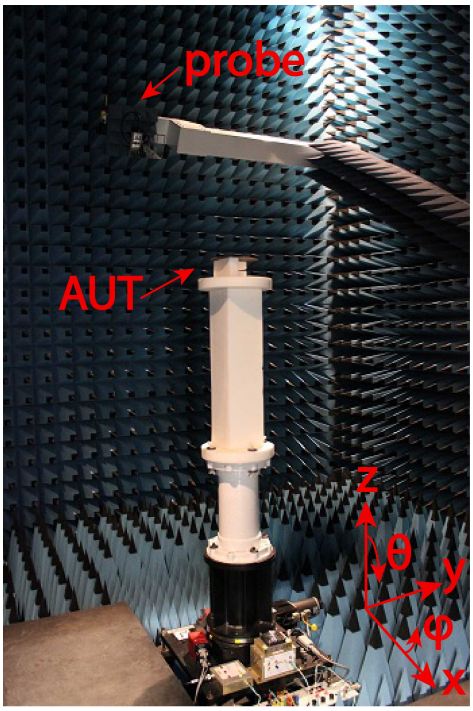

Figure 1.1: Measurement setup in the institute's anechoic chamber. An antenna under test (AUT) is placed on a Rohacell column stacked on a column made from glass-fiber reinforced polymer. ©2014 IEEE, reprinted with permission from [3].

tem. Far-field patterns are obtained from measurements in the near-field via a near-field-to-far-field transformation. A detailed discussion of near-field measurements and transformations is available in [121]. The chamber operates in a wide frequency range from 800 MHz to 40 GHz. The probe antenna is located on an arm which can move up to polar angles $\theta \leq 160°$. The Antenna Under Test (AUT) is placed on a column on an azimuth φ rotary stage. The influence of the column on the antenna measurements should be small. For this purpose a column made from Rohacell is used for lightweight antennas. Rohacell is a polymethacrylimide hard foam; its dielectric properties are close to the those of air [122]. It is often used in measurements of lightweight antennas, as it can be machined into fixtures and has negligible influence on the results. The Rohacell column is presented in [17], where also the performance of the chamber at TU Wien is discussed. A column made from glass-fiber reinforced polymer is used for heavier objects (e.g. car roofs, cavities). An aluminum fixture is added when necessary. A typical measurement setup is depicted in Fig. 1.1.

Sec. 3.4.3 presents measurements of pattern reconfigurable antennas, that are performed in cooperation with Karlsruhe Institute of Technology (KIT). These measurements are performed in the anechoic chamber at KIT.

Chapter 2

Carbon Fiber Reinforced Polymer for Antennas

Carbon fiber composites are generally composites which contain carbon fibers that reinforce a matrix. Polymers are widely used as matrix and these materials are then referred to as Carbon Fiber Reinforced Polymer (CFRP). Other matrices are in use too e.g. carbon fiber reinforced concrete [123]. Carbon fiber strands can be woven into fabrics. The most commonly used fabrics use plain or twill weave, other fabrics are used for special requirements e.g. drapability. Sheets of unidirectional fibers are also used, fiber strand are then sparsely connected with other materials like nylon. CFRP parts are typically built as laminates from fibers preimpregnated with epoxy (prepreg) and cured in an autoclave, but other production processes exist such as resin transfer molding. CFRP are now widely used in lightweight construction due to their large Young's modulus relative to their weight. Applications are hulls for airplanes, boats and sports cars and CFRP are also used in civil engineering and sports equipment. Various methods for recycling of CFRP are in use [124]. CFRP offer high corrosion resistance for electric applications, as the fibers are protected inside the matrix. Their radio frequency properties vary widely with fiber volume fraction, weave and wavelength. The microwave material properties of CFRP are estimated in this chapter and CFRP are evaluated by measurement for their use for chassis antenna cavities.

2.1 Radio Frequency Properties of CFRP

The direct current properties of CFRP are not of interest for antenna applications, as the material properties in general show a large dependence on frequency. For automotive antenna applications the electromagnetic proper-

ties of CFRP in the range from megahertz to terrahertz are of interest. The electromagnetic properties of CFRP are expected to be anisotropic due to the nature of carbon fiber composites, where conductive fibers are embedded in a dielectric matrix.

Electric conductivity and permittivity of unidirectional CFRP are measured from $10^2 - 10^{10}$ Hz both in fiber direction and transversal to fiber direction in [125]. The influence of fiber volume fraction is also investigated. [125] concludes that CFRP are good conductors up to 10 GHz. Graphite, carbon-black and unidirectional CFRP are compared in [126] from $0 - 10^9$ Hz; fiber orientation is also considered. Composites with interwoven carbon fibers and glass fibers are considered in [127]. [128] measures the S-parameters of unidirectional and $[0\ 45\ 90\ -45]_{2s}$ material samples between two horn antennas, and in a second measurement setup compares the radar cross section of CFRP parallel and perpendicular to fiber direction, both for $8 - 12$ GHz. The diamagnetic behavior of unidirectional CFRP is measured in [129] where it is found that the real part of the permeability varies between $0 \leq \mu_r \leq 1$ depending on fiber orientation.

The most prominent method to estimate the material parameters of CFRP is to measure the S-parameters of a sample inside a waveguide and use the Nicolson-Ross-Weir (NRW) method [130, 131] to obtain conductivity, permittivity and permeability [125, 129]. Other methods exist. CFRP fabrics are measured between two loop antennas in [132]. Conductivity is estimated from the radiation efficiency of a carbon-fiber monopole antenna in [133].

There are several models for CFRP. The need for models of different complexity arises from the issue that simulations of individual fibers in large structures is not feasible. Properties of fibers and fiber strands are smeared to obtain macroscopic material parameters. Macroscopic descriptions of the materials then use homogenous anisotropic properties. A detailed discussion of equivalent layer models in [134] studies models with different levels of detail. In [135] microscopic material properties are translated into impedance networks. In [136] CFRP are described as tensors: A macroscopic description is derived from virtual materials, that are generated from bubble meshes. Conductivity in fiber direction is estimated from fiber volume fraction with a rule of mixture model. As the investigated materials are below the percolation threshold, conductivity perpendicular to fiber direction is very low. Perpendicular to fiber direction conductivity is based on the capacity between monte-carlo placed fiber cross sections.

In automotive applications such models might not be necessary to model CFRP ground planes. As will be shown in Sec. 2.2.2, ground planes from woven CFRP have negligible influence on automotive antennas' radiation patterns, and can therefore be modeled as isotropic.

2.1.1 Material Characterization with the NRW Method

The CFRP investigated in literature are typically laminates with unidirectional plies; sometimes stacked with different ply alignment to obtain more isotropic Young's modulus and electric conductivity. Unidirectional CFRP are of wide theoretical interest, as the anisotropy is more pronounced and material models are simpler than those of woven materials. But these materials are not necessarily the ones which are used in the automotive industry. Materials in the automotive industry are subject to stringent recycling requirements. Carbon composites used in mass produced cars therefore typically contain a large percentage of recycled fibers. From an electromagnetic viewpoint, the radio frequency conductivity, permittivity and permeability of materials with short, recycled fibers shreds will significantly differ from unidirectional CFRP, which are typically investigated.

Currently the most important automotive, wireless communication service is V2X communications, as it is safety critical communication. Communication between vehicles of similar height, such as C2C, might be affected by the change from metal to composite car roofs. The service uses the DSRC $5.875 - 5.905\,\mathrm{GHz}$ frequency band in Europe [137] and similar bands in other countries [22]. A frequency band around $5.9\,\mathrm{GHz}$ is therefore chosen for the estimation of the constitutive material properties of automotive carbon composites.

In this section the electromagnetic properties of a twill weave CFRP and a CFRP with short carbon fiber shreds in random alignment on its top layer are measured at $5.9\,\mathrm{GHz}$. Material properties are estimated from measurements of laminate samples inside a rectangular waveguide using the Nicolson-Ross-Weir (NRW) method. This section is based on [2, 13].

Two CFRP are investigated. One is a 2/2 twill weave CFRP laminate whit plies stacked as [45 90 45 90 45]. The twill-CFRP is $0.9\,\mathrm{mm}$ thick and has approximately 1000 filaments per roving. The second material is a laminate with unidirectional fiber plies, but on its top layers there are fiber shreds of approximately $1\,\mathrm{cm}$ length in random alignment. The thickness of the shred-CFRP is $2.26\,\mathrm{mm}$.

The S-parameters of samples from the Material Under Test (MUT) are measured inside rectangular waveguides. The standard operating frequency range of rectangular waveguides is in monomode operation. The waveguide is used in a frequency range above the cutoff frequency of its fundamental TE_{10} mode, but below the cutoff frequencies of other modes. This measurement procedure is therefore suitable to characterize material anisotropy, as the electric field vectors within the waveguide are all aligned parallel to the shorter waveguide walls. A rectangular waveguide WR187 is used (nomi-

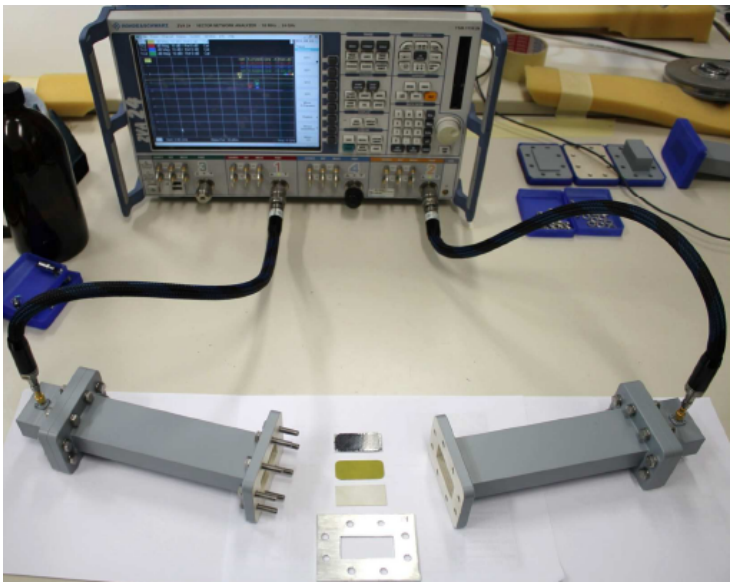

Figure 2.1: Setup to measure the S-parameters of material samples inside a rectangular waveguide. Reprinted with permission from [2].

nal frequency range $3.94 - 5.99\,\mathrm{GHz}$ and TE_{10} cutoff $3.152\,\mathrm{GHz}$. Samples with different orientations are cut from the MUT to characterize material anisotropy. Samples are cut from 0° to 90° in 10° steps for the twill-CFRP. The shred-CFRP is investigated from 0° to 110° in 5° steps. As the material has short carbon fiber shreds in random alignment on its top layer, it was suspected that the material might by inhomogeneous on the investigated size scale. This material inhomogeneity is investigated by cutting four samples with the same alignment (0°) from different locations of the MUT. All samples are taken from the same sheet, not from different batches. The measurement setup is depicted in Fig. 2.1.

The NRW method allows the estimation of intrinsic electromagnetic material properties from measures S-parameters. The NRW method was developed in the 1970s and has since become a standard method to estimate material properties. The original method is described in a paper by Nicolson and Ross [130] and a paper by Weir [131].

The first step is typically to move the calibration planes from the sample fixture to the surface of the material samples, as the location of the MUT inside the fixture may vary depending on the investigated material. This is done according to [138],

$$R_i = e^{-\gamma_0 L_i}, i \in \{1,2\} \tag{2.1}$$

$$S_{11}^C = \frac{S_{11}}{R_1^2} \tag{2.2}$$

$$S_{21}^C = \frac{S_{21}}{R_1 R_2} \tag{2.3}$$

with the scattering parameters S_{mn} from port n to port m and L_i being the distance from the calibration plane at port i to the material sample. S_{11}^C and S_{21}^C are then used in the NRW equations [131],

$$\Gamma = X \pm \sqrt{X^2 - 1} \tag{2.4}$$

$$X = \frac{(S_{11}^C)^2 - (S_{21}^C)^2 + 1}{2S_{11}^C} \tag{2.5}$$

$$\frac{1}{\Lambda^2} = -\left(\frac{1}{2\pi d}\ln\left(\frac{1}{P}\right)\right)^2 \tag{2.6}$$

$$P = \frac{S_{11}^C + S_{21}^C - \Gamma}{1 - (S_{11}^C + S_{21}^C)\Gamma} \tag{2.7}$$

where d is the thickness of the MUT and P is the propagation factor.

As P is a complex number in general, the logarithm in Eq. 2.6 is ambiguous by $2\pi n$, $n \in \mathbb{N}_0$. The ambiguity of the logarithm is a well known problem of the NRW method and several solutions have been proposed. The most common disambiguation method (e.g. [139]) used for CFRP is to limit measurements to thin samples with $d < \lambda$. As CFRP are often built as thin laminates, this condition is typically fulfilled at microwave frequencies. The method proposed in [131] compares group delays from estimated results to the group delay obtained from the slope of the propagation factor P. This requires to calculate the NRW equations for a large amount of n as the solution is chosen a posteriori. Instead of comparing the phase difference at each frequency point, it is possible to compare it to the preceding frequency point [140]. No branching is then needed, but the method requires knowledge of a frequency point with defined n. Wavelengths much larger than sample thickness d can easily be measured in coaxial cables and lead to defined $n = 0$. In waveguides this is not possible, as waveguides have a cutoff frequency and the method would need to be used in conjunction with a starting method that defines n for one frequency. Phase ambiguity can also be resolved by measuring two samples with different thickness [138]. The results obtained in this section are obtained with the assumption that the samples are thin $d < \lambda$, and are checked with the method from [131].

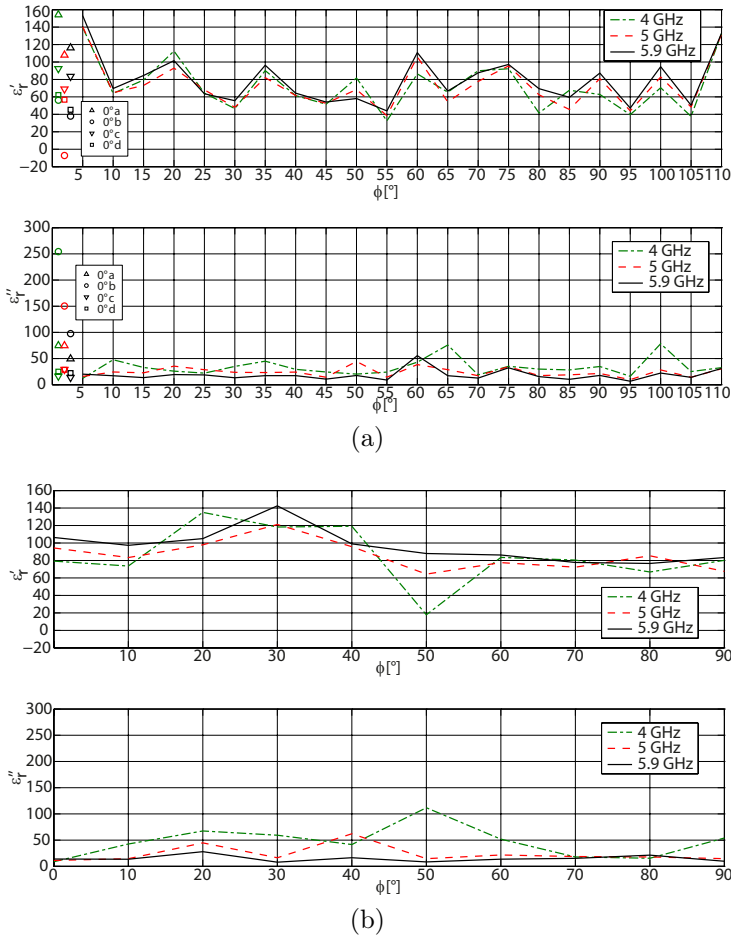

(a)

(b)

Figure 2.2: Estimated permittivity of a) shred-CFRP and b) twill-CFRP based on rectangular waveguide measurements. Reprinted with permission from [2].

Following the disambiguation of the logarithm and calculation of the NRW equations, the complex magnetic permeability μ_r and electric permittivity ϵ_r are estimated according to [131, 138], as

$$\mu_r = \mu_r' - j\mu_r'' = \frac{1+\Gamma}{\Lambda(1-\Gamma)\sqrt{\frac{1}{\lambda_0^2}-\frac{1}{\lambda_c^2}}} \tag{2.8}$$

$$\epsilon_r = \epsilon_r' - j\epsilon_r'' = \frac{\lambda_0^2}{\mu_r}\left(\frac{1}{\lambda_c^2}+\frac{1}{\Lambda^2}\right) \tag{2.9}$$

where λ_0 is the wavelength in free space and λ_c is the cut-off frequency of the waveguide.

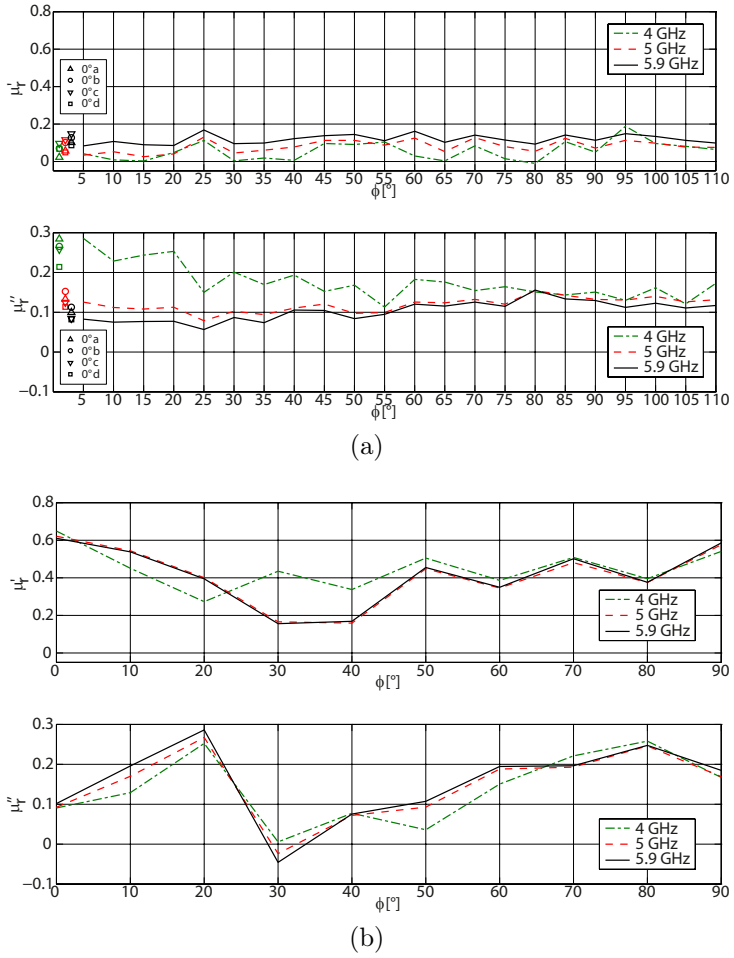

(a)

(b)

Figure 2.3: Estimated permeability of a) shred-CFRP and b) twill-CFRP based on rectangular waveguide measurements. Reprinted with permission from [2].

Estimated permittivity is depicted in Fig. 2.2 and permeability is depicted in Fig. 2.3. The permeability of both the shred-CFRP and the twill-CFRP are between 0 and 1, with the relative permeability of shred-CFRP being low independent of the orientation and an anisotropic permeability of the twill-CFRP varying between 0.1 and 0.6. Results are in accordance with the strong diamagnetic behavior described in [129].

The NRW equations allow negative estimates of the permittivity and permeability. Slightly negative values are estimated, although passive materials are investigated, as is evident for sample 0°d in Fig. 2.2a, a few values in Fig. 2.3a and the 30° sample in Fig. 2.3b.

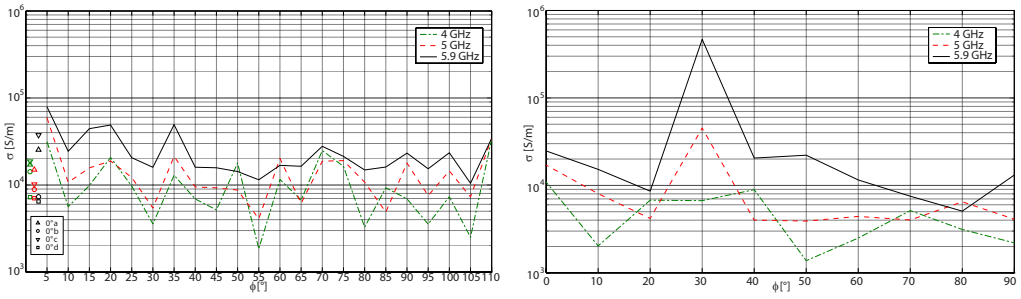

(a) (b)

Figure 2.4: Estimated conductivity of a) shred-CFRP and b) twill-CFRP based on rectangular waveguide measurements. Reprinted with permission from [2].

Conductivity is estimated directly from S_{11} as in [141]:

$$\sigma = \frac{4\pi\mu_0 f \left(1 - |S_{11}|^2\right)^2}{Z_0^2 \left((1 + |S_{11}|^2) - \sqrt{-|S_{11}|^4 + 6|S_{11}|^2 - 1}\right)^2}, \tag{2.10}$$

where μ_0 is the magnetic constant, f the frequency and Z_0 is the free space impedance.

Estimated conductivity is depicted in Fig. 2.4. Compared to the anisotropic conductivity of unidirectional CFRP (see Sec. 2.1), the anisotropies of the conductivities of shred-CFRP and twill-CFRP are much less pronounced. The conductivity of the CFRP with shredded fibers in random alignment varies only within one order of magnitude.

There are several implications from these findings:

- As antenna measurements in Sec. 2.2.2 confirm, the quasi-isotropic conductivity of these CFRP results in only negligible influence on the radiation patterns of automotive antennas on CFRP ground planes.

- The quasi-isotropic conductivity of the investigated CFRP implies that complex material models are not required in antenna simulations. The geometry of the weave does not need to be considered in the investigated frequency range. Layered models are not necessary and permittivity, permeability and conductivity can be modeled as approximately isotropic, instead of being modeled as tensors.

- The skin depth of the electric current is only very small at microwave frequencies. It is therefore possible to only manufacture the top layer

from a CFRP with properties favorable in antenna applications. The remaining plies of the laminate can be designed in accordance with mechanical considerations.

- The conductivity of the CFRP with recycled fiber shreds on the top layer is slightly more isotropic than the conductivity of the twill weave. The use of fiber shreds obtained from recycled carbon fiber composites is beneficial from an antenna viewpoint.

2.2 CFRP in Antenna Applications

2.2.1 CFRP Antennas and Reflectors

CFRP are electric conductors and therefore suitable to build antennas, as is discussed in Sec. 2.1. In practice lightweight construction is not necessary for most antennas, as only antennas for low frequencies are physically large and therefore heavy. But some areas benefit from lightweight construction of antennas such as large reflector dishes for radio astronomy and reflectors for satellite antennas in space applications. CFRP are also used if lightweight construction of the antenna is not necessary, but when CFRP are already present on the structure and are then used for antennas. This is the case for most vehicles, where the hull or chassis is built from CFRP and used as reflector or ground plane for antennas. Nevertheless, construction of antennas from CFRP is certainly possible and might replace other technologies such as Printed Circuit Board (PCB) antennas or punched, bent sheet metal parts. In this section the state of the art of CFRP in antenna applications is reviewed, before my own contributions are discussed in Sec. 2.2.2 and Sec. 2.2.3.

First applications of CFRP for military aircraft date back to at least the 1960s [142]. Conference proceedings on "Electromagnetic Effects of (Carbon) Composite Materials upon Avionics Systems" by the Advisory Group for Aerospace Research & Development (AGARD) of the North Atlantic Treaty Organization (NATO) from 1980 are published in [143].

CFRP reflectors are measured in X-band in [144] and a gain difference to aluminum $< 0.8\,\mathrm{dB}$ is found. Measurements at L- and S-band in [145] found a difference $< 0.1\,\mathrm{dB}$. A dual-offset reflector antenna is discussed in [146], but it was metalized as the specification for cross-polarization discrimination could not be met otherwise. A Ka-band dual reflector antenna and a Ku/Ka-band dual gridded reflector are presented in [147]. Reflectivity measurements with different methods for antenna refletorcs in the range from $110 - 200\,\mathrm{GHz}$ are found in [148, 149]. High reflectivity of $96 - 97\,\%$ in fiber direction and

75 % perpendicular to fiber direction are found. Deployable CFRP booms for Synthetic Aperture Radar (SAR) antennas are described and manufactured in [150]. A CFRP reflector for the detection of power lines by helicopters at 76 GHz is presented in [151, 152]. In [153] the use of horn antennas instead of open-ended waveguides is investigated. The production process and practical problems of a CFRP reflector for the square kilometer array are elaborated in [154].

The reflection properties of CFRP are not only important for antenna reflectors, but also as a target for radars. A recent investigation of the radar cross section at 7 - 12 GHz found that the orientation of twill weave samples to the polarization of the incident wave was not important [155]. But the reflection from unidirectional CFRP varied by 5 - 8 dB depending on orientation.

Several antennas manufactured from CFRP are found in the literature. A bow-tie antenna is presented in [156] and the influence of fiber direction and weave is investigated. A lozenge monopole antenna is manufactured and measured in [157]. In [158] a monopole antenna is presented, where the monopole consists of carbon fiber strands.

Antennas are often built on or into CFRP, in case such structures are already available. A blade antenna for 1 GHz is measured on a carbon composite ground plane in [159]. Microstrip patch antennas are measured on unidirectional CFRP stacked as [0 45 -45 90] in [141, 160]; it is found that the orientation of the top ply shifts the resonance frequency and reduces antenna gain. Microstrip antennas on CFRP are also investigated in [161]. The anisotropy of unidirectional CFRP is utilized in [162] to build a mechanically reconfigurable antenna. Modes are suppressed, by rotating the antenna against the anisotropic ground plane.

Slotted waveguide antennas are developed in [163], that can be built into CFRP airplane hulls. The antennas use rectangular CFRP support structures as electromagnetic waveguides and are load-bearing. A single CFRP slotted waveguide is presented in [164]; decreased antenna gain is explained to be cause by the anisotropic conductivity around the slots. A production manual is available in [165]. Single slotted waveguide antennas are combined to an array - the slotted waveguide antenna stiffened structure [166]. Slot antennas without waveguides can be backed by cavities [167]. A loop feed is discussed in [168]. Beam steering is demonstrated by building the slot array as a rectangular coaxial structure instead of a rectangular waveguide [169].

2.2.2 CFRP as Antenna Ground Plane

Antennas located on the car roof are often built as monopole antennas, such that they use the car roof as antenna ground plane. Monopole antennas provide omnidirectional radiation, which is necessary as the vehicle's orientation towards a transmitter and/or receiver is in general unknown. Monopole antennas can be seen as one half of a dipole antenna, which is then mirrored on a conductive ground plane. While in theory an infinitely large, perfect conductive ground plane is required, in practice a large metallic ground plane is sufficient. The car roof offers a large conductive ground plane and most vehicular services require omnidirectional radiation patterns, such as C2X, mobile telephony, terrestrial radio and WLAN.

CFRP are introduced as construction material to reduce vehicle weight. This is especially important for electric cars, as reduced vehicle weight directly increases the range per battery charge. Investigations are required, whether CFRP chassis can still be used as antenna ground planes. As presented in Sec. 2.1, CFRP are electric conductors, but their conductivity is anisotropic in general. To the best of the author's knowledge, the first measurement of a monopole antenna on a CFRP ground plane was conducted in [159] in 1982. A quarter-wavelength blade antenna for 1 GHz was measured on a CFRP ground plane and it was found that anisotropy effects were undetectable within measurement accuracy. In this section measurements of several CFRP with different fiber weave are performed and evaluated to determine if CFRP as ground plane materials influence antenna performance. The section is based on [2, 3, 9].

Investigation of CFRP ground planes with narrowband wire monopole antennas

Simple quarter-wavelength long wire monopole antennas for the Industrial, Scientific and Medical (ISM) 2.4 GHz band and the V2X 5.9 GHz band are measured on circular ground planes made from CFRP. For measurements coaxial cables are attached to SubMiniature version A (SMA) flanges The wire monopole antennas are soldered to the flanges' inner conductors and the flanges are screwed to threaded holes in the ground planes. The wire monopole antenna for 5.9 GHz on the shred-CFRP is depicted in Fig. 2.5. Three different CFRP are investigated. The first is a 0.9 mm thick sheet with a 2/2 twill weave and is denoted as twill-CFRP. The investigated twill-CFRP is stacked as a laminate with [45 90 45 90 45]. The twill-weave has approximately 1000 filaments per roving and an overall fill level of about 45 %. A photograph of the twill-CFRP is depicted in Fig. 2.6a. The second

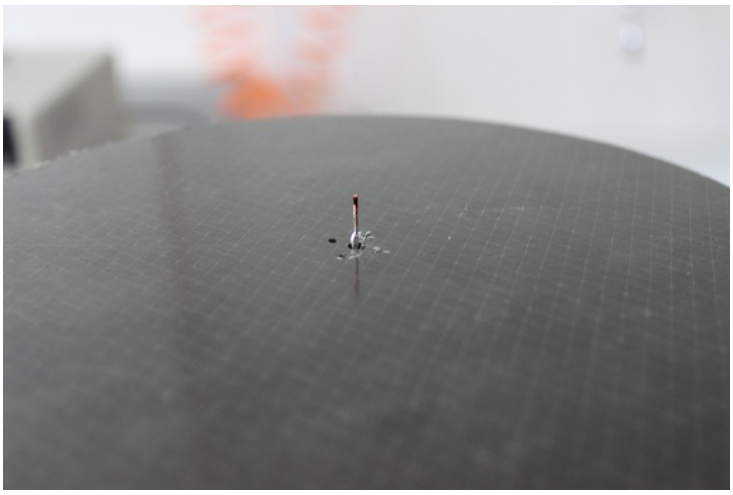

Figure 2.5: A wire monopole antenna for 5.9 GHz on a circular ground plane made from CFRP.

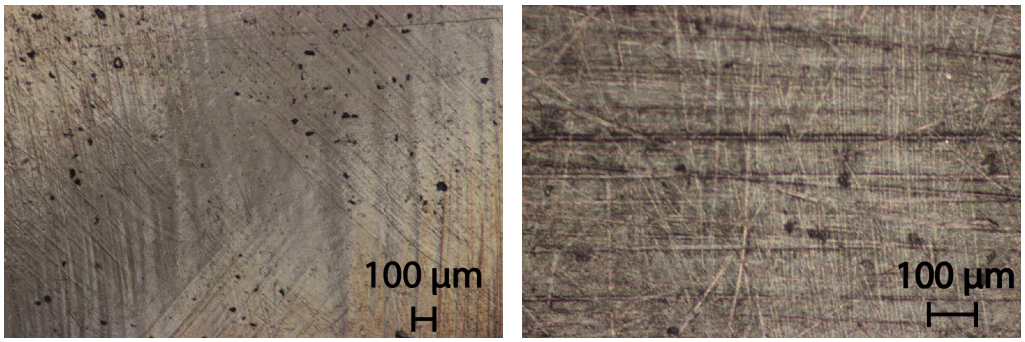

(a) (b)

Figure 2.6: Photograph of the a) twill-CFRP and b) shred-CFRP. ©2014 IEEE, reprinted with permission from [3].

material consists of unidirectional plies, but has short carbon fiber shreds in random alignment on the top layer, it is denoted as shred-CFRP. The shred-CFRP disk has a thickness of 2.26 mm. A photograph of the material is depicted in Fig. 2.6b. The third CFRP is again a 2/2 twill-weave, it is thereafter called twill-CFRP2. Twill-CFRP2 is commercially available from CG TEC, its plies are arranged as $[0\ 90]_N$ and it has a fiber volume fraction of approximately 60%. The materials are compared to a 2 mm thick aluminum disk. All circular ground planes have a diameter of 195 mm.

The measured return losses of the antennas are depicted in Fig. 2.7. The wire monopole antennas were cut to length, such that they are resonant on

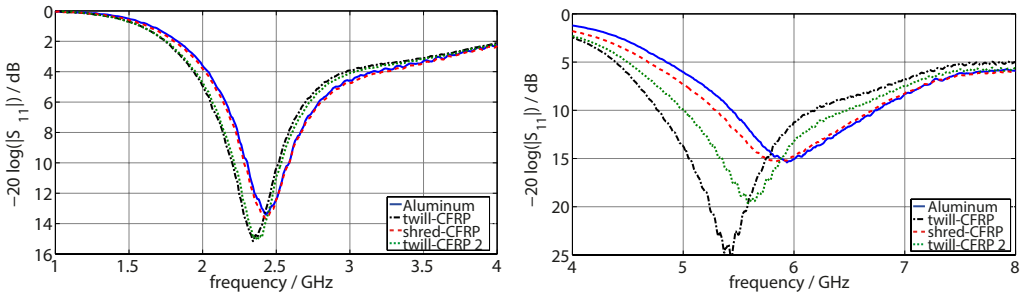

Figure 2.7: Measured return loss of the monopole antennas on CFRP ground planes at a) 2.45 GHz and b) 5.9 GHz. ©2014 IEEE, reprinted with permission from [3].

the aluminum ground plane at the desired frequencies 2.45 GHz and 5.9 GHz. When placed on the CFRP ground planes the resonance frequencies are then slightly shifted. However, the return loss of the monopole antennas is still better than 10 dB on all ground planes and this effect can easily be compensated in antenna design by changing the length of the antenna.

The gain patterns of the antennas are measured in the institute's anechoic chamber. Vertical cuts of the normalized gain patterns at azimuth $\varphi = 0°$ are depicted in Fig. 2.8. The horizontal cuts of the normalized gain patterns at $\theta = 90°$ are depicted in Fig. 2.9. The vertical gain patterns show almost no difference between materials. Small variations are evident close to zenith for $0° \leq \theta \leq 15°$ and for the backlobes at 2.45 GHz, see Fig. 2.8a. In Fig. 2.8b minor variations are evident at 5.9 GHz again close to zenith for $0° \leq \theta \leq 30°$. In the important region for monopole antennas $\theta < 90°$ the patterns are almost identical. Variations in radiation patterns in the horizontal plane in Fig. 2.9 are smaller than 1 dB. For automotive monopole antennas these variations are smaller than most other vehicular influences. CFRP can therefore be assumed to have no influence on monopole antennas' radiation patterns at 2.45 GHz and 5.9 GHz. This implies, that the investigated CFRP can be modeled as isotropic in automotive antenna simulations. These simplifications do not apply to CFRP with unidirectional fiber alignment, as will be shown in the second part of this section.

The radiation efficiency on the CFRP ground planes was also measured and is given relative to the efficiency on aluminum in Tab. 2.1. Depending on the CFRP and frequency the radiation efficiency is reduced to 76.9 % of the efficiency on an aluminum ground plane. In automotive applications such an efficiency reduction of up to 1.2 dB will be acceptable.

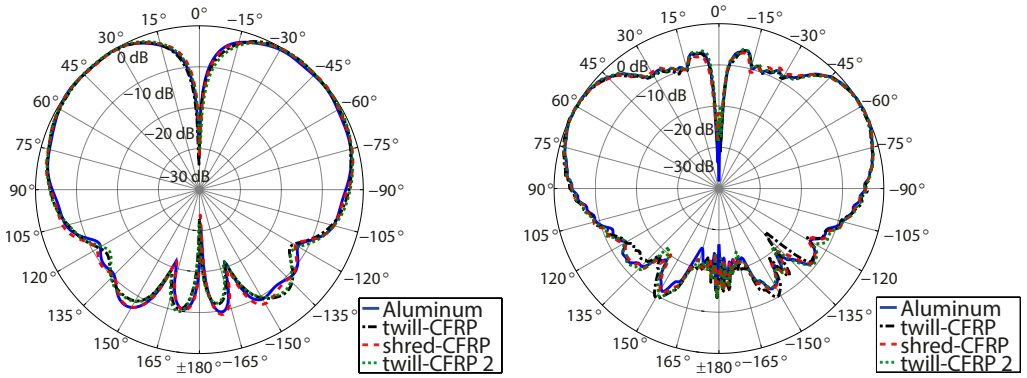

(a) (b)

Figure 2.8: Measured normalized gain patterns of wire monopole antennas on CFRP ground planes, vertical cut at $\varphi = 0°$ for a) 2.45 GHz and b) 5.9 GHz. ©2014 IEEE, reprinted with permission from [3].

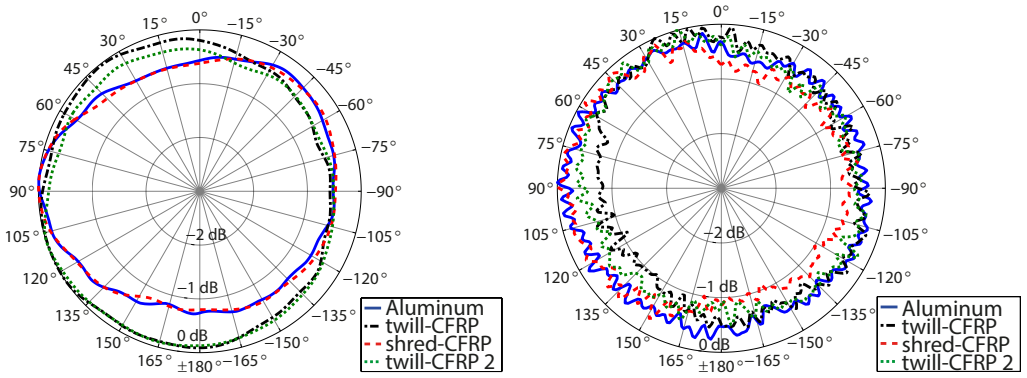

(a) (b)

Figure 2.9: Measured normalized gain patterns of wire monopole antennas on CFRP ground planes, horizontal cut at $\theta = 90°$ at a) 2.45 GHz and b) 5.9 GHz. ©2014 IEEE, reprinted with permission from [3].

Investigation of CFRP ground planes with wideband conical monopole antennas

To obtain measurement results in a wider frequency range, the results with wire monopole antennas from [3] are repeated with wideband conical monopole antennas. The first twill-CFRP is no longer investigated. The disk was quite thin which caused problems, as the holes could not be threaded properly. The twill-CFRP investigated in this section is again the commercially

2.45 GHz	Al	twill-CFRP	shred-CFRP	twill-CFRP2
10dB bandwidth [GHz]	0.29	0.32	0.31	0.32
relative 10dB BW [%]	11.8	13.1	12.7	13.1
maximum gain [dBi]	2.1	2.0	1.4	1.6
relative efficiency [%]	100.0	102.3	91.0	94.4
5.9 GHz				
10dB bandwidth [GHz]	1.30	1.42	1.43	1.48
relative 10dB BW [%]	22.0	24.1	24.2	25.1
maximum gain [dBi]	4.2	3.2	3.0	3.5
relative efficiency [%]	100.0	82.2	76.9	87.3

Table 2.1: Comparison of measured antenna properties with different ground plane materials. ©2014 IEEE, reprinted with permission from [3].

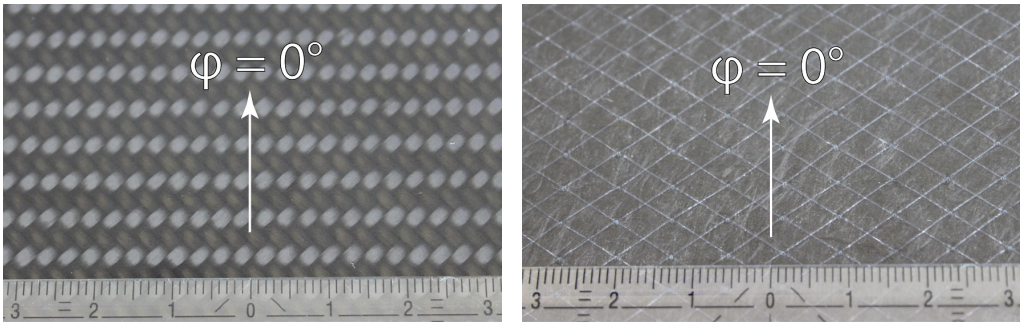

(a) (b)

Figure 2.10: Photograph of the a) twill-CFRP and b) shred-CFRP. ©2017 IEEE, reprinted with permission from [9].

available material from CG TEC. The plies of the 2/2 twill weave are again stacked as $[0\ 90]_N$ to a total thickness of 1.6 mm and the fiber volume fraction is 63 % according to manufacturer. A photograph of the twill-CFRP is depicted in Fig. 2.10a. Again the shred-CFRP is investigated, a photograph with larger scaling is depicted in Fig. 2.10b. The third CFRP investigated with conical monopole antennas has plies with unidirectional fiber alignment, all oriented in the same direction $\varphi = 0°$. The plate has a thickness of 4 mm, quite thick as unidirectional CFRP plates break easily. All ground planes have a diameter of 300 mm. The disks are cut by waterjet; again SMA flanges are screwed to threaded holes in the center of the disks.

The conical monopole antennas are standard designs, which are dimensioned according to [170]. The lowest frequency of operation is defined by

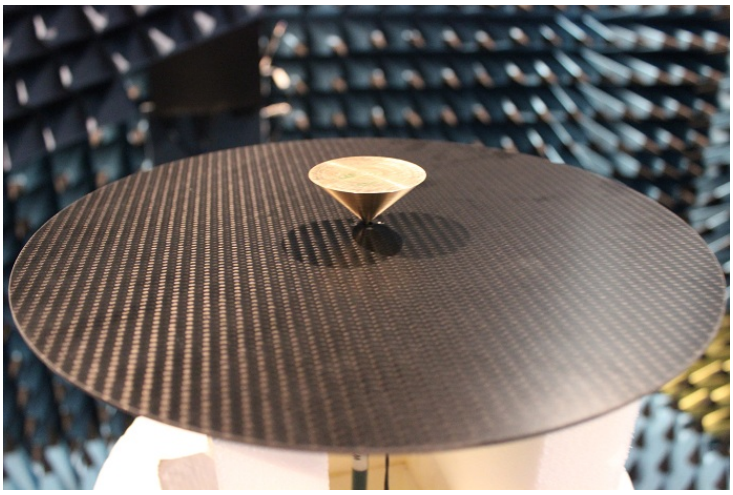

Figure 2.11: Conical monopole antenna on twill weave CFRP. The antenna is placed on a Rohacell pillar in the institute's anechoic chamber. ©2017 IEEE, reprinted with permission from [9].

the height of the antenna; the operation at higher frequencies is defined by the manufacturing precision of the cone tip. The impedance is adjusted by the angle between cone and ground plane. The length of the cylindrical extension on the bottom is adjusted to the thickness of the different ground planes, such that the cone tip is positioned at the ground plane surface. All cones are turned from brass. The tubes on the bottom of the cones tightly fit onto the inner conductors of the SMA flanges. Soldering is not required. A photograph of a conical monopole antenna on the twill weave CFRP is depicted in Fig. 2.11.

Measured S-parameter are depicted in Fig. 2.12. Above 2 GHz the S-parameters of the conical monopole antennas are better than -10 dB on all investigated materials. Below 2 GHz the return loss is lower than 10 dB. This would influence the gain patterns, as they are measured as realized gain in the anechoic chamber and the antenna mismatch would then be included in the gain patterns. The antenna gain according to the IEEE definition, which is based on power accepted by the antenna, is therefore calculated from the measured realized gain, which is based on power supplied to the antenna. The depicted IEEE gain no longer contains the antenna mismatch.

The vertical cuts of the gain patterns (IEEE gain definition) are depicted in Fig. 2.13. The left sides of the plots show the vertical cuts at azimuth $\varphi = 0°$ and the right sides of the plots show the vertical cuts at $\varphi = 90°$. For the unidirectional CFRP $\varphi = 0°$ corresponds to fiber direction and $\varphi = 90°$ is perpendicular to fiber direction. The first important observation is, that

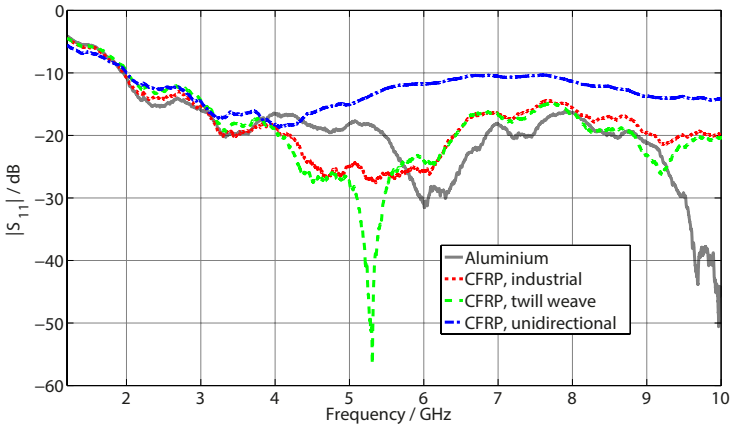

Figure 2.12: Measured S-parameters of conical monopole antennas on different ground plane materials. ©2017 IEEE, reprinted with permission from [9].

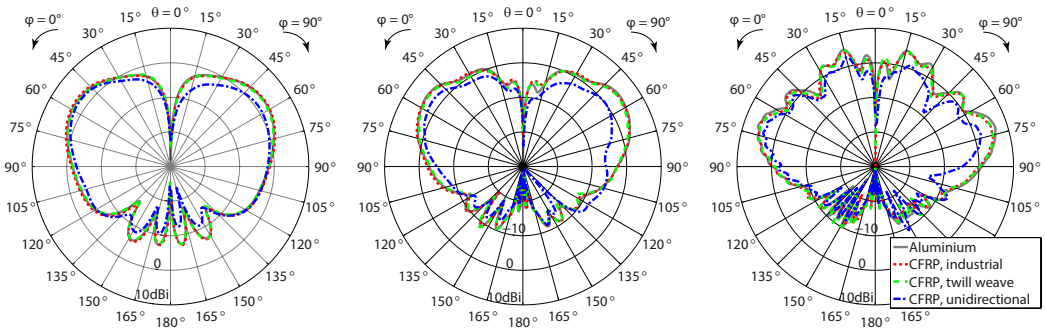

(a) (b) (c)

Figure 2.13: Vertical cuts of the conical monopole antennas' measured gain patterns (IEEE gain definition) on different ground plane materials. Each plot shows the pattern at $\varphi = 0°$ on the left and the pattern at $\varphi = 90°$ on the right side. Cuts are shown for a) 2 GHz, b) 5 GHz and c) 10 GHz ©2017 IEEE, reprinted with permission from [9].

the gain patterns on the industrial and twill CFRP are almost identical to the gain patterns on aluminum. The second observation is, that the gain patterns on the unidirectional CFRP differ from those on aluminum. In fiber direction the gain is reduced, but the shape of the patterns are almost the same as on an isotropic material. Perpendicular to fiber direction the gain is reduced, but more importantly the shapes of the gain patterns are also changed. In the region from 1 - 10 GHz unidirectional CFRP clearly behave as an anisotropic material, when used as antenna ground plane.

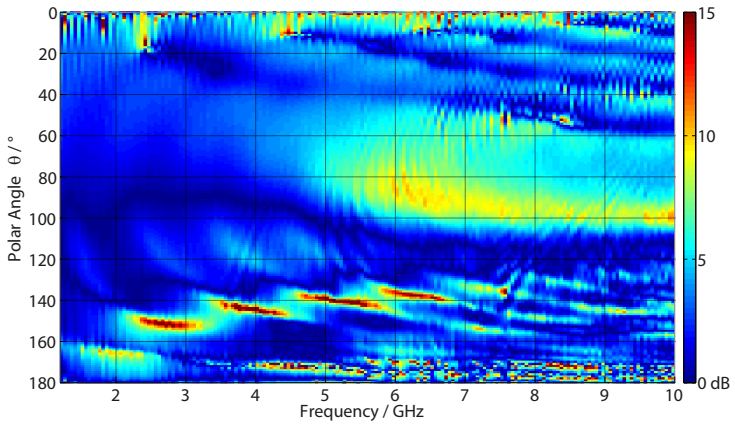

Figure 2.14: Absolute difference between the vertical cuts of the gain patterns on aluminum and unidirectional CFRP for azimuth $\varphi = 90°$ (perpendicular to fiber direction). ©2017 IEEE, reprinted with permission from [9].

To further investigate the anisotropic behavior of unidirectional CFRP over frequency, the absolute difference of the vertical cuts perpendicular to fiber direction of the gain patterns on unidirectional CFRP and aluminum are depicted in Fig. 2.14. Monopole antennas do not radiate towards zenith or nadir, and variations at $\theta \approx 0°$ and $\theta \approx 180°$ can be neglected. Changes in the backlobes ($120° \leq \theta \leq 160°$) are not important, as radiation below the ground plane is unwanted in most applications. But the gain pattern changes at $\theta \approx 90°$ are very concerning. Changes in gain patterns from isotropic ground planes of 10 dB are quite large. The more so as the anisotropy influences become very large at 5.9 GHz, a frequency which is used for V2V communication.

The changed gain patterns result in a changed directivity, as is shown in Fig. 2.15. But not only the directivity is changed; the unidirectional CFRP results in reduced radiation efficiency. Fig. 2.16 shows that the radiation efficiency on CFRP is reduced by up to 4 dB from the efficiency on aluminum. It should be noted, that the radiation efficiency is estimated from IEEE gain values, which are calculated from measured realized gain patterns of the antennas and S-parameter measurements, and the absolute gain value measured with reference horn antennas. This leads to inaccuracies in the estimation of the efficiency and results in efficiency values slightly above 100 %.

As a conclusion to these investigations it can be said that CFRP with twill weave and with shredded carbon fibers in random alignment act as isotropic ground plane materials in the gigahertz-range. The anisotropy of unidirectional CFRP ground planes cause large changes in the gain patterns

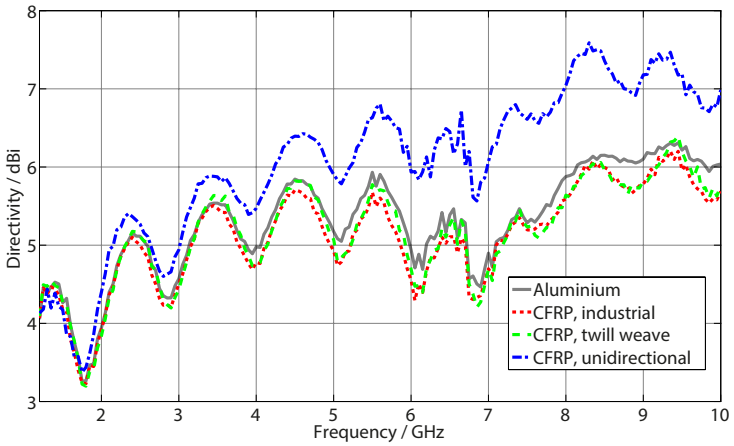

(a)

Figure 2.15: Measured directivity of conical monopole antennas on different ground plane materials. ©2017 IEEE, reprinted with permission from [9].

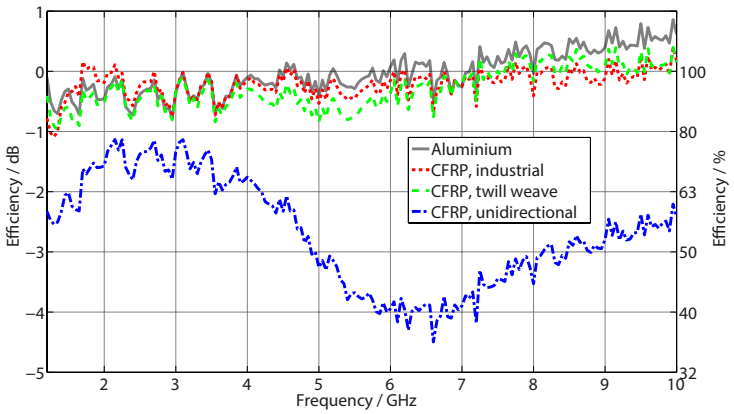

Figure 2.16: Calculated radiation efficiency of conical monopole antennas on different ground plane materials. ©2017 IEEE, reprinted with permission from [9].

of monopole antennas.

2.2.3 Automotive Antennas on a CFRP Car Roof

CFRP are investigated as ground plane material on the example of flat disks in Sec. 2.2.2. This simplified ground plane geometry is very useful, as it is circularly symmetric and together with circularly symmetric antennas it can be used to measure anisotropy in antenna gain patterns. Although it could be assumed, that these results obtained on small disks translate to the

(a) (b)

Figure 2.17: Shark-fin automotive antenna module on half of a CFRP car roof: a) top view and b) front view.

behavior on whole car roofs; one can not be certain until quantitative results are obtained by measurement.

The goal of the measurements in this section is to quantify the influence of CFRP car roofs on automotive antennas. CFRP ground planes are therefore no longer simplified, and the ground plane now has the size and geometry of a car roof. The antennas are also no longer simplified to wire monopole antennas or conical monopole antennas, but a whole automotive antenna module from mass production is measured. The section is based on [5].

An unpainted CFRP car roof from mass production is obtained. Practical problems arise, when comparing a CFRP car roof to a metal roof. Vehicles either use a CFRP or metal roof and different car models have different roof geometry. It is therefore not possible to obtain mass produced car roofs with the same geometry made from these two materials. Furthermore, CFRP and aluminum roofs use different production processes and production of the exact same roof geometry from aluminum is economically not reasonable. As a tradeoff a flat $1 \times 1\,\mathrm{m}^2$ aluminum sheet is used. The shark-fin fixture and contour of the aluminum are laser cut. Only half of the CFRP roof is measured, as the institute's anechoic chamber is not large enough for a whole car roof. The roof's CFRP has fiber shreds in random alignment on the top layer. The investigated automotive antenna module is a shark-fin housing which contains several antennas, two of them are C2C antennas manufactured in PCB technology on FR4. The antenna module on half of the CFRP car roof is shown in Fig. 2.17. Only the results for one C2C antenna are presented in this dissertation; the results of both C2C antennas are published in [5].

The CFRP roof and aluminum sheet are mounted with a fixture on a glass

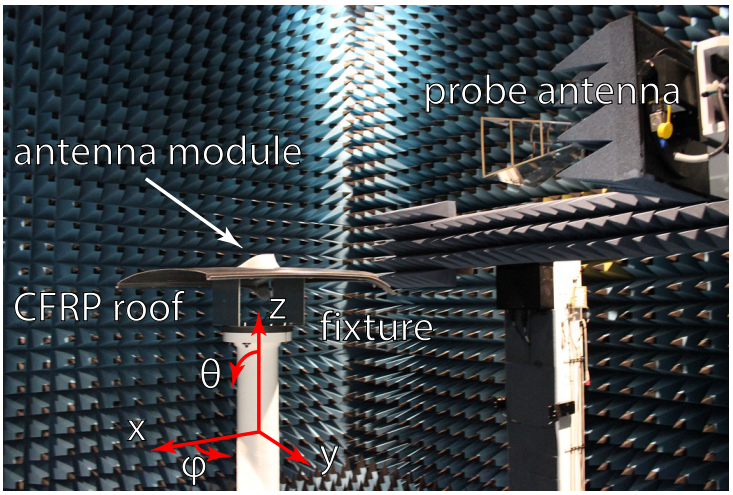

Figure 2.18: Automotive antenna module mounted on a CFRP car roof inside an anechoic chamber. ©2016 IEEE, reprinted with permission from [5].

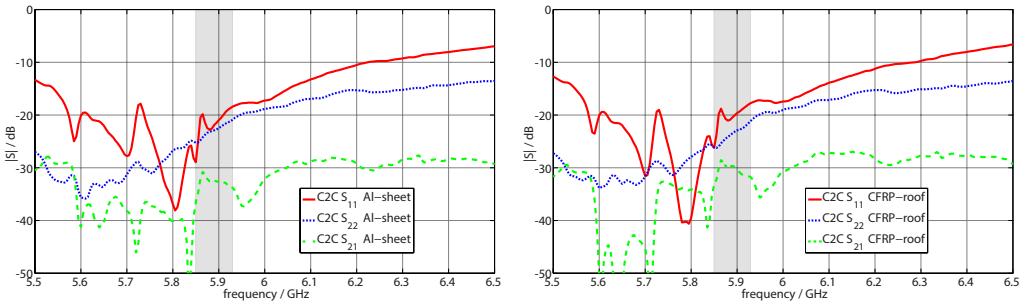

(a) (b)

Figure 2.19: Measured S-parameters of the C2C antennas a) on an aluminum sheet and b) on a CFRP car roof. ©2016 IEEE, reprinted with permission from [5].

fiber reinforced polymer column in the anechoic chamber, as is depicted in Fig. 2.18. The antenna is mounted in a horizontal position, it might be tilted when mounted on the rear end of a car roof.

Measured S-parameters are depicted in Fig. 2.19. Fig. 2.19a shows the results on the aluminium sheet and Fig. 2.19b shows the results on the CFRP car roof. The return loss of both C2C antennas is excellent with $\approx 20\,\mathrm{dB}$ in the desired frequency band. Antenna isolation is also excellent with $\approx -30\,\mathrm{dB}$. Only small differences are noticeable between the aluminum and CFRP ground plane.

Gain patterns are shown in Fig. 2.20. Differences of about 2 dB are in the

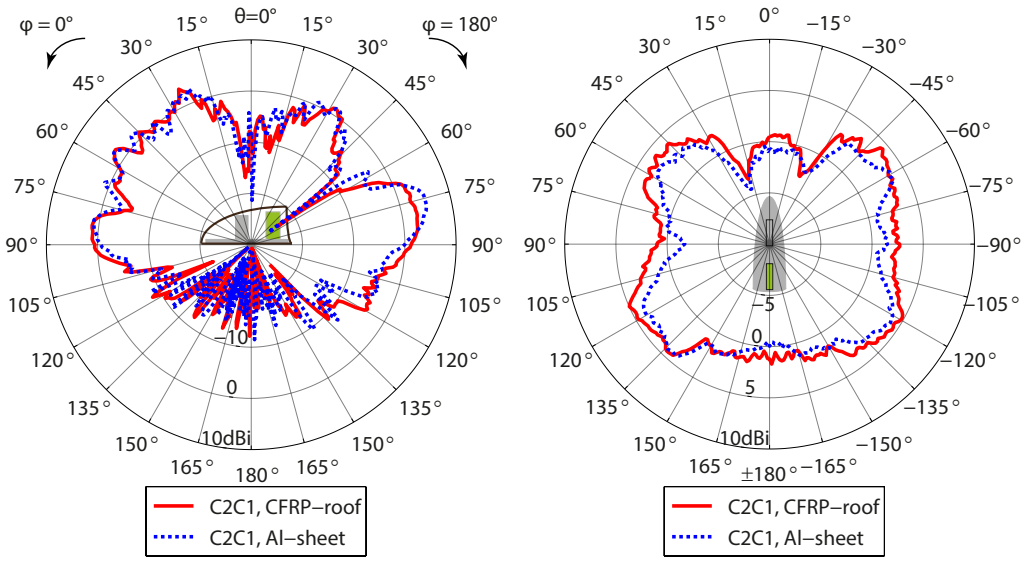

(a) (b)

Figure 2.20: Measured gain patterns of a C2C antenna on an aluminum sheet and a CFRP car roof at 5.9 GHz, a) vertical cut at $\varphi = 0°$ b) horizontal cut at $\theta = 90°$. ©2016 IEEE, reprinted with permission from [5].

same magnitude as known influences of room curvature. No additional zeros are caused by the CFRP and there are no large changes in gain patterns, as they occur for unidirectional CFRP in Sec. 2.2.2.

Measured radiation efficiency is shown in Fig. 2.21 on the aluminum sheet and on the CFRP car roof. The efficiency on the CFRP car roof relative to the efficiency on aluminum is also given. The radiation efficiency is reduced by 10 % on the CFRP roof, which is less than the 23 % reduction found in Sec. 2.2.2 on a small CFRP disk. A possible explanation is the aluminum base of the automotive antenna module. A 10 % reduction in radiation efficiency can be neglected in automotive applications.

As a conclusion to measurements of an automotive antenna module on a CFRP car roof it can be said, that small influences of the material on the antenna exist. Radiation efficiency is reduced by 10 %. As the material's influence of the gain pattern could not be measured independent of the roof geometry, the conclusion is, that the influence of CFRP on the automotive antenna is at least less than the influence of the roof curvature. These influences are smaller than most other influences on automotive antennas (see Sec. 1.4.4) and do not need to be considered in practice.

As a general conclusion to this chapter it is found that CFRP with shred-

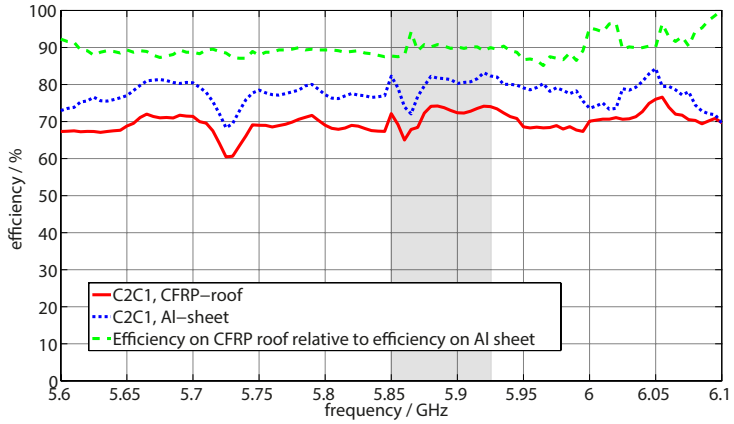

Figure 2.21: Measured radiation efficiency of a C2C antenna on an aluminum sheet and on a CFRP car roof. ©2016 IEEE, reprinted with permission from [5].

ded fibers and CFRP with woven fabrics are quasi-isotropic conductors in the single-digit gigahertz region. The conductivity of these CFRP varies within one order of magnitude. CFRP made from unidirectional fibers are anisotropic. Accordingly, measurements of CFRP as ground plane material for antennas show that shred-CFRP and woven CFRP have no significant influence on gain patterns, while unidirectional CFRP drastically change the gain patterns of antennas placed on it. Measurements of an automotive antenna module on a shred-CFRP car roof also show that the CFRP behaves as an isotropic conductor. From an antenna design viewpoint shredded and woven CFRP can be used as antenna ground planes. For simulations these CFRP can be modeled as isotropic materials.

Chapter 3

Concealed Vehicle Chassis Antenna Cavity

3.1 Design Considerations for Chassis Antenna Cavities

This section starts with claiming design goals for new antenna mounting positions. The aim is to get an abstract view on automotive antenna design, define requirements for a new automotive antenna module, find suitable locations for an automotive antenna module and then design a new antenna module that fits these requirements. The prove, that this mounting position is indeed a good position for antennas and that antennas inside the module function properly, is given in later sections of this chapter by building a prototype and measuring several state of the art antennas inside the new module.
The following requirements are demanded of the antenna module:

- The antenna module must to be located in an optimum position for antennas on the vehicle.
- The antenna module must be concealed.
- The antenna module must be dedicated antenna space.
- The antenna module must be large.
- The antenna module must be compatible with existing antenna designs to allow a smooth transition to the new technology.

Antenna Positions on Vehicles

Several scientific works investigate optimal vehicular and automotive antenna mounting positions. An early investigation is published in [89], which considers six antenna positions on a police car, three on the roof, two on the trunk and one on the front fender. For a long time the design principal was that automotive antennas should be omnidirectional, as the vehicle might be oriented in an arbitrary direction towards a transmitter. For most services (audio broadcasts, telephony, etc.) the antenna's position on the vehicle was chosen such that omnidirectional radiation patterns were possible, typically antennas were mounted on the roof. As vehicular antenna systems consisted of a simple single antenna per service, advanced functionality like beam steering was not feasible. For satellite reception [171] investigates positions for GPS antennas and concludes that the roof and trunk are preferable positions.

This view changes when MIMO antenna systems are introduced on vehicles. The evaluation becomes increasingly more difficult as MIMO antennas involve both pattern diversity and spatial diversity. Pattern diversity is either deliberately designed or caused by the vehicle itself e.g. shadowing from large vehicle parts. The electromagnetic waves are also not immediately radiated, but wave propagation along vehicles is a complicated process involving edge diffraction, reflections, waves guided inside dielectric parts and interference of these waves [97]. A large number of investigations research optimal vehicular mounting positions for MIMO antennas [52–54, 61, 63, 100, 115, 172, 173]. For repeatability ray tracing simulations are used to investigate automotive antenna positions [56, 66, 114, 115, 174]. [66] investigates antenna height. [113, 114, 175] compare 16 locations, including bumpers, roof, side mirrors and roof pillars. It is found that the best MIMO positions are the side mirrors and the roof and near-optimum radiation patterns for these positions are synthesized. [56] compares antenna positions in virtual test drives. [52] measures five different positions on the roof and one antenna on the upper end of the windshield. From the same measurements [54] draws the conclusion that vertical spacial diversity (roof and windshield) is important for C2C communication, as it counteracts destructive interference from road reflections (compare two-ray models, [176]). [172] considers polarization diversity. In [173] channel capacity is measured for 2×2 MIMO systems with 15 locations on the car's hood, roof and trunk.

The car roof is an available and feasible position for antennas. It might contain panorama roof windows, sunroof, overhead consoles, cables. The roof is a structural component of the car chassis, but there is technical precedence that such modules can penetrate the roof without degrading its structural

integrity, again for example roof windows. Antennas in this position might get damaged in the event of an accident, e.g. overturning, but the roof is not part of the car's deformable zone. It can be expected, that the antennas and communication modules in the roof stay intact in most accidents, or at least they are a lot less vulnerable than antennas in the side mirrors or bumpers.

Concealed Vehicular Antennas

Why is it demanded, that the antenna module should be concealed? The aesthetic appearance of a vehicle is a major selling point for mass produced consumer cars. Protruding antennas or antenna modules interfere with this design and would in return lower sales. Protruding antennas also influence vehicles' drag coefficients. These limitations apply to mass produced cars sold to consumers, but might not apply in other sectors, e.g. for military vehicles [31].

To conceal antennas is a design choice – but not a technical choice! This design choice is currently made for most consumer electronics. The most prominent example is the concealment of antennas in mobile phones.

Several concealed antennas have been researched for automotive applications. Slot antennas around the car (e.g. in doors, behind license plates) are proposed in [177]. [178] considers concealed antennas inside rear-view-mirrors, spoilers, engine hood and back shelf. In [179] hidden antennas at three different positions are discussed: Very High Frequency (VHF) antenna on the rear windscreen, a planar inverted-F antenna for 900 MHz telephony in the bumpers and a top-loaded monopole for telephony placed on the rear window just below the roof. As expected the antenna in the bumpers is severely shadowed by the vehicle. Two antennas in the front and rear bumpers are combined to achieve omnidirectional radiation, but several nulls appear in the region between the two patterns. The monopole antenna shows better performance, but gain in driving direction is reduced by 10 dB. The windows are a popular location for radio antennas [180, 181]. [30, 182] use the windshield instead of the rear window for an antenna reconfigurable between FM and DAB.

Low et al. propose an antenna module placed in an aperture at the rear end of the roof [183, 184]. The module contains antennas for AM, FM, DAB and television. The problem of an aperture is, that is does not isolate the vehicle interior from the antennas. In [184, p. 3708] the authors note that fields within the body cavity need to be modeled in addition to the car's exterior. Antennas in the side mirror are investigated in [185, 186]. [186]

presents a conformal antenna on the cover of a side mirror. Antennas inside the rear-view mirror are shown in [187] and [188]. LTE and IEEE 802.11p antennas inside the spoiler are investigated in [189]. A WLAN antenna for the roof spoiler is described in [190]. A transmitter in a roof pillar is depicted in [191]. Usage of vehicles' characteristic modes [32] or parts of it (such as rear-view mirrors [33]) is currently under research [192].

Several authors consider small cavities, which only house one single antenna. A SDARS antenna inside a $40 \times 40 \times 10\,\mathrm{mm}^3$ cavity is presented in [193]. [194] adds an antenna for GPS. An aircraft antenna for distance measurement equipment inside a circular cavity ($\varnothing 280\,\mathrm{mm}$, height 43 mm) is proposed in [195]. Simulations of a LTE antenna inside a $200 \times 200 \times 30\,\mathrm{mm}^3$ cavity are presented in [196]. For measurements the cavity protrudes from the roof (sic, see [196, Fig. 11]). At 2.6 GHz the pattern has variations up to 20 dB.

Patents similar to the proposed cavity are [197, 198]. [197] proposes several hidden antenna modules in the chassis, which are embedded into holes cut after production. [197, Fig. 3 and Fig. 4] describe a very complicated process of crimping the roof sheet and adding reinforcing profiles around the cutout, along with several measures to isolate the gaps. For commercial systems this shows the huge advantage of building antenna cavities directly as part of the chassis. [198] depicts an antenna module which is inserted into a hole in the car roof. The module reaches from the exterior to the interior of the car [198, Fig. 4]. Complicated modifications to the roof are again necessary around the hole to attach the module inside the roof and insulate the gaps [198, Fig. 2].

Concealed antennas are also investigated for Unmanned Aerial Vehicles (UAVs). A monopole array in the wings of a small UAV is manufactured and measured in [199]. Slotted waveguide antennas in the arms of small UAVs are discussed in [200].

Dedicated Antenna Space

Evidence suggests, that vehicular antenna modules should be dedicated antenna space.

It is well known that areas surrounding antennas should be empty, such that free-space waves can form and propagate. Objects in the vicinity of antennas, especially metal parts, interfere with the antennas' operation. While it is in principle possible to compensate some influences of these objects by adapting the antennas' design, this requires additional effort during develop-

ment. In practice most of these problems stem from the design process of the whole vehicle. The vehicle is not designed by a single company, but design and manufacturing of parts is outsourced. The final design of the vehicle and its components is in general not available during antenna design, as modules are developed simultaneously [108]. Combining antennas with independently designed parts might have unforeseen consequences, which would arise late in development and therefore close to market release.

Antennas in side mirrors are discussed in detail as an example, because they are under consideration as mounting position for automotive antennas [185, 186, 201–203]. Side mirror modules already serve a purpose. They already contain several mirrors, indicators, electronics, and cables. Some influences of these parts on antennas can be compensated, or minimized by shielding the antenna, e.g. by introducing a metal sheet underneath it. Other influences can not be compensated, for example the influence of the moveable mirrors. This creates dependencies in the development, as the antenna design can not be adapted until the side mirror's design is final. Antenna designs can not be reused for future vehicles, as the side mirrors will change. The size of side mirror modules can not grow excessively; they are already too small to fully replace shark-fin modules.

Similar problems appear for antennas in bumpers, windows, etc. The compelling argument for the vastly successful shark-fin antenna modules is, that they eliminate these interdependencies. The influence on the vehicle's aesthetic appearance and mechanical properties is fixed, as the size and geometry of the shark-fin casing is fixed. The antennas can be independently developed by external supply companies, as long as the volume fits within the shark-fin casing. The only remaining influences on the antennas are the geometry of the car model's roof and the presence of roof windows and rails. As single large antenna modules can also contain electronics, they only need to be connected by a power supply and a data bus, small distributed antenna systems each require a cable.

In order to be successful, a new automotive antenna module must be dedicated antenna space that strives to eliminate interdependencies with other functional units.

On the Size of Automotive Antenna Modules

A cavity is proposed as automotive antenna module. Cavities offer large space dedicated for antennas and can be fully concealed. The electronics and passengers in the vehicle interior are isolated from the radiation. The

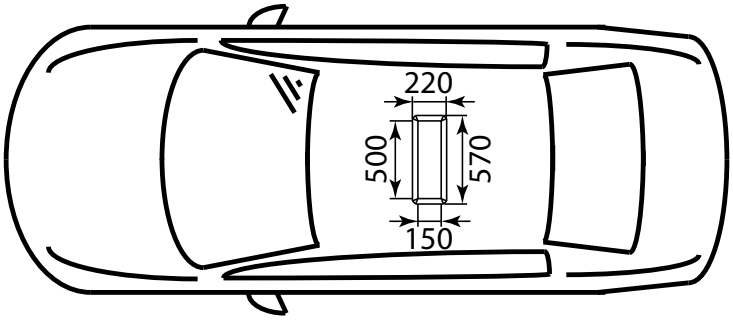

Figure 3.1: Sketch of a chassis antenna cavity in the center of a car roof. ©2016 IEEE, reprinted with permission from [1].

cavity can be built into the chassis, and preferably it is manufactured as part of the roof. The width of the antenna cavity should be chosen as large as possible, but such that it fits the width of the car roof, trunk and hood of most car models. The length of the antenna cavity should be chosen such that it fits in front or behind a panorama roof window or a sunroof. The height of the antenna cavity should be chosen according to the height of car roofs. The shape of the cavity must be chosen such that manufacturing of the cavity as part of the chassis is possible and it needs to fulfill mechanical requirements. Following these design choices results in an antenna module, which is applicable for most vehicle types. Just like shark-fin modules it can be used on sedan type vehicles, humvees, vans, etc. For vehicles without roof – convertibles are prominent examples – a cavity of the same size can be built into the trunk lid or hood.

The exact shape of the cavity is not that important. In practice an antenna module will be inserted into the cavity. For antenna applications the shape of the module inside the cavity can then be altered, as the metal parts of the module can be shaped as required for antenna design. It can be expected, that this won't be necessary, as rectangular modules have been used with great success, e.g. for base station antennas.

For production the cavity is designed with inclined walls. For a prototype inner dimensions of $150 \times 500 \times 40\,\mathrm{mm}^3$ and outer dimensions of $220 \times 570 \times 40\,\mathrm{mm}^3$ are chosen. The cavity is larger than current roof mounted shark-fin antenna modules. The cavity has a volume of about $3\,\mathrm{dm}^3$, while the largest commercially used automotive antenna modules [72] have a volume of about $0.2\,\mathrm{dm}^3$ [1]. An example of the cavity placed in the center of a car roof is depicted in Fig. 3.1. Production of a prototype from CFRP is described in Sec. 3.3.1. The cavity was new at the time of invention, the literature research of the Austrian patent office is attached in Appendix A.

Performance of Current Automotive Antennas Inside the Antenna Module

The new module is a cavity and therefore allows antenna designs, which are not suitable for shark-fin modules. Possible examples are slot antennas [167], slotted waveguides [169], cavity backed antennas [204], partially reflecting sheet arrays [205] etc. The cavity can be divided into sub-cavities and it is large enough to also contain elements for antenna isolation, such as isolation fences and slots [206].

There are several concerns when placing automotive antennas inside a cavity. Radiation can be blocked by the cavity walls. Reflections from the walls can interfere with waves from the antenna. Destructive interference then causes nulls in the radiation pattern. The position below the roof could shadow radiation in the horizontal plane. Resonance frequencies of the cavity can influence antenna operation. The proximity to conductive walls could detune the antennas.

To allow a smooth transition from roof-mounted shark-fin antenna modules to chassis antenna cavities, it needs to be demonstrated, that state-of-the-art automotive antennas function in antenna cavities without major design changes. The focus will be on antennas, which are currently placed inside roof mounted shark-fin modules, as these modules will be replaced by the cavity. Antennas for AM/FM, radar, tire monitoring, etc. are not discussed as they are already concealed in suitable places. Measurements in this chapter proof the proper operation of monopole antennas, IFAs and pattern reconfigurable antennas inside the chassis antenna cavity. Influences of the chassis antenna module onto antennas are quantized and discussed.

3.2 Simulation Models for CFRP Chassis Antenna Cavities

The manufactured geometry of the chassis antenna cavity is derived from extensive simulations. The material model is based on estimation of the material properties of CFRP and measurements of the influences of CFRP onto antennas in Chapter 2. For the sake of shortness only exemplary simulations of the final cavity and antenna designs are discussed. Simulations are compared to measurement results of prototypes that are presented in detail in Sec. 3.4.

Various antenna simulation tools are commercially available for a wide selection of solvers such as finite elements, method of moments etc. All these simulation methods require, that the antenna and its surroundings are modeled. Two things are required: a geometric description and the material parameters (conductivity, permittivity, permeability) at the right frequencies. The precision of the model will in practice be limited in order to reduce the simulation time. This is typically achieved by limiting the complexity of the geometry. Several methods exist for different solvers, e.g. limiting the number of tetrahedrons in finite element simulations.

This section only considers simulation of the antenna characteristics itself. In automotive antenna simulation the complex geometry of the vehicle is simplified by removing curvatures and parts that are small compared to wavelength. Sometimes additional simulations are required and design automotive antennas and evaluate their performance, e.g. propagation models for GPS antennas under foliage [207], channel models for V2V communication [208], channel models for intra-vehicular communication [209], or ray-tracing simulations to determine capacity maximizing radiation patterns [210].

In Chapter 2 it is shown, that the material properties of CFRP can be modeled as isotropic, as long as woven fabrics or materials with fiber shreds in random alignment on top are used. More complicated CFRP models such as tensors [136] or equivalent layer models [134] are then not required. The anisotropy of UD-CFRP influences antennas in the gigahertz range (compare Sec. 2.2.2) and therefore the anisotropy also needs to be modeled. In this section the validity of these assumptions is checked, by comparing simulation results of an antenna in a chassis antenna cavity obtained from a finite element simulation with measurement results.

Ansys High Frequency Structural Simulator (HFSS) is used as simulation software, which is now part of the Ansys Electronics Desktop. HFSS uses primarily finite element methods. The simulation of the LDS monopole antenna inside the chassis antenna cavity (Sec. 3.4.2) is discussed as an ex-

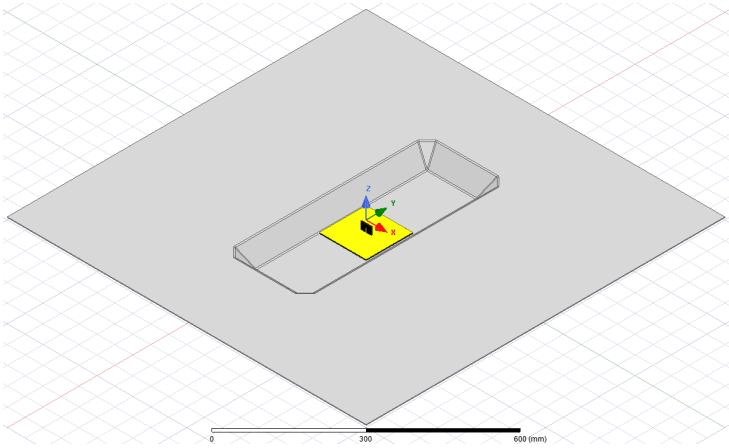

Figure 3.2: Simulation model of the LDS monopole antenna inside a chassis antenna cavity in Ansys HFSS.

ample. This is a good example for several reasons. The antenna and cavity both use semi-complex geometries and materials, which help to illustrate the tradeoffs required in contemporary antenna simulations. The geometry of the monopole antenna itself is simple, which allows to draw conclusions without too many details, e.g. the IFA in Sec. 3.4.2 has a more detailed structure. At 5.9 GHz the gain pattern of the antenna inside the cavity becomes quite complex as several zeros appear close to zenith; this is helpful for evaluating the simulations precision. Also at this frequency the cavity and the surround ground plane becomes electrically large, which increases simulation durations and helps to illustrate model tradeoffs to increase simulation speed. The simulation's geometry model is given in Fig. 3.2, which shows the LDS monopole antenna from Sec. 3.4.2 inside a chassis antenna cavity.

The geometric model of the monopole antenna is simplified by omitting the SMA connector. The monopole antenna's substrate (XANTAR LDS 3720) is modeled according to [101]. The LDS metal layer (a stack of copper, nickel and gold) is modeled as a solid gold layer.

The chassis antenna cavity's model is also simplified. The corners of the cavity are modeled to be sharply angled instead of round, as this simplification significantly reduces mesh size and therefore simulation time. The vehicle around the chassis antenna cavity is not modeled. This would limit the validity of the results to a specific vehicle type or car model. Nevertheless, simulation with a specific vehicle model is advised for manufacturers. For scientific investigation a $1 \times 1\,\mathrm{m}^2$ ground plane is big enough to show the general influence of a large ground plane, while omitting influences of roof curvature, roof rails, and so on. As is shown in Sec. 2.1.1 the conduc-

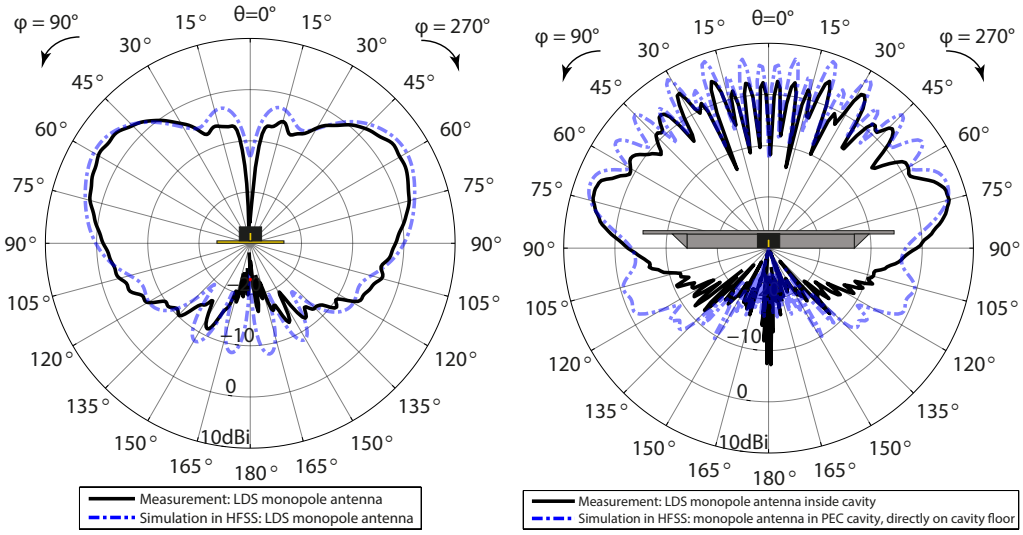

(a) (b)

Figure 3.3: Simulation results compared to measurements: a) LDS monopole antenna b) LDS monopole antenna placed directly on the floor of a chassis antenna cavity, which is modeled as a perfect conductor PEC.

tivity of woven CFRP is quasi-isotropic at 5.9 GHz. Measurements of CFRP as antenna ground plane material in Sec. 2.2 show no significant influence of plain-weave CFRP on antenna performance in the investigated frequency range. The CFRP is therefore modeled either as an isotropic quasi-conductor or as a perfect conductor.

The model antenna is excited by a lumped port and is surrounded by an airbox with a radiation boundary condition (now shown in Fig. 3.2). The simulation iteratively increases the mesh precision, until a termination condition is met. The simulation is stopped when difference in S-parameters to the previous iteration drops below a defined threshold, which is a widely used termination condition.

Measurements in the anechoic chamber require several modifications to the antennas and their surrounding, but these measurement specific additions are not modeled. Coaxial cables required for measurements are not modeled. The support pillar and aluminum fixture are not modeled. Angles $\theta > 160°$ can not be measured inside the anechoic chamber, as the θ-arm with the probe antenna can't move below the column with the AUT.

Two simulation results are discussed. The first is a simulation of the LDS monopole antenna on the LDS ground plane without the cavity. Fig. 3.3a compares vertical cuts of a measurements to simulation results. Note, that

the backlobes from the simulation for $\theta > 160°$ are missing in the measurements as the θ-arm in the anechoic chamber can not measure at these angles. Otherwise the simulation result resembles the measured gain pattern, but overestimates the gain in the desired area by about 2 dB. Fig. 3.11 compares a measurement of the monopole antenna inside the chassis antenna cavity to a heavily simplified model. The antenna is not placed on a separate LDS ground plane, as is the case in the measurement, but instead directly on the cavity floor. The cavity's rounded corners are not modeled and the material is modeled as Perfect Electric Conductor (PEC). Still the number and positions of the many zeros around zenith are simulated quite accurately. The region of interest $60° \geq \theta \geq 90°$ is also quite accurate. Large deviations are only found below the large ground plane for $\theta > 90°$. The simulation results show backlobes around $105° > \theta > 120°$, which have no correspondence in the measurement data. It must be noted, that these backlobes are present in almost all simulations of the cavity and that they are missing in almost all measurements of the cavity. This disagreement is yet without explanation. The backlobes might arise from an unknown problem from the simulation, either from the configuration of the software or inaccuracies in the geometric model, but they might also be the result of modifications for measurements, such as fixtures and holes in the cavity floor. The radiation towards $\theta = 180°$ displayed in the measurement results is definitively an artifact. Nevertheless, this example shows that even heavily simplified simulation models are in good agreement with measurement results.

(a) (b)

Figure 3.4: Cavity mold a) before surface treatment and b) after surface treatment.

3.3 Manufacturing Process of a CFRP Chassis Antenna Cavity

3.3.1 Prototype Production With the Autoclave Method

Prototypes of the chassis antenna cavity are manufactured to prove feasibility of production and enable measurements. The prototypes are built from CFRP to prove the possibility of manufacturing the antenna cavity as part of CFRP car chassis, but also of airplane and boat hulls. This section is based on [6].

Prototypes of the CFRP chassis antenna cavity are built with the autoclave method. The cavity design has a rectangular shape with a size of $500 \times 200\,\mathrm{mm}^2$ and inclined walls. The walls' inclinations are chosen such that they are suitable for the antennas and production. As representation of a car roof, the cavity is embedded in the center of a $1 \times 1\,\mathrm{m}^2$ sheet. A mold is milled from Raku-Tool WB-0700 tooling material in a machining center. All cavity edges are built with a 5 mm radius. The mold's surface is treated with Chemlease MPP 712 EZ and Chemlease PMR EZ. The mold is depicted in Fig. 3.4a, the mold with surface treatment is presented in 3.4b and closeups of edges and corners are shown in Fig. 3.5.

The CFRP part is built as orthotropic laminate with fiber axes at 0° and 90°. The plies are a plain weave CFRP from Isovolta prepreg with $200\,\mathrm{g/m}^2$ weight. The matrix is an epoxy resin, with a resin content of $\approx 30\,\%$. Eight layers are stacked to a total thickness of 2 mm as $[(0°\ 90°)_4]$. After the layup is done by hand, the specimen is vacuum bagged and cured in an autoclave at 4 bar and 130 °C. The prepreg layup on the mold is depicted in Fig. 3.6a and

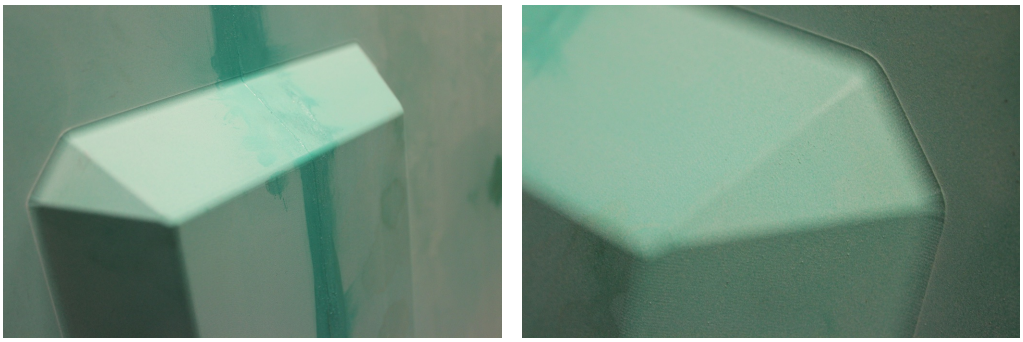

(a) (b)

Figure 3.5: Closeups of the cavity mold. a) edges and b) corner

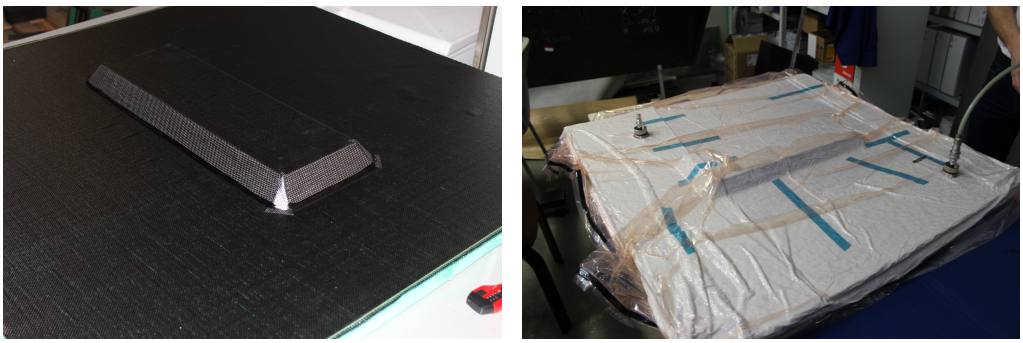

(a) (b)

Figure 3.6: a) Finished prepreg layup before vacuum bagging. b) Vacuum bagged specimen before curing in the autoclave.

the vacuum bagged specimen is depicted in 3.6b. Four parts were produced.

The first produced part has blowholes around the edges between cavity and sheet as is depicted in Fig. 3.7a, and unidirectional filaments are added to these edges under the visible ply for subsequent prototypes, see Fig. 3.7b. A finished part with added dimensions is depicted in Fig. 3.8.

The produced part is an exemplar of an antenna cavity built into a large CFRP sheet, such as a car roof, trunk, hood or door. The cavity can also be located at the roof end, where the cavity can be open in one direction. Radiation towards the opening is then increased, because no cavity wall is present. The CFRP chassis antenna cavity prototype is cut open in one direction to allow measurements of this mounting position in Sec. 3.4.4. A vertical cut would not be practical in cars roofs, as the cavity's opening would be adapted to match the roof curvature and the window-roof transition will

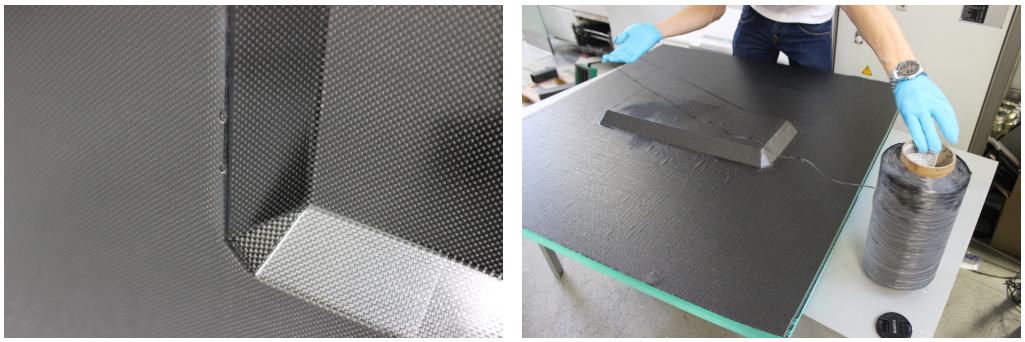

(a) (b)

Figure 3.7: a) Blowholes in the first prototype. b) Unidirectional filaments are added to the edges to counteract blowholes.

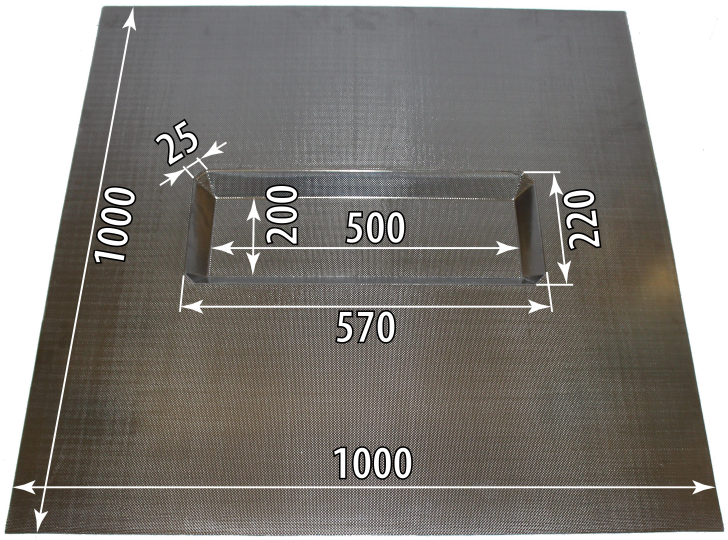

Figure 3.8: Finished part with added dimensions. All dimensions in millimeter. ©2016 IEEE, reprinted with permission from [6].

be designed to fit mechanical requirements. However, measurements with a cavity, which is cut open vertically, are reproducible and not bound to a specific car model. Measurement results of antennas inside a chassis antenna cavity for the roof end are presented and discussed in Sec. 3.4.4.

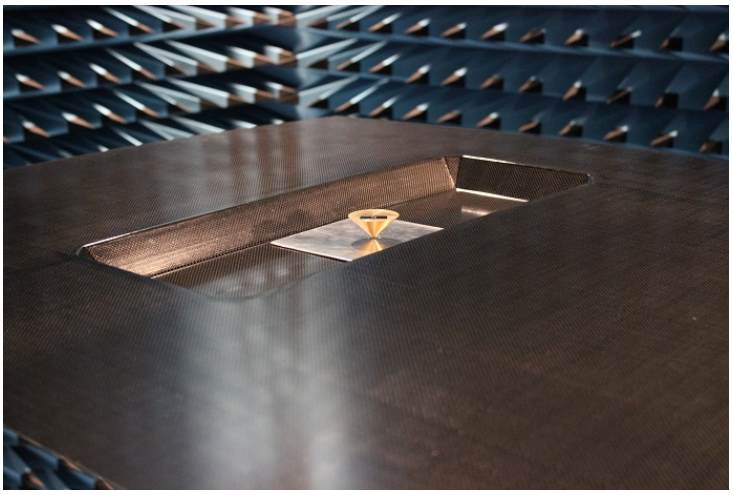

Figure 3.9: A conical monopole antenna inside the chassis antenna cavity.

3.4 Antenna Performance Inside the Chassis Antenna Cavity

3.4.1 Wideband Conical Monopole Antenna

It needs to be verified, whether the chassis antenna cavity is a suitable mounting position for automotive antennas. The proper operation of contemporary antennas intended for the module is tested. In practice it is sufficient to test antenna types, as small deviations in performance can be accounted for in antenna design. Antennas with radiation towards zenith, such as GNSS and SDARS antennas are not investigated. Their proper operation inside a smaller cavity of size $40 \times 40 \times 10\,\mathrm{mm}^3$ is already proven in [193, 194, 202].

A wideband antenna is measured to evaluate the cavity in a wide frequency range. A conical monopole antenna is chosen for this purpose. Monopole antennas are often used when large ground planes are available and are already widely used in automotive applications. Conical monopole antennas are a wideband type of monopole antennas. The cone used in this section are the ones presented in Sec. 2.2.2. The antenna inside the antenna cavity is shown in Fig. 3.9. This section is based on [1].

The measured S-parameters of the conical monopole antenna inside the cavity are depicted in Fig. 3.10. The antenna is measured on a small quadratic aluminum sheet and placed on the same ground plane inside the cavity. As is evident from the measurements the return loss is better than 10 dB for frequencies $> 2\,\mathrm{GHz}$. The cavity has some influence on the S-parameters, but the return loss stays better than 10 dB. Shifts in frequency caused by the

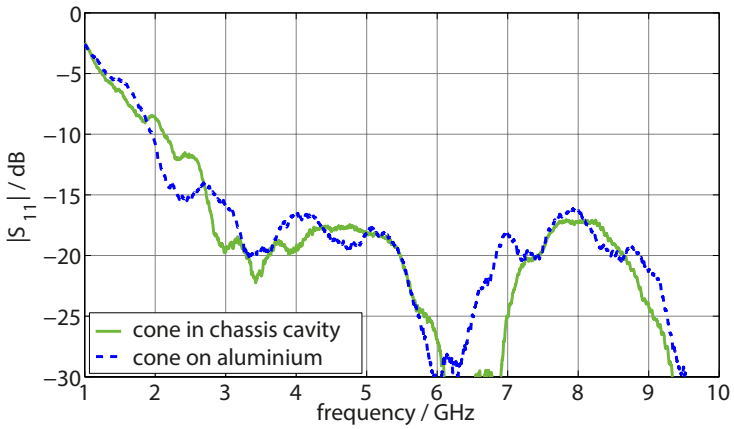

Figure 3.10: Measured S-parameters of the conical monopole antenna inside the CFRP chassis antenna cavity. ©2016 IEEE, reprinted with permission from [1].

cavity are better evaluated with narrowband antennas and will be discussed in Sec. 3.4.2 and Sec. 3.4.3.

The gain patterns are again measured inside the anechoic chamber. Plots are shown for 2 GHz because it the smallest frequency with a good return loss of about 10 dB and the operating frequency of the IFA in Sec. 3.4.2. Results for 5.9 GHz are shown because IEEE 802.11p for V2X operates at this frequency and radiation around the horizontal plane is especially critical for this service. The vertical cuts are depicted in Fig. 3.11. Interference patterns are caused by reflections from the cavity walls and are visible near zenith. This interference causes nulls in the antenna's gain pattern, which impairs proper functionality. The cavity becomes electrically large with increasing frequency and size. More nulls are therefore present at 5.9 GHz than at 2 GHz, and more are present along the long side of the cavity then the short side. The angle of these nulls can be controlled by changing the cavity walls' inclination and a tradeoff is found for V2X antennas at 5.9 GHz. For polar angles $\theta > 60°$ near-omnidirectional radiation is maintained. At lower frequencies (here 2 GHz, but WLAN, etc. are similar) the cavity's influence on the antennas' gain patterns is small, and the typical shape of monopole antenna patterns is kept without any added nulls. This is an astonishing result, considering that the antenna is placed below the surface.

The horizontal cuts of the gain patterns are depicted in Fig. 3.12. Due to the large ground plane size ($1 \times 1\,\mathrm{m}^2$) the pattern is pushed upwards (towards lower polar angles θ), which results in reduced gain in the horizontal plane. This is not an influence of the cavity, but of the presence of a large

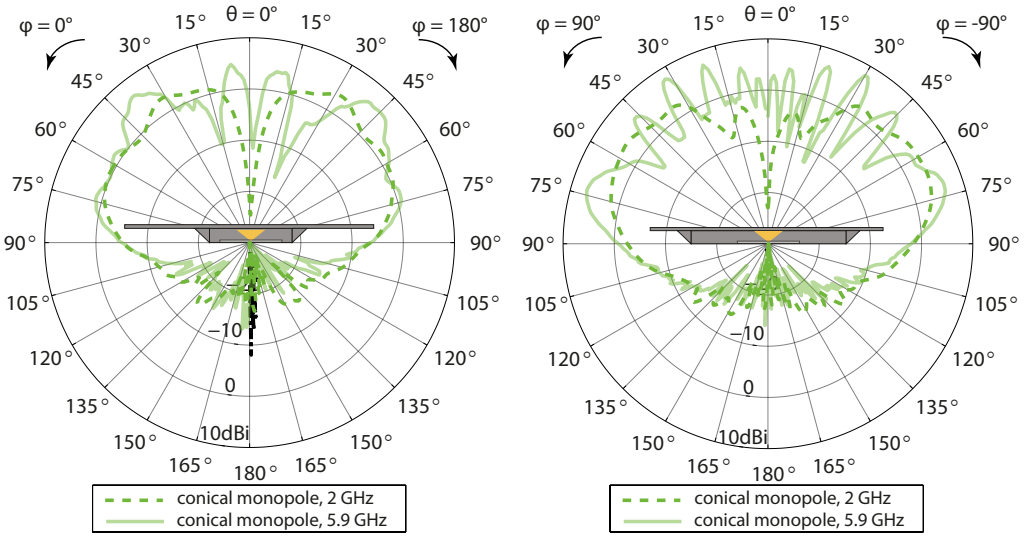

(a) (b)

Figure 3.11: Vertical cuts of the measured gain patterns. The conical monopole antenna is placed in the center of a chassis antenna cavity for measurements. a) cut along the short cavity side, b) cut along the long cavity side. ©2016 IEEE, reprinted with permission from [1].

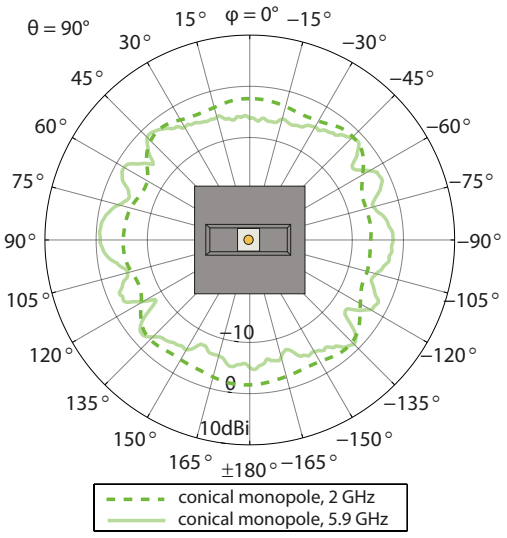

Figure 3.12: Conical monopole antenna inside the chassis antenna module. Horizontal cuts of the measured gain patterns at $\theta = 90°$. ©2016 IEEE, reprinted with permission from [1].

ground plane, such as a car roof. At lower frequencies the influence of the quadratic shape of the ground plane influences the gain pattern in horizontal plane. While the pattern on a circular ground plane would be rotationally symmetric, variations of about 3 dB are clearly visible towards the ground plane corners. The shape of the cavity has some influence at 2 GHz, but it is quite small. With increasing frequency the shape of the cavity starts to significantly influence the gain pattern. About 5 dB ripples appear in the direction of the cavity corners.

Based on these measurements, special care should be taken at higher frequency when designing the cavity's corners. The corners of the produced specimen are designed for easy manufacturing. This does not necessarily have to be changed for mass production. Typically the antenna module will be manufactured as a separate part and inserted into the cavity. The module can then be designed to fit the cavity on the outside and with rounded corners on the inside.

3.4.2 Antennas in Laser Direct Structuring Technology

Three antennas are designed for production with Laser Direct Structuring (LDS) technology and measured as part of this thesis: a dipole antenna, a monopole antenna and an Inverted-F Antenna (IFA). A group photo of the antennas is shown in Fig. 3.13. After a short introduction to Molded Interconnect Devices (MIDs) the antennas are described in this section and measurements of the antenna both in the cavity and on their own are presented and discussed. This section is based on [1, 4, 6, 7, 14].

Laser Direct Structuring (LDS) is a production technology for Molded Interconnect Devices (MIDs). MIDs use injection molded polymers as substrates for electronic circuits. Injection molded MID substrates can assume more complex shapes than PCBs, which are in general planar. While punched and bent sheet metal parts and flexible foils often need to be attached to a structural part, this is not necessary for MIDs. Typically molded plastic parts are already available in the device in the form of spacers, fixtures or covers. In practice this eliminates an additional manufacturing step which is prone to error.

Several production processes for MIDs are currently in use, the most prominent are two-shot molding [211], hot embossing [212] and laser techniques. LDS is a laser technique that uses polymers with an additive [213]. Desired areas are activated by laser. Plating is done in current-less metal baths, where the metal atoms bond with the activated additives. However, MID manufacturing processes are less precise than PCBs, and multilayer designs are not possible. Detailed descriptions of MID materials, the LDS

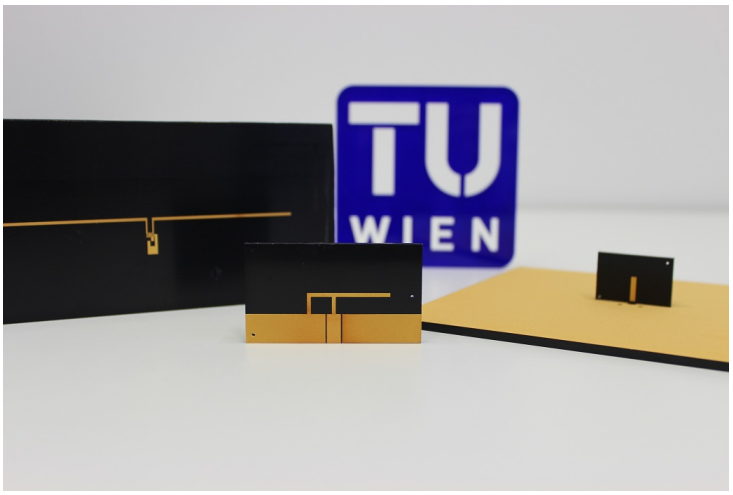

Figure 3.13: Antennas manufactured with LDS, from left to right: dipole antenna, IFA and monopole antenna.

process, quality control and applications are available in [213, 214].

Antenna geometries are usually simple enough to allow manufacturing with LDS. Conformal antennas can be designed in many applications, often on a preexisting plastic housing. Microstrip waveguides can be built as MID [215] and electronic components such as baluns, matching networks, filters, amplifiers and connectors can be soldered to the metalized parts.

A bent LDS patch antenna is presented and measured in [216]. In [217] two logarithmic-periodic antennas are manufactured on a conical substrate. A feeding network is added in [218]. Several applications of LDS antennas are found in mobile phones [219, 220]. An active MID antenna for GPS is designed in [221] and a low noise amplifier is placed on the underside. LDS is also suitable to build dielectric filled rectangular waveguides by plating rectangular polymer parts, antennas can then be designed as dielectric horn antennas [222]. In automotive applications LDS can be used to build conformal antennas directly on the shark-fin plastic part, which usually acts as protective cover for the antennas inside. A design for LTE MIMO communication is measured in [71]. A drive-test measurement of the antenna is described in [100].

A half-wavelength dipole antenna is presented in [7] and is shown in Fig. 3.14. A balun is placed next to the antenna on the MID and for measurements a coaxial connector and strain relief are included. The antenna design, simulation model and measurement results are available in [7]. A typical application of dipole antennas are Ultra High Frequency (UHF) RFID tags, e.g. [223, 224]. Conformal LDS antennas can be plated onto the packaging.

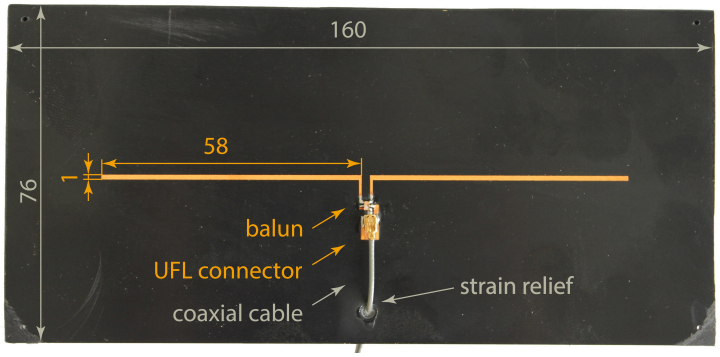

Figure 3.14: Dipole antenna manufactured in LDS technology with balun, connector and strain relief. All dimensions are in millimeter. ©2016 IEEE, reprinted with permission from [7].

A Laser Direct Structured Monopole Antenna

Monopole antennas can also be manufactured with LDS, but more importantly the antenna's ground plane can also be produced with LDS as is described in [4, 14]. [4] presents a quarter-wavelength long monopole antenna for ITS DSRC at 5.9 GHz. The substrate material is XANTAR LDS 3720 from Mitsubishi Engineering. The substrate is activated by laser and plated with 6-8 μm copper, 5-7 μm nickel and 0.1 μm gold. The ground plane has a size of $150 \times 150\,\text{mm}^2$ and the monopole antenna is a $10 \times 2\,\text{mm}^2$ rectangle metalized onto a $30 \times 20 \times 3\,\text{mm}^3$ substrate. The antennas are simulated with HFSS. The simulation model uses material parameters for LDS substrate materials estimated from measurements in [101]. A semi-rigid coaxial cable is soldered to the ground plane. The monopole is soldered to its inner conductor. Dimensions of the LDS monopole antenna on an aluminum ground plane are depicted in Fig. 3.15.

Measurements compare LDS antenna performance on ground planes made from aluminum, CFRP and with LDS. The CFRP ground plane is made from the shred-CFRP, which was investigated in Sec. 2.1.1 and Sec. 2.2.2. The measured S-parameters are depicted in Fig. 3.16. The measured resonance frequency on the LDS ground plane is lower than the simulated as the substrate material's properties from [101] were not available in the design phase. Nevertheless, return loss at 5.9 GHz is better than 6 dB, which is acceptable for automotive applications.

Radiation patterns are measured inside the institute's anechoic chamber. The measured radiation patterns are depicted in Fig. 3.17 and compared to simulations in HFSS. The radiation patterns are very similar on the CFRP, LDS and aluminum ground plane.

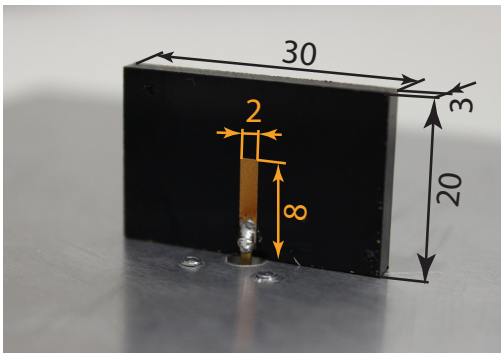

Figure 3.15: Monopole antenna in LDS technology on an aluminum ground plane. All dimensions are in millimeter. ©2016 IEEE, reprinted with permission from [1].

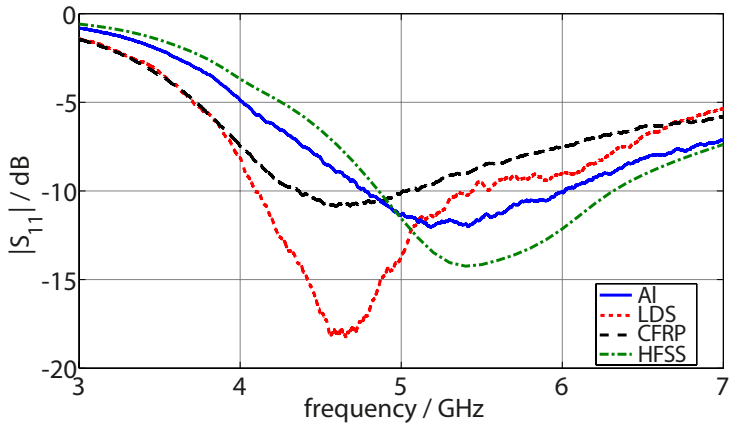

Figure 3.16: S-parameters of a LDS monopole antenna on measured on different ground plane materials and simulated as PEC in HFSS. ©2015 IEEE, reprinted with permission from [4].

Laser Direct Structured Monopole Antenna Inside the Chassis Antenna Cavity

The monopole antenna is measured inside the antenna cavity to quantify the cavity's influence on the antenna's matching and gain pattern. The antenna is again placed on the small $150 \times 150\,\mathrm{mm}^2$ ground plane when measured inside the cavity, as the CFRP sheet is too thin to be threaded, in order to attach a SMA flange. The measured $|S_{11}|$ on the small ground plane and inside the cavity is shown in Fig. 3.18. There is some influence of the antenna cavity on the return loss, but the influence is small and the return loss stays better than 10 dB. The cavity does not cause a shift in resonance frequency.

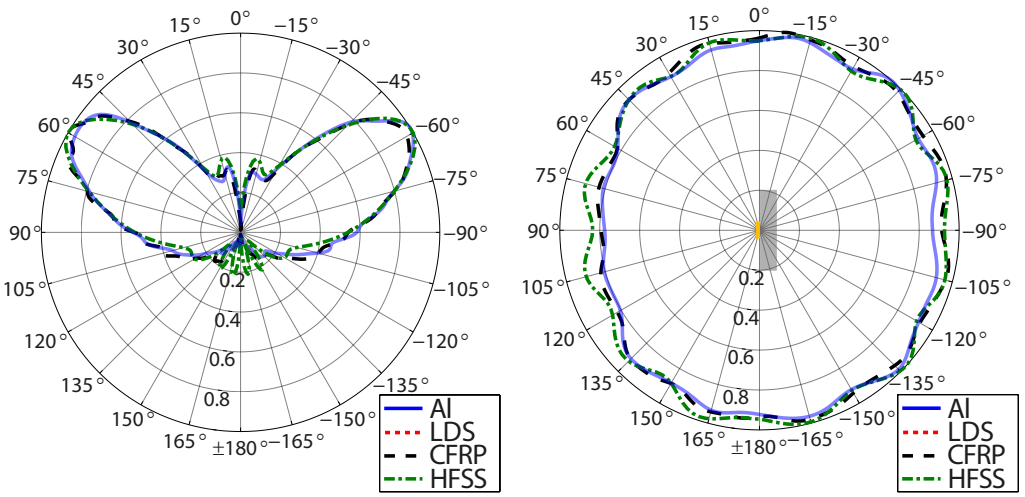

(a) (b)

Figure 3.17: Measured radiation patterns of a LDS monopole antenna on different ground plane materials and simulation in HFSS at 5.9 GHz. a) vertical cut of the radiation pattern at azimuth $\varphi = 0°$, b) horizontal cut of the radiation pattern at polar angle $\theta = 60°$. ©2015 IEEE, reprinted with permission from [4].

However, in the cavity center the influence of the cavity on the return loss is expected to be small. Antenna matching might be influenced, when the antennas are placed too close to the cavity walls and currents couple into the walls.

The vertical cuts of the monopole antenna's gain pattern are depicted din Fig. 3.19. On the small ground plane the pattern is that of a typical monopole antenna on a finite size ground plane. The zero at zenith ($\theta = 0°$) is characteristic for monopole antennas. As the ground plane size is finite, the antenna radiates below the ground plane ($\theta > 90°$) and the pattern's maximum is tilted upwards to $\theta \approx 60°$. When placed inside the antenna cavity located on a large conductive ground plane ($1 \times 1\,\mathrm{m}^2$), several changes happen in the antennas gain pattern. The first evident change is that radiation below the ground plane is significantly reduced. This is a direct consequence of the increase ground plane size. The maximum is now tilted from the theoretical 90° angle on an infinite ground plane to $\theta \approx 75°$. The cavity causes additional zeros in the pattern, as it is already several wavelengths large at 5.9 GHz. The larger the cavity gets in one direction, the more zeros appear in the pattern, as can be easily seen by comparing the cuts along the short and long cavity sides in Fig. 3.19. Radiation towards angles $\theta < 30°$ is no longer

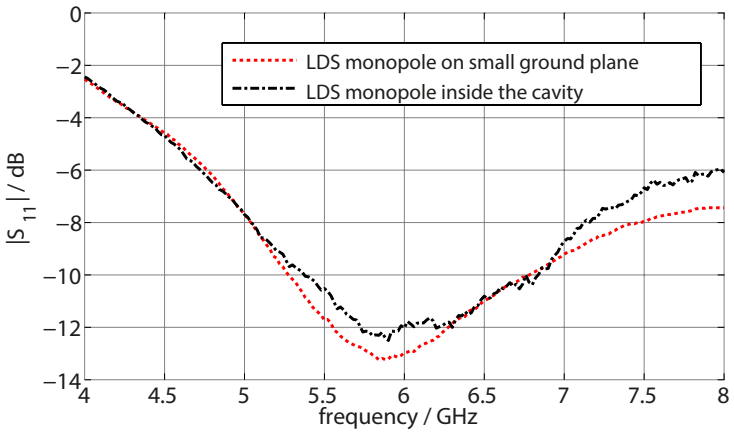

Figure 3.18: Measured S-parameters of the LDS monopole antenna on a small ground plane and inside the antenna cavity. ©2016 IEEE, reprinted with permission from [6].

possible, as fast fading would be present, while the vehicles moves through the close notches in the pattern. However, monopole antennas are not used for radiation towards these angles, as monopole antennas intrinsically have a zero at zenith already. The polar angles around 90° are of importance for monopole antennas used for $V2X$ communication. For monopole antennas used for mobile communication with base stations in cellular systems, polar angles at 90° and below are important, depending on the distance and height of the base station antenna. As the pattern is somewhat smooth for polar angles $45° \leq \theta \leq 90°$, monopole antennas inside chassis antenna cavities are suitable solutions for these services.

Of particular interest is $C2C$ communication, as it is safety relevant and the antennas are placed at similar heights. This means that antenna radiation is important close to $\theta \approx 90°$ and intuitively the cavity walls would block radiation in these directions. This is not the case, as the horizontal gain pattern cut in Fig. 3.20 shows. Gain in the horizontal plane is reduced by 1-4 dB due to the increased ground plane size. The gain pattern is still quite omnidirectional in the horizontal plane, and it is suitable for automotive applications. The cavity does however influence the pattern in the area of the cavity corners. In the direction of the corners the cavity causes about 4 dB large ripples.

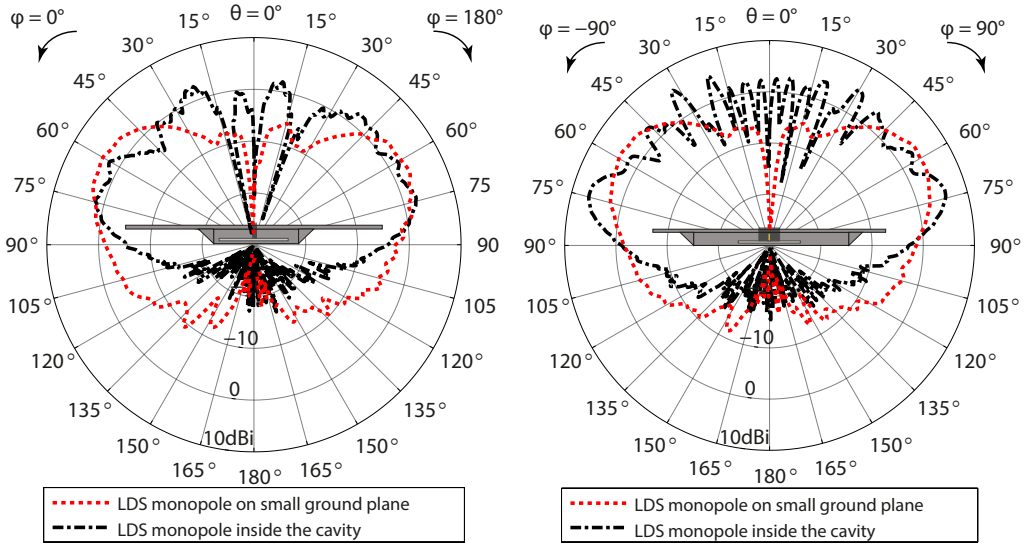

Figure 3.19: Vertical cuts of the measured gain patterns of the 5.9 GHz LDS monopole antenna measured without the cavity on a small ground plane and placed in the center of the chassis antenna cavity. a) cut along the short cavity side for azimuth $\varphi = 0°$ and b) cut along the long cavity side for azimuth $\varphi = 90°$ ©2016 IEEE, reprinted with permission from [6].

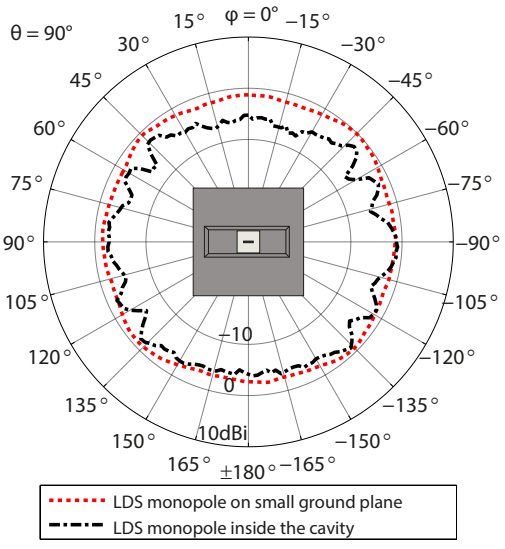

Figure 3.20: Horizontal cut at polar angle $\theta = 90°$ of the measured gain pattern of the 5.9 GHz LDS monopole antenna on a small ground plane and inside the antenna cavity. ©2016 IEEE, reprinted with permission from [6].

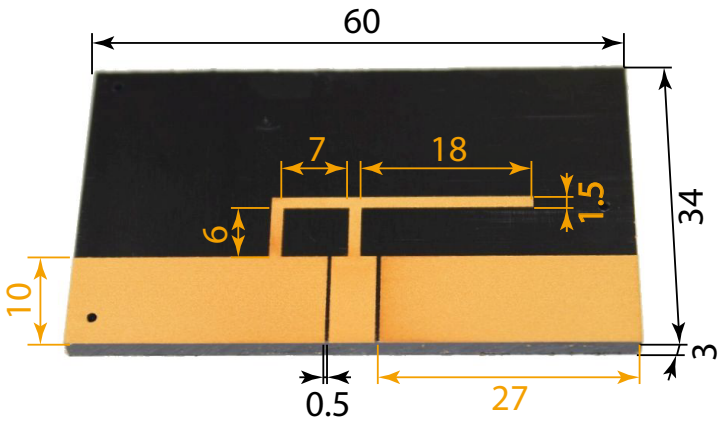

Figure 3.21: IFA in LDS technology. All dimensions are in millimeter. ©2016 IEEE, reprinted with permission from [1].

Laser Direct Structured Inverted-F Antenna

An Inverted-F Antenna (IFA) is designed for LDS and measurements show the feasibility in the vehicular antenna cavity. Fig. 3.21 displays the LDS IFA and its dimensions. The IFA radiates at 2 GHz, to demonstrate the feasibility of antennas inside the cavity for frequencies used in cellular network services. IFAs are widely used in mobile phones.

The LDS IFA is measured inside the chassis antenna cavity. For measurements the antenna is placed in the cavity center. The IFA is measured in the cavity with and without a $150 \times 150\,\mathrm{mm}^2$ aluminum ground plane and in different orientations. The results are omitted here, as the influence of the cavity does not change significantly. For comparison and briefness, the results of the IFA are shown already in comparison with the LDS monopole antenna and the conical monopole antenna.

Measured S-parameters of the LDS antennas and the conical monopole antenna inside the chassis antenna cavity are depicted in Fig. 3.22. The conical monopole antenna is a broadband antenna, while the LDS monopole antenna and the IFA are, by design, narrowband antennas. The return loss of all antennas is better than 10 dB in their designated frequency band.

The vertical cuts of the gain pattern are depicted in Fig. 3.23 and the horizontal cuts in Fig. 3.24. The vertical cuts are typical IFA patterns with only minor influences of the cavity. Like for the conical monopole antenna the influence of the cavity is larger at higher frequencies, where the cavity is large relative to wavelength. In the horizontal cuts at 2 GHz mainly show the quadratic shape of the ground plane.

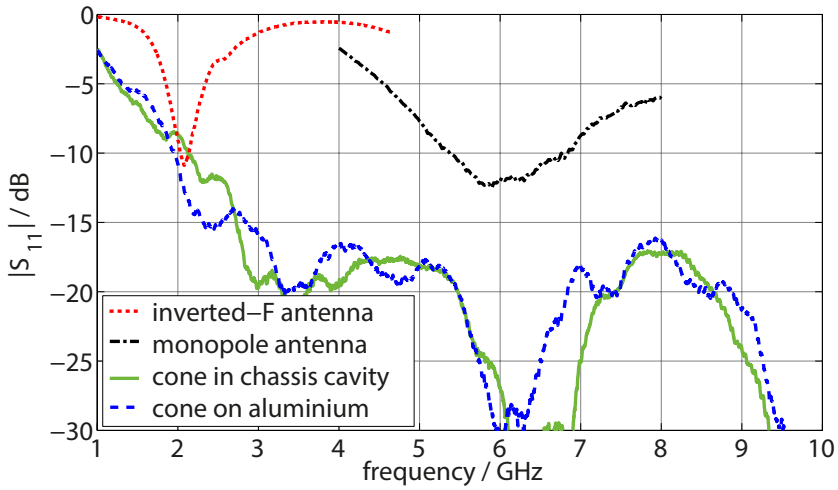

Figure 3.22: Measured S-parameters of the LDS monopole antenna and IFA and the conical monopole antenna inside the CFRP chassis antenna cavity. ©2016 IEEE, reprinted with permission from [1].

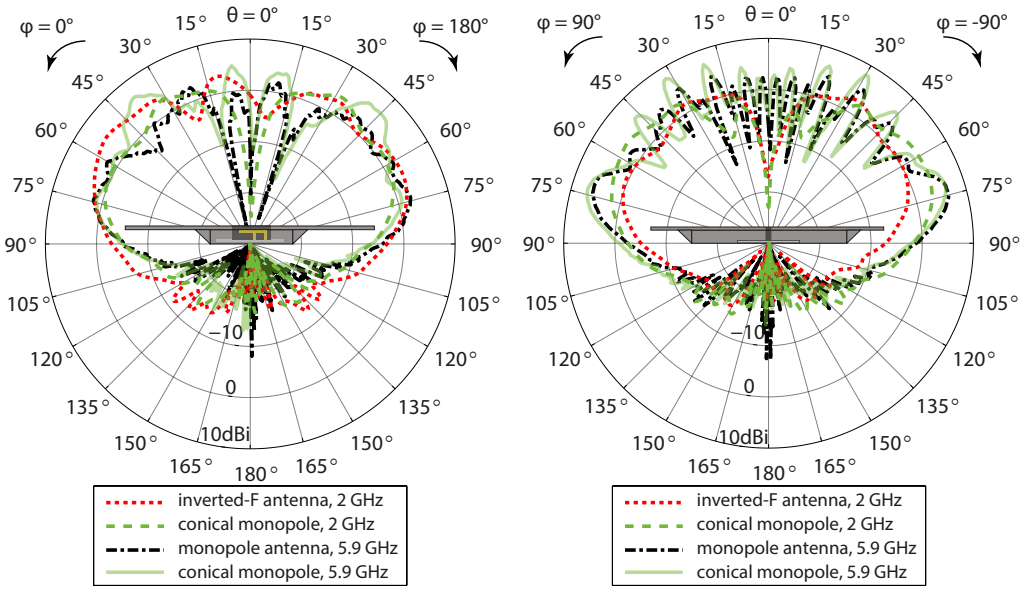

(a) (b)

Figure 3.23: Vertical cuts of the measured gain patterns. The antennas are placed in the center of a chassis antenna cavity for measurements. a) cut along the short cavity side, b) cut along the long cavity side. ©2016 IEEE, reprinted with permission from [1].

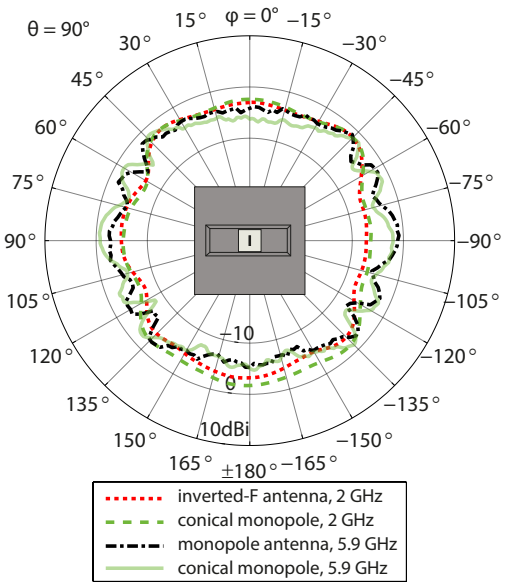

Figure 3.24: Conical monopole antenna, IFA and LDS monopole antenna inside the chassis antenna module. Horizontal cut of the measured gain patterns at $\theta = 90°$. ©2016 IEEE, reprinted with permission from [1].

These measurement results show that antennas in LDS technology are suitable for chassis antenna cavities. Moreover, they show that the standard antenna types IFA and monopole antenna are feasible inside the cavity. The cavity is large enough such that these antennas can be fully contained and concealed within the cavity. Together with patch antennas for GNSS, these are antenna types currently used in roof mounted shark-fin antenna modules. There is substantial know-how in adapting these antenna types for automotive applications and their application can continue inside antenna cavities.

At lower frequencies around 1 GHz the influence of the antenna cavity is small. Radiation in the horizontal plane is not blocked by the cavity walls as could be intuitively assumed. With increasing frequency the cavity becomes larger relative to wavelength and several influences of the cavity on the gain patterns of antennas become evident. The most influential is that several zeros appear close to zenith. At 5.9 GHz several of these zeros are already present up to polar angles of about 30° to 40°. Ripples of about 4 dB appear in the horizontal plane towards the directions of the cavity corners.

3.4.3 Pattern Reconfigurable Antennas

Antennas for advanced beamforming methods such as phased arrays are currently not feasible on vehicles [76]. Pattern reconfigurable antennas have been developed for vehicular communication in the recent years. Pattern reconfigurable antennas offer pattern diversity without the requirement for different physical antennas with these patterns [84]. This saves space on the vehicle and doesn't require the allocation of space for several antennas. MIMO systems are also improved by using pattern reconfigurable antennas instead of antennas with fixed patterns [77].

It should be noted, that switching based on diversity gains other than pattern diversity is possible. In [85] spatial diversity is used by switching between antennas at different positions with Microelectromechanical Systems (MEMS). [225] shows a frequency reconfigurable antenna inside a $240 \times 240 \times 48\,\mathrm{mm}^3$ cavity.

For the application in automotive systems, pattern reconfigurable antennas must satisfy several requirements. The reconfiguration must be done electrically; antennas which are thermally, mechanically or otherwise reconfigurable can typically not be used in automotive applications, e.g. a director made from shape memory allow in [78]. Due to vehicle movement the communication channels change fast and antennas have to be reconfigured quickly. Usually the switching is done with PIN-diodes or MEMS switches. The antennas must operate in a wide temperature range and the production cost must be competitive. Therefore, typical vehicular reconfigurable antennas are built as PCB on FR4, which also allows the attachment of switches, capacitors and chokes.

Usually automotive antennas are either switched between four radiation patterns (left, right, front or back) or two radiation patterns (left/right or front/back). A Yagi-Uda antenna reconfigurable into four directions for a bus roof is measured in [226]. A 2.6 GHz LTE antenna, which can be reconfigured between a left, right, front or back radiation pattern is presented in [79]. In [227] four vertical elements are placed around a monopole antenna, and the electrical length of the elements is adjusted with PIN-diodes to act as director or reflector and therefore form a Yagi-Uda antenna in four directions.

An antenna for 2.6 GHz LTE is presented in [80], the antenna consists of four monopoles separated by reflectors. It can be reconfigured between a left/right and a front/back radiation pattern, which are obtained from a pattern synthesis process. The switching is done with PIN-diodes. In [81] the phase between two bent monopole antennas is switched with a tapered line balun. In [82] two monopole antennas are used, the second monopole is connected via $3/4\,\lambda$ long lines on top and bottom. The second monopole is

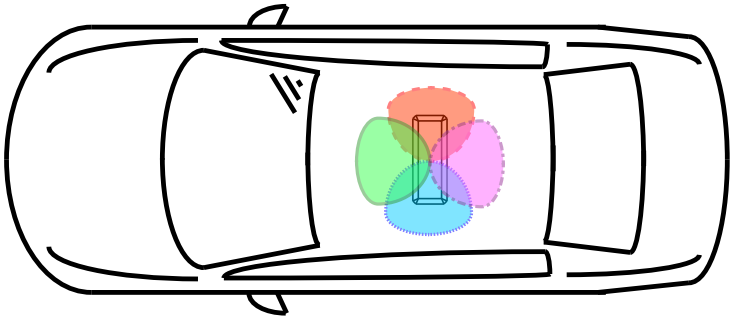

Figure 3.25: Exemplary mounting location of the chassis antenna cavity in the center of the car roof with a pattern reconfigurable antenna oriented such that it can radiate towards the left, right, front or back of the vehicle. ©2017 IEEE, reprinted with permission from [8].

fed either on its top or bottom, which is selected with MEMS. The phase difference between two IFAs spaced by $\lambda/2$ [83] is switched with PIN-diodes on a back-to-back balun.

The measurements of pattern reconfigurable antennas inside the chassis antenna module are the result of a collaboration with Jerzy Kowalewksi from the Institut für Hochfrequenztechnik und Elektronik, Karlsruhe Institute of Technology (KIT). Measurements in this section are performed inside the anechoic chamber at KIT. This section is based on work by J. Kowalewski et al. [79] and on [8].

Antenna Reconfigurable Between Radiation Towards Four Directions Inside the Chassis Antenna Cavity

An automotive antenna reconfigurable between radiation patterns in front, back, left or right direction is presented in [79]. It is investigated if this antenna operates properly, when embedded inside a chassis antenna cavity and measurements are performed to quantize the influence of the antenna cavity on pattern reconfigurable antennas. Measurements in previous sections proved the proper functionality of antennas with unidirectional radiation patterns inside the chassis antenna module. The operation of directional antennas inside the cavity might be impaired, i.e. from reflections from the cavity walls. As an example the antenna could be placed inside a chassis antenna cavity in the vehicle roof oriented such that it radiates toward the left, right, front or back of the vehicle, as is depicted in Fig. 3.25. This configuration provides improved gain over omnidirectional antennas, when communicating with one other vehicle and the decreased gain towards the other directions decreases interference.

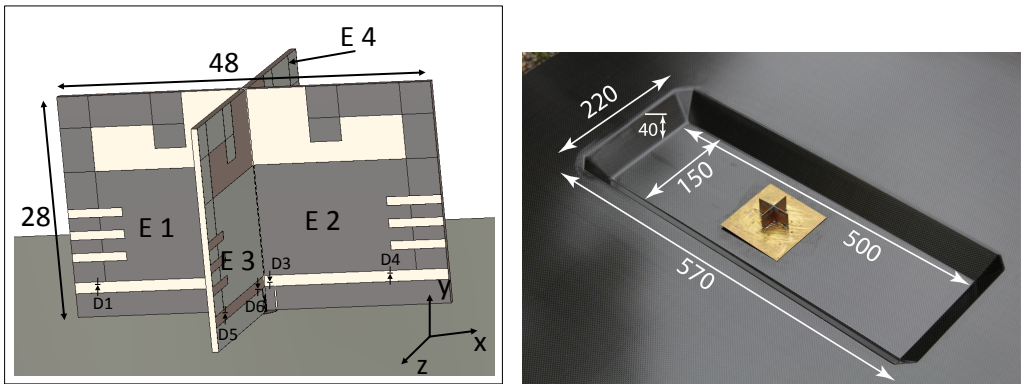

(a) (b)

Figure 3.26: a) Schematic of the pattern reconfigurable antenna with four directions. b) Pattern reconfigurable antenna placed inside the chassis antenna cavity. ©2017 IEEE, reprinted with permission from [8].

A schematic of the antenna is depicted in Fig. 3.26a. On top the antenna has four monopole elements which are bent to reduce antenna height. The elements are connected via pin diodes to either the inner conductor of a coaxial connector or to the ground plane. If the antenna is configured for radiation towards the right, then the monopole element on the right (E 2) is configured as a radiator by activating diode D3. The element on the opposite side (E 1) is configured as a reflector by connecting it to ground with diode D1. The remaining two elements are also grounded. Radiation towards the other directions is configured accordingly. The antenna elements are built in PCB technology and are printed on FR4. Two PCBs are stuck together perpendicular. Fig. 3.26b shows the antenna prototype inside the chassis antenna cavity.

Measured return loss is better than 15 dB; the frequency dependency is omitted here, but published in [8]. The measured vertical cuts of the gain patterns are depicted in Fig. 3.27. As the antenna is symmetric, only two patterns are depicted, the pattern towards the front and the pattern towards the right. Generally the pattern along the short side of the cavity is influenced more than the pattern towards the long cavity side. In the desired front direction, the gain from $20° \leq \theta \leq 85°$ the antenna gain varies around 0 dBi, at $\theta = 90°$ it is about -5 dBi (Fig. 3.27a). The antenna radiates a significant amount of power towards the back, when the front state is selected. Gain towards the back, when front is selected, is around 0 dBi between $40° \leq \theta \leq 75°$. When the right state is selected, radiation towards the front is about 10 dB lower than with a selected front state (also Fig. 3.27a).

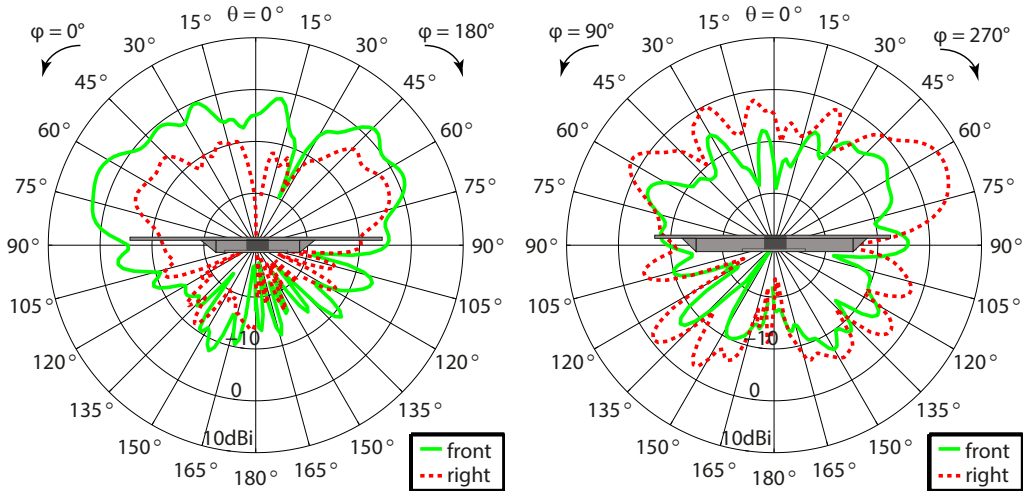

Figure 3.27: Vertical gain pattern cuts of the pattern reconfigurable antenna at 2.6 GHz and a) $\varphi = 0°$ and b) $\varphi = 90°$. ©2017 IEEE, reprinted with permission from [8].

The cut along the long cavity side in Fig. 3.27b shows that the beam towards the right (when right is selected) has more gain than the front state, but that it is also confined to a narrower angle. Towards the right a maximum gain of 6.5 dBi is achieved. The radiation towards the left, with right selected, is generally better in direction of the long cavity side, than it is for the cut along the short cavity side. The difference between right state and front state is about 10 dB in Fig. 3.27b. It must also be noted, that the measurements show very large back lobes. This hints that a hole in the ground plane for coaxial cables and pin-diode voltage supply was not properly covered.

Several differences are noticeable, when comparing the results in the cavity to the patterns measured on a small ground plane in [79]. The first difference is again that the pattern is tilted upwards due to the larger ground plane. The pattern is smoother in a wider vertical angle in [79] and gain is a bit higher in that region (about 3 dBi vs 0 dBi). Towards the short cavity side, the difference between radiation in (desired) front direction and (undesired) back direction is a slightly worse. Towards the long cavity side, the gain of the right direction pattern is increased, but confined to a narrower angle. Overall the pattern reconfigurable antenna works inside the chassis antenna cavity, but there are influences from the cavity on the gain patterns which need to be addressed in antenna design.

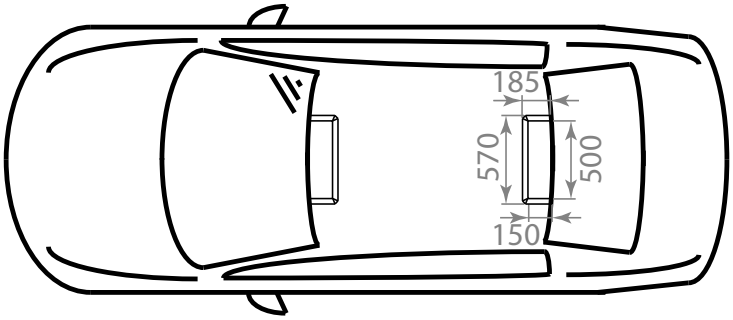

Figure 3.28: Sketch of two chassis antenna cavities located on both roof ends of a car.

3.4.4 Chassis Antenna Cavities for the Roof Edge

A variant of the chassis antenna cavity is investigated. Antenna cavities can not only be located in the center of large conductive sheets, as was investigated previously, they can also be placed at the edge. In automotive applications this is the case at the roof edges, prominently above the windshield or rear window, but edges of large ground planes are also available with the engine hood (bonnet) or the trunk lid. A sketch depicting two chassis antenna cavities located at both ends of a car roof is shown in Fig. 3.28. Several patents propose the usage of antenna cavities at these positions, but to the best of my knowledge, the first prototype of this antenna mounting position and the first scientific investigation with measurements is published in [10]. There the LDS monopole antenna is compared between mounting positions: on a small ground plane, in a chassis antenna cavity and in a prototype of the cavity modified for edges. This section is based on [10].

As explained throughout this dissertation, a major problem for C2C antennas is, that transmit and receive antenna are placed at roughly the same height. But due to the large metal ground plane, patterns of antennas placed on the roof are tilted upwards. Other mounting positions such as bumpers, spoilers or side mirrors offer good radiation towards one direction, but are completely shadowed in the opposite direction by the vehicle. Antenna cavities located at the front and/or rear end of the car roof can substantially improve radiation towards these directions, while maintaining the radiation patterns achieved from a standard chassis antenna cavity towards the other directions, as will be shown in this section.

Similar antenna modules are described in several patents. [228] suggests to use border, edge and corner areas in the vehicle chassis to form hollow areas for the reception of antennas for various applications. As preferred areas it lists the windows, roof edges, spoilers and C-holms. Nagy describes

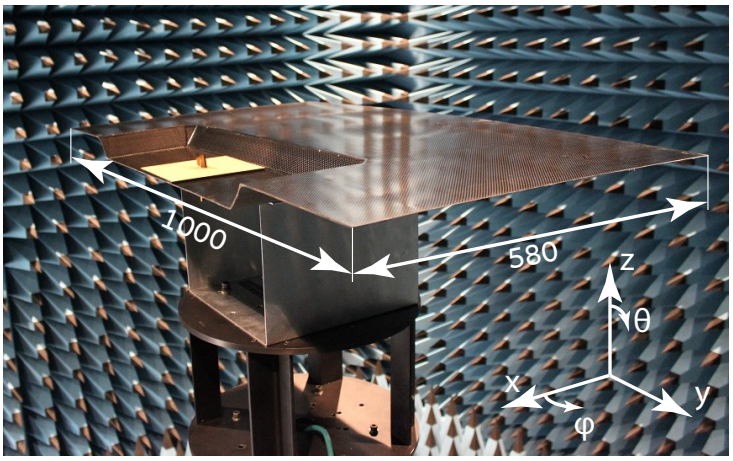

Figure 3.29: LDS monopole antenna for 5.9 GHz inside a CFRP chassis antenna cavity modified for the roof edge. ©2017 IEEE, reprinted with permission from [10].

a roof antenna shelf positioned below an extension of the windshield or rear window [229]. An overhead console located between windshield and roof is proposed in [230]. The overhead console contains antennas and is covered by a resin roof portion. An antenna location similar to [230] is proposed in [231], where an antenna volume is proposed for convertibles, which is located in the roof frame support above the windshield. [232] describes a "Transmission and/or reception unit arrangement for use at e.g. roof frame part of motorvehicle, has transmission and/or reception device arranged in hollow space, which is defined by body component or external component and cladding part" (Englisch title).

A chassis antenna cavity prototype for the edge of a ground plane is depicted in Fig. 3.29. The prototype is a modified version of the regular CFRP chassis antenna cavity, which is cut open along the long side of the cavity. The cavity is therefore open in one direction, as would be the case on the edge of a ground plane. In a commercial application this cavity might be placed in the roof directly above the windshield. The opening of the cavity would then of course not be vertical, but adapted to the roof curvature. Window glass would be present below the cavity opening and a suitable mechanical window-roof transition would be designed to close gaps. Such vehicle specific details are not included, to obtain a more general description.

Gain patterns are measured inside the institute's anechoic chamber. An important conclusion is found, when comparing the results obtained for the regular antenna cavity, the edge antenna cavity and the small ground plane (with size exactly as the width of the cavity). Towards the opening the

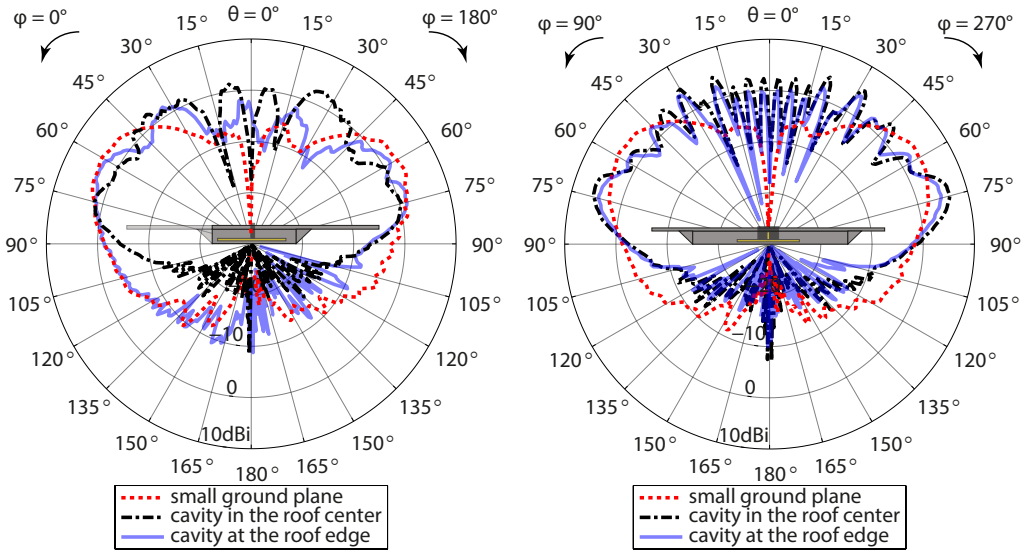

Figure 3.30: Measured gain patterns a 5.9 GHz LDS monopole antenna on small ground plane, inside a chassis antenna cavity and inside a chassis antenna cavity for the roof edge. Vertical cuts for a) $\varphi = 0°$ and b) $\varphi = 90°$. ©2017 IEEE, reprinted with permission from [10].

pattern of the antenna is that of the antenna placed on the small ground plane, as is evident from Fig. 3.30a towards $\varphi = 0°$. Towards the other directions, the gain pattern of the antenna inside the edge cavity is that of the antenna placed inside a regular cavity (Fig. 3.30a and Fig. 3.30b). This also holds true for the horizontal cuts of the gain pattern in Fig. 3.31.

When placed on the edge of a large ground plane, the cavity for the roof edge acts like a small ground plane in the direction of the opening, and like a regular chassis antenna cavity in the other directions. This means, that radiation in one direction can be improved by placing the cavity on one (or both) edges of the car roof. This finding motivates the development of a smart car roof for MIMO antenna applications. Antenna cavities placed at several locations, e.g. at the front roof edge, the center and the rear roof edge; provide spatial diversity and offer enough space for future automotive antenna requirements. Cable losses can be reduced by placing communication hardware and other electronics under the car roof, where they are close to the antenna modules.

The antenna cavities investigated here can be completely concealed and therefore do not influence the aesthetic design of consumer cars. The antenna

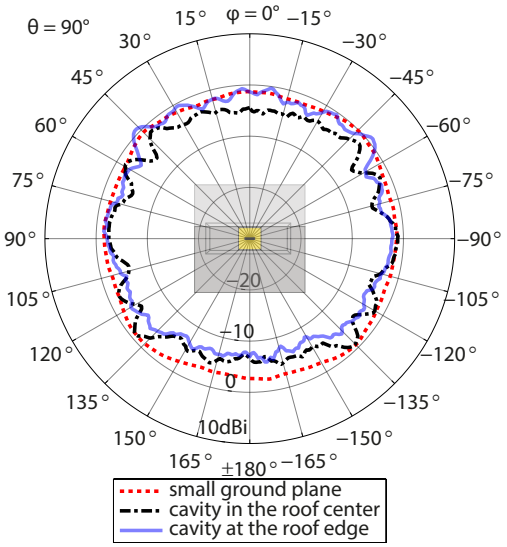

Figure 3.31: Horizontal cuts of the measured gain patterns of a 5.9 GHz LDS monopole antenna on small ground plane, inside a chassis antenna cavity and inside a chassis antenna cavity for the roof edge. ©2017 IEEE, reprinted with permission from [10].

cavity concept forms the technical basis for the communicative vehicle, which exchanges information with vehicles, pedestrians and buildings around it, while being connected to sensor networks and the internet. Antenna diversity, spatial diversity, pattern diversity, frequency diversity and smart antenna systems are enabled by reserving more space for antennas on vehicles. The design and development of vehicular antennas is thus freed from the burden of additional mechanical, aerodynamic, and aesthetic requirements. Engineers finally focus on the optimization of vehicular connectivity.

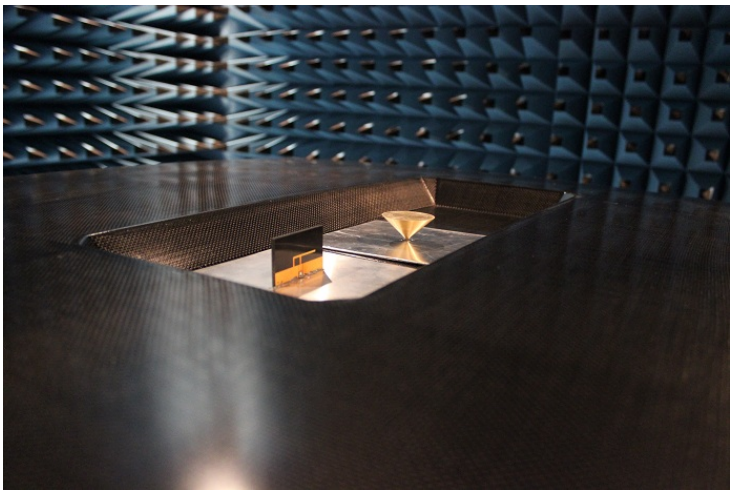

Figure 3.32: Conical monopole antenna and IFA inside the chassis antenna cavity. ©2017 IEEE, reprinted with permission from [12].

3.4.5 Multiple Antennas Inside the Cavity

Measurements of multiple antennas inside a chassis antenna cavity are published in [12] and this section is based on this work.

Measurements are conducted to quantify the influences of multiple antennas inside the chassis cavity on each other. Antennas can be separated farther inside the cavity, as it is larger than current shark-fin antenna modules. The size of the cavity also allows the inclusion of decoupling slots and fences. On the other hand reflections from the walls might negatively influence antenna coupling. Additionally, the antennas are always placed in the cavity center in previous sections and the radiation characteristics of off-center antennas is expected to change. The LDS IFA and the conical monopole antenna are measured inside the cavity simultaneously, with the cone placed in the center and the IFA placed off-center. The setup is shown in Fig. 3.32.

Measurement results are shown in Fig. 3.33. The vertical cut along the short cavity side is omitted, as only minor changes in pattern are found [12]. The vertical cut along the long cavity side (Fig. 3.33a) shows only small changes in the conical monopole antenna's gain pattern towards low polar angles θ. This observation holds for the horizontal cuts in Fig. 3.33b. The data suggests that the influence of multiple antennas on each other gain pattern is small, if the antennas are reasonably spaced. The off-center position of the IFA has a much larger influence on the IFA's gain pattern.

Results for 5.9 GHz are available in [12]. The number of possible antenna configurations are limited during the prototyping stage, as each antenna is

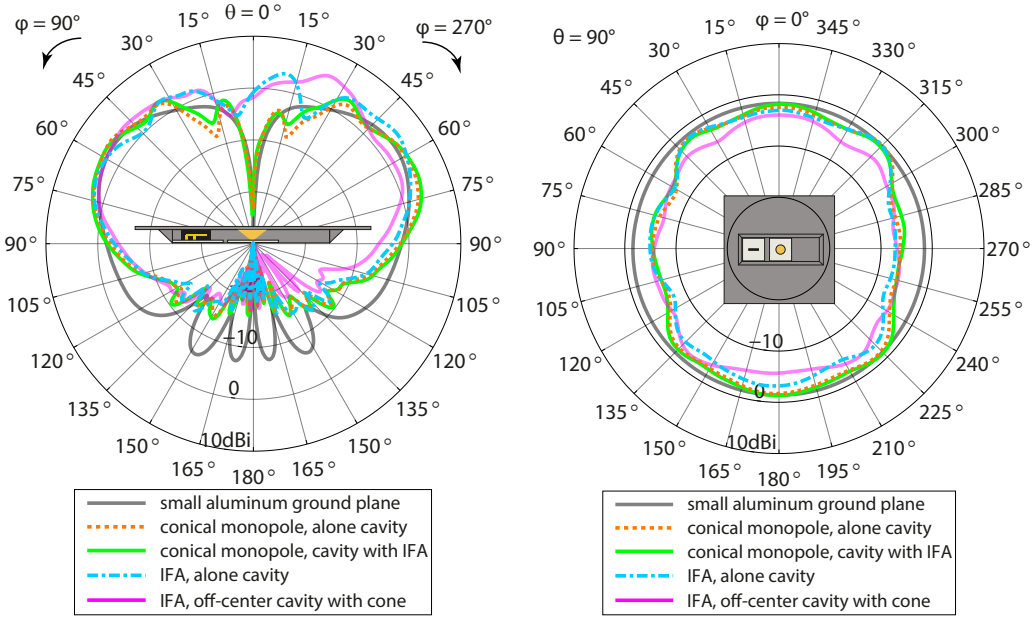

Figure 3.33: Measured gain patterns at 2 GHz of conical monopole antenna in cavity center and IFA placed off-center: a) vertical cut, b) horizontal cut. ©2017 IEEE, reprinted with permission from [12].

connected to measurement equipment through a hole in the cavity floor. Exchangeable cavity bases are developed and described in the next section, which will allow the measurement of position sweeps and more sophisticated antenna arrangements inside the cavity.

3.4.6 Exchangeable Cavity Bases

Exchangeable cavity bases are developed, manufactured and verified by measurement. Results are published in [11] and this subsection is based on this work.

In previous investigations the antennas have to be placed on a separate metal ground plane, which is subsequently placed inside the cavity. This is necessary, as the CFRP sheet of the cavity prototype is too thin to be threaded. SMA flanges, which connect the antennas with the coaxial feeding cables, can therefore not be directly mounted to the cavity. To avoid this problem, the coaxial cables are attached to separate metal ground planes in previous chapters and the coaxial cables are routed to the anechoic chamber's equipment via holes cut into the cavity floor. While this solution is found useful for single antenna measurements due to its simplicity, measurements of multiple-antenna systems inside the cavity require a more sophisticated solution, as uncovered holes in the cavity floor influence measurement results. The method also limits the experimental verification of antenna position sweeps obtained from simulations.

Most antennas used in vehicular applications require a connection to a ground plane. A hole needs to be cut, such that cables can be connected to the antennas inside the cavity. In case the antenna is mounted on the cavity's floor or walls, additional holes are required to connect flanges. The production of a whole cavity prototype with a large surrounding ground plane is expensive. Therefore, it is not feasible during development to build a new cavity prototype for every antenna or when measuring an antenna on different positions. The most common solution is to cut out some area and insert exchangeable modules. An example are shark-fin antenna modules, where the antennas are combined on a common metal base, which is then inserted into a cutout in the car roof. For mass production this is optional. While the whole cavity floor can still be removed, it is also feasible to place the antenna module inside the chassis cavity and route the cables through the cavity walls.

For sheets made from CFRP an additional problem arises: The conductive fibers are embedded inside the insulating matrix. A preferable way to mount exchangeable ground planes would be to design them as inlays, but tightly fitting the two material with different temperature expansion coefficients is hard and the materials might not be connected stable enough to withstand vibration during drive tests or tilting during measurements. Therefore, it is proposed to place the exchangeable ground plane on the chassis antenna floor and contact the fibers inside the CFRP to the aluminum antenna base via screws. Fig. 3.34a shows the CFRP cavity prototype with cutout floor and

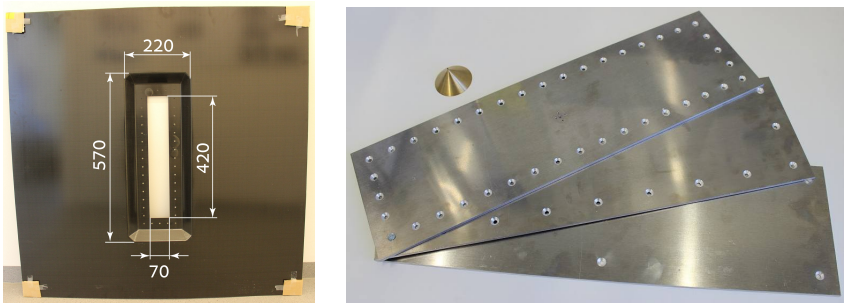

(a) (b)

Figure 3.34: a) Cut-out and holes in a CFRP chassis antenna cavity, ©2017 IEEE, reprinted with permission from [12]. b) Exchangeable aluminum cavity bases with different number of holes together with a conical monopole antenna. ©2016 IEEE, reprinted with permission from [11].

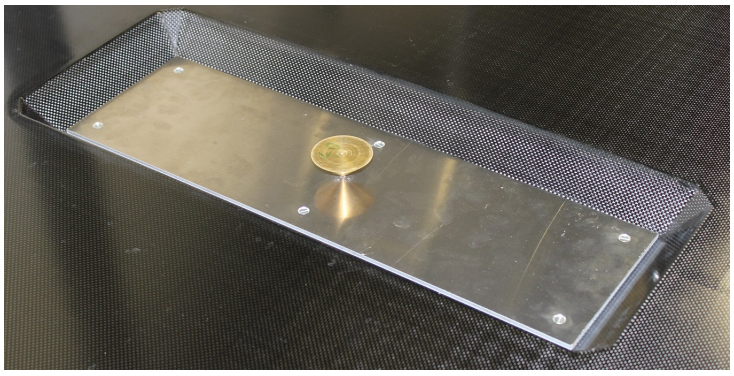

Figure 3.35: Conical monopole antenna mounted on an exchangeable cavity base. ©2017 IEEE, reprinted with permission from [11].

holes. Fig. 3.34b shows exchangeable aluminum bases with different number of holes together with a conical monopole antenna.

As a rule of thumb vias are spaced about $\lambda/10$ in high frequency engineering when connecting ground planes. While vias can be closely spaced on small PCBs, it is not feasible to maintain such tightly placed vias for the chassis cavity at frequencies approaching 10 GHz. Evaluation by measurement is therefore required to assure proper operation of the exchangeable cavity bases. Measurement results show, that the exchangeable cavity base concept is feasible [11]. Measured patterns up to 5.9 GHz coincide with patterns where the antenna is placed on a separate ground plane (compare Sec. 3.4.1), providing that a sufficient number of screws connect the exchangeable base with the cavity.

Chapter 4

Conclusion

In this dissertation I investigate the possibility of concealing whole antenna modules inside chassis. I develop a chassis antenna cavity based on simulations. I prove the feasibility of the antenna cavity by building a prototype. I evaluate the concept by performing extensive measurements of widely used antenna designs. I simulate, measure and evaluate a dipole antenna, a monopole antenna and an Inverted-F Antenna (IFA) in Laser Direct Structuring (LDS) technology. LDS is a process to manufacture Molded Interconnect Device (MID) and is considered as replacement for automotive antennas on Printed Circuit Boards (PCBs). The antennas investigated for the cavity include cellular networks, Vehicle-to-Any (V2X) communication, wideband operation, pattern reconfigurability, and multiple antenna systems. I prototype and measure a variant of the cavity for the roof edge that provides better coverage at low elevation angles. In Chapter. 2.1 I estimate the material properties of CFRP, evaluate CFRP as ground plane material for narrowband and wideband antennas and measure a contemporary automotive antenna module on a CFRP car roof. Simulation results show good agreement with measurements, even when the CFRP is modeled as isotropic conductor or even as Perfect Electric Conductor (PEC).

- Angle-dependent measurements of shredded and woven CFRP in Chapter 2.2 show, that they are quasi-isotropic conductors in the single-digit gigahertz range. Further measurements of these CFRP as antenna ground plane show that their influence on antenna performance is negligible in vehicular applications. These findings are in direct contrast to previously published literature, which investigates CFRP with unidirectional fiber alignment that have anisotropic conductivity and a strong influence on antennas. CFRP can therefore be used as ground plane for vehicular antennas without the requirement for metallization.

- Materials with recycled carbon fibers show great radio frequency performance compared to other CFRP. CFRP consisting of shredded fibers have more isotropic conductivity than both unidirectional and woven CFRP. Shred-CFRP also behaves as an isotropic antenna ground plane. The efficiency on the investigated material was reduced by 10 % but overall shred-CFRP is a good antenna ground plane material.

- Construction of vehicular antenna cavities from CFRP is proven to be possible and feasible by building a prototype (see Sec. 3.3.1). Viability to operate antennas inside the cavity is demonstrated with measurement based evaluations of standard antenna types inside the cavity.

- The antenna cavity frees automotive antenna development of aesthetic limitations imposed by designers, and it doesn't influence a vehicle's drag coefficient. This allows to allocate more space for vehicular antennas. The increased number of vehicular antennas increases the diversity of the system and in turn increases throughput and/or reliability of vehicular communication. The chassis antenna cavity enables intelligent transport systems, the vehicular Internet of Things (IoT), automatic and cooperative driving, automotive Multiple-Input and Multiple-Output (MIMO) communication and smart antenna systems.

- The cavity has significant influence on the performance of antennas. Both the cavity and the CFRP influence the return losses of antennas, although the influence is small for practical purposes. The cavity causes large changes in antennas gain patterns. For monopole antennas additional zeros appear close to zenith. The number of zeros increases with frequency, as the cavity becomes electrically large. Measurement results in Sec. 3.4 show, that the cavity introduces additional zeros in the gain patterns of monopole antennas at 5.9 GHz. In the horizontal plane ripples of a about 4 dB appear in the gain patterns towards the cavities corners. Measurement of an IFA and a conical monopole antenna for 2 GHz show that these influences are smaller at low frequencies. There no additional zeros appear in the gain patterns close to zenith.

- Automotive antenna development does not need to adapt for the cavity. Monopole antennas and IFAs work well inside the cavity. These are well-understood antenna types that are widely used by vehicular antenna designers.

Appendix A

Literature Research of the Austrian Patent Office

Recherchenbericht zu **RG 50004/2016**

österreichisches patentamt

Klassifikation des Anmeldungsgegenstands gemäß IPC:
B60R 11/02 (2006.01)

Klassifikation des Anmeldungsgegenstands gemäß CPC:
B60R 11/02 (2013.01); *B60R 2011/0028* (2013.01)

Recherchierter Prüfstoff (Klassifikation):
B60R

Konsultierte Online-Datenbank:
WPI; EPODOC; TXTnn

Dieser Recherchenbericht wurde zu den am **31.03.2016** eingereichten Ansprüchen **-** erstellt.

Kategorie*)	Bezeichnung der Veröffentlichung: Ländercode, Veröffentlichungsnummer, Dokumentart (Anmelder), Veröffentlichungsdatum, Textstelle oder Figur soweit erforderlich	Betreffend Anspruch
A	EP 1921708 A1 (KOJIMA PRESS KOGYO KK) 14. Mai 2008 (14.05.2008) gesamtes Dokument	
A	US 6118410 A (NAGY) 12. September 2000 (12.09.2000) gesamtes Dokument	
A	EP 2860820 A1 (VOLVO CAR CORP) 15. April 2015 (15.04.2015) gesamtes Dokument	
A	JP 2012232679 A (KOJIMA PRESS KOGYO KK) 29. November 2012 (29.11.2012) Figuren, Zusammenfassung	
A	DE 102011106829 A1 (DAIMLER AG) 08. März 2012 (08.03.2012) gesamtes Dokument	
A	DE 102009036727 A1 (DAIMLER AG) 25. März 2010 (25.03.2010) gesamtes Dokument	
A	DE 20002426 U1 (SERCO GMBH & CO KG) 13. April 2000 (13.04.2000) gesamtes Dokument	
A	DE 4403643 A1 (KOLBE & CO HANS) 10. August 1995 (10.08.1995) gesamtes Dokument	

Datum der Beendigung der Recherche:	Seite 1 von 1	Prüfer(in):
17.05.2016		WAGNER Sascha

*) **Kategorien** der angeführten Dokumente:

X Veröffentlichung **von besonderer Bedeutung**: der Anmeldungsgegenstand kann allein aufgrund dieser Druckschrift nicht als neu bzw. auf erfinderischer Tätigkeit beruhend betrachtet werden.

Y Veröffentlichung **von Bedeutung**: der Anmeldungsgegenstand kann nicht als auf erfinderischer Tätigkeit beruhend betrachtet werden, wenn die Veröffentlichung mit einer oder mehreren weiteren Veröffentlichungen dieser Kategorie in Verbindung gebracht wird und diese **Verbindung für einen Fachmann naheliegend** ist.

A Veröffentlichung, die den allgemeinen **Stand der Technik** definiert.

P Dokument, das von **Bedeutung** ist (Kategorien **X** oder **Y**), jedoch **nach dem Prioritätstag** der Anmeldung veröffentlicht wurde.

E Dokument, das **von besonderer Bedeutung** ist (Kategorie **X**), aus dem ein „**älteres Recht**“ hervorgehen könnte (früheres Anmeldedatum, jedoch nachveröffentlicht, Schutz ist in Österreich möglich, würde Neuheit in Frage stellen).

& Veröffentlichung, die Mitglied der selben **Patentfamilie** ist.

Bibliography

[1] G. Artner, R. Langwieser, and C. F. Mecklenbräuker, "Concealed CFRP Vehicle Chassis Antenna Cavity", *IEEE Antennas and Wireless Propagation Letters*, vol. 16, no. 1, pp. 1415–1418, 2017. DOI: 10.1109/LAWP.2016.2637560.

[2] G. Artner, P. K. Gentner, J. Nicolics, and C. F. Mecklenbräuker, "Carbon Fiber Reinforced Polymer With Shredded Fibers: Quasi-Isotropic Material Properties and Antenna Performance", *International Journal of Antennas and Propagation*, vol. 2017, no. Article ID 6152651, 2017. DOI: 10.1155/2017/6152651.

[3] G. Artner, R. Langwieser, G. Lasser, and C. F. Mecklenbräuker, "Effect of Carbon-Fiber Composites as Ground Plane Material on Antenna Performance", in *IEEE-APS Topical Conference on Antennas and Propagation in Wireless Communications (APWC)*, Palm Beach, Aruba, 2014, pp. 711–714. DOI: 10.1109/APWC.2014.6905580.

[4] G. Artner, R. Langwieser, and C. F. Mecklenbräuker, "Material Induced Changes of Antenna Performance in Vehicular Applications", in *IEEE International Conference on Microwaves, Communications, Antennas and Electronic Systems (COMCAS)*, Tel Aviv, Israel, 2015. DOI: 10.1109/COMCAS.2015.7360442.

[5] G. Artner and R. Langwieser, "Performance of an Automotive Antenna Module on a Carbon-Fiber Composite Car Roof', in *10th European Conference on Antennas and Propagation (EuCAP)*, Davos, Switzerland, 2016. DOI: 10.1109/EuCAP.2016.7481852.

[6] G. Artner, R. Langwieser, R. Zemann, and C. F. Mecklenbräuker, "Carbon Fiber Reinforced Polymer Integrated Antenna Module", in *IEEE-APS Topical Conference on Antennas and Propagation in Wireless Communications (APWC)*, Cairns, Australia, 2016. DOI: 10.1109/APWC.2016.7738118.

[7] G. Artner, R. Langwieser, and C. F. Mecklenbräuker, "A MID Dipole Antenna in LDS Technology", in *24th Telecommunications Forum (TELFOR)*, Belgrade, Serbia, 2016. DOI: 10.1109/TELFOR.2016.7818832.

[8] G. Artner, J. Kowalewski, C. F. Mecklenbräuker, and T. Zwick, "Pattern Reconfigurable Antenna With Four Directions Hidden in the Vehicle Roof',

in *International Workshop on Antenna Technology (iWAT)*, Athens, Greece, 2017, pp. 84–87. DOI: 10.1109/IWAT.2017.7915323.

[9] G. Artner, R. Langwieser, and C. F. Mecklenbräuker, "Carbon Fiber Reinforced Polymer as Antenna Ground Plane Material Up to 10 GHz", in *European Conference on Antennas and Propagation (EuCAP)*, Paris, France, 2017, pp. 3612–3616. DOI: 10.23919/EuCAP.2017.7928128.

[10] G. Artner, R. Langwieser, and C. F. Mecklenbräuker, "Vehicular Roof Antenna Cavity for Coverage at Low Elevation Angles", in *IEEE AP-S Symposium on Antennas and Propagation and USNC-URSI Radio Science Meeting*, San Diego, USA, 2017.

[11] G. Artner and C. F. Mecklenbräuker, "Exchangeable Bases for Rapid Prototyping of Carbon Fiber Reinforced Polymer Antenna Cavities", in *IEEE-APS Topical Conference on Antennas and Propagation in Wireless Communications (APWC)*, Verona, Italy, 2017.

[12] G. Artner, "The Communicative Vehicle: Multiple Antennas in a Chassis Antenna Cavity", in *IEEE Vehicular Technology Conference Fall (VTC)*, Toronto, Canada, 2017.

[13] G. Artner and C. Mecklenbräuker, "Carbon-Fiber Composites in Antenna Applications", in *Vienna young Scientists Symposium (VSS)*, Vienna, Austria: Book-of-Abstracts.com, Heinz A. Krebs, 2015, pp. 108–109, ISBN: 978-3-9504017-0-7.

[14] G. Artner and R. Langwieser, "Lightweight Antenna Materials For The Internet Of Things", in *Vienna young Scientists Symposium (VSS)*, Vienna, Austria: Book-of-Abstracts.com, Heinz A. Krebs, 2016, pp. 80–81, ISBN: 978-3-9504017-2-1.

[15] P. S. Douglas-Hamilton, "Device for Indicating the Intended Movements of Vehicles", *U.S. Patent No. 912,831*, 1909.

[16] N. Guinart, R. Benbouhout, and J.-C. Huard, "Method and Equipment for Monitoring Tyre Wear and Vehicle On-Board Wear-Monitoring System", *U.S. Patent Application No. 15/127,178*, 2017.

[17] G. Lasser, "Passive RFID for Automotive Sensor Applications", Dissertation, Technische Universität Wien, 2014.

[18] G. Lasser, L. W. Mayer, Z. Popović, and C. F. Mecklenbräuker, "Low-Profile Switched-Beam Antenna Backed by an Artificial Magnetic Conductor for Efficient Close-to-Metal Operation", *IEEE Transactions on Antennas and Propagation*, vol. 64, no. 4, pp. 1307–1316, 2016. DOI: 10.1109/TAP.2016.2526044.

[19] B. Fleming, "Tire Pressure-Monitoring Systems Rollout", *IEEE Vehicular Technology Magazine*, vol. 4, no. 3, pp. 6–10, 2009. DOI: 10.1109/MVT.2009.933465.

[20] *Verordnung (EG) Nr. 661/2009 des Europäischen Parlaments und des Rates vom 13. Juli 2009.*

[21] M. Boban, R. Meireles, J. Barros, P. Steenkiste, and O. K. Tonguz, "TVR - Tall Vehicle Relaying in Vehicular Networks", *IEEE Transactions on Mobile Computing*, vol. 13, no. 5, pp. 1118–1131, 2014. DOI: 10.1109/TMC.2013.70.

[22] P. Alexander, D. Haley, and A. Grant, "Cooperative Intelligent Transport Systems: 5.9-GHz Field Trials", *Proceedings of the IEEE*, vol. 99, no. 7, pp. 1213–1235, 2011. DOI: 10.1109/JPROC.2011.2105230.

[23] *ETSI EN 302 571 v2*, 2016.

[24] C. A. Balanis, *Antenna Theory: Analysis and Design*, 4. John Wiley & Sons, 2016, ISBN: 978-1118642061.

[25] A. Krischke, *Rothammels Antennenbuch*, 13. DARC, 2013.

[26] *The ARRL Antenna Book For Radio Communications*, 22. Radio Society of Great Britain, 2011, ISBN: 978-0872596948.

[27] R. C. Hansen and R. E. Collin, *Small Antenna Handbook*, 2. John Wiley & Sons, IEEE Press, 2011, ISBN: 978-0470890837.

[28] V. Rabinovich, N. Alexandrov, and B. Alkhateeb, *Automotive antenna design and applications*. CRC Press/Taylor & Francis, 2010.

[29] J. P. Coon, "Flexible Antenna Mounting", *U.S. Patent No. 2,546,026*, 1951.

[30] A. Boege, L. Reiter, and S. Lindenmeier, "High-Impedance Amplifier in Combination with Coated FM Windscreen Diversity Antennas", in *IEEE International Symposium on Antennas and Propagation (APSURSI)*, 2016, pp. 113–114. DOI: 10.1109/APS.2016.7695765.

[31] M. Ignatenko, S. A. Sanghai, G. Lasser, B. Allen, R. Smith, M. Notaros, and D. S. Filipovic, "Antennas for Military Vehicles", *IEEE Antennas and Propagation Magazine*, vol. 58, no. 6, pp. 64–74, 2016. DOI: 10.1109/MAP.2016.2609806.

[32] T.-Y. Shih and N. Behdad, "Design of Vehicle-Mounted, Compact VHF Antennas Using Characteristic Mode Theory", in *European Conference on Antennas and Propagation (EuCAP)*, Paris, 2017, pp. 1774–1777. DOI: 10.23919/EuCAP.2017.7928334.

[33] E. Safin, R. Valkonen, and D. Manteuffel, "Reconfigurable LTE MIMO Automotive Antenna System Based on the Characteristic Mode Analysis", in *9th European Conference on Antennas and Propagation (EuCAP)*, 2015, ISBN: 9788890701856.

[34] A. Walbeoff and R. Langley, "Multiband PCB antenna", *IEE Proceedings - Microwaves, Antennas and Propagation*, vol. 152, no. 6, pp. 471 –475, 2005. DOI: 10.1049/ip-map:20050053.

[35] R. Leelaratne and R. Langley, "Multiband PIFA Vehicle Telematics Antennas", *IEEE Transactions on Vehicular Technology*, vol. 54, no. 2, pp. 477–485, 2005. DOI: 10.1109/TVT.2004.841535.

[36] A. Malarky, G. Z. Rafi, S. Safavi-Naeini, and L. Delgrossi, "A Planar Dual Band GPS and DSRC Antenna for Road Vehicles", in *IEEE 66th Vehicular Technology Conference*, 2007, pp. 2096–2100. DOI: 10.1109/VETECF.2007.440.

[37] I. A. Jensen and J. K. H. Gamage, "Versatile automobile antenna unit for roadside communication", in *10th European Conference on Wireless Technology (ECWT)*, 2007, pp. 213–216. DOI: 10.1109/ECWT.2007.4403984.

[38] M. Cerretelli, V. Tesi, and G. B. Gentili, "Design of a Shape-Constrained Dual-Band Polygonal Monopole for Car Roof Mounting", *IEEE Transactions on Vehicular Technology*, vol. 57, no. 3, pp. 1398–1403, 2008. DOI: 10.1109/TVT.2007.912153.

[39] M. Gallo, S. Bruni, and D. Zamberlan, "Design and Measurement of Automotive Antennas for C2C Applications", in *6th European Conference on Antennas and Propagation (EUCAP)*, 2012, pp. 1799–1803. DOI: 10.1109/EuCAP.2012.6205985.

[40] N. Guan, H. Chiba, Y. Yamaguchi, and H. Tayama, "A flat car-roof antenna module for phone and GPS applications", in *IEEE-APS Topical Conference on Antennas and Propagation in Wireless Communications (APWC)*, 2013, pp. 299–302. DOI: 10.1109/APWC.2013.6624884.

[41] N. Guan, H. Chiba, Y. Yamaguchi, Y. Niihara, and H. Tayama, "A Flat Roof Automobile Antenna Module for LTE, GPS and SDARS Applications", in *IEEE-APS Topical Conference on Antennas and Propagation in Wireless Communications (APWC)*, 2014, pp. 11–14. DOI: 10.1109/APWC.2014.6905517.

[42] F. Carrera, D. Navarro, M. Cabedo, D. Sanchez, M. Ferrando, M. Gallo, S. Bruni, M. Pannozzo, and D. Zamberlan, "Wideband monopole for mobile, WLAN and C2C services in vehicular applications", in *IEEE Antennas and Propagation Society, AP-S International Symposium (Digest)*, 2013, pp. 2071–2072. DOI: 10.1109/APS.2013.6711694.

[43] M. Gallo, S. Bruni, M. Pannozzo, and D. Zamberlan, "Performance Evaluation of C2C antennas on Car Body", in *European Conference on Antennas and Propagation (EuCAP)*, 2013, pp. 3136 –3139, ISBN: 9788890701818.

[44] M. Gallo, S. Bruni, and D. Zamberlan, "A Novel Fully Integrated Fin Antenna for Automotive Application", in *8th European Conference on Antennas and Propagation (EuCAP)*, 2014, pp. 2986–2989. DOI: 10.1109/EuCAP.2014.6902455.

[45] E. Ghafari, A. Fuchs, D. Eblenkamp, and D. N. Aloi, "A Vehicular Rooftop, Shark-fin, Multiband Antenna for the GPS/ LTE/ Cellular/ DSRC Systems", in *IEEE-APS Topical Conference on Antennas and Propagation in Wireless Communications (APWC)*, 2014, pp. 237–240. DOI: 10.1109/APWC.2014.6905546.

[46] I. Goncharova and S. Lindenmeier, "A High Efficient Automotive Roof-Antenna Concept for LTE, DAB-L, GNSS and SDARS with Low Mutual Coupling", in *9th European Conference on Antennas and Propagation (EuCAP)*, 2015, ISBN: 9788890701856.

[47] M. A. B. Diez and S. Lindenmeier, "A Highly Efficient Car2Car-Multiband Rooftop Automotive Antenna", in *IEEE International Symposium on An-*

tennas and Propagation & USNC/URSI National Radio Science Meeting (APS-URSI), 2015, pp. 1606–1607. DOI: 10.1109/APS.2015.7305192.

[48] M. M. Bilgic and K. Yegin, "Modified Annular Ring Antenna for GPS and SDARS Automotive Applications", *IEEE Antennas and Wireless Propagation Letters*, vol. 15, no. 1, pp. 1442–1445, 2016. DOI: 10.1109/LAWP.2015.2512558.

[49] D. V. Navarro-Mendez, L. F. Carrera-Suarez, D. Sanchez-Escuderos, M. Cabedo-Fabres, M. Baquero-Escudero, M. Gallo, and D. Zamberlan, "Wideband Double Monopole for Mobile, WLAN, and C2C Services in Vehicular Applications", *IEEE Antennas and Wireless Propagation Letters*, vol. 16, pp. 16–19, 2017. DOI: 10.1109/LAWP.2016.2552398.

[50] I. Goncharova and S. Lindenmeier, "A Compact Satellite Antenna Module for GPS, Galileo, GLONASS, BeiDou and SDARS in Automotive Applications", in *European Conference on Antennas and Propagation (EuCAP)*, 2017, pp. 3639–3643. DOI: 10.23919/EuCAP.2017.7928117.

[51] Y. Tashiro, "Antenna Device", *U.S. Patent Application US2017/0093028 A1*, 2017.

[52] S. Kaul, K. Ramachandran, P. Shankar, S. Oh, M. Gruteser, I. Seskar, and T. Nadeem, "Effect of Antenna Placement and Diversity on Vehicular Network Communications", in *4th Annual IEEE Communications Society Conference on Sensor, Mesh and Ad Hoc Communications and Networks*, 2007, pp. 112–121. DOI: 10.1109/SAHCN.2007.4292823.

[53] A. Rasku, "Multi-Antenna Solutions for Automotive Environment", Master's Thesis, Tampere University of Technology, 2008.

[54] S. Oh, S. Kaul, and M. Gruteser, "Exploiting Vertical Diversity in Vehicular Channel Environments", in *IEEE 20th International Symposium on Personal, Indoor and Mobile Radio Communications (PIMRC)*, 2009, pp. 958–962. DOI: 10.1109/PIMRC.2009.5449728.

[55] D. Kornek, M. Schack, E. Slottke, O. Klemp, I. Rolfes, and T. Kurner, "Effects of Antenna Characteristics and Placements on a Vehicle-to-Vehicle Channel Scenario", in *IEEE International Conference on Communications Workshops*, 2010. DOI: 10.1109/ICCW.2010.5503935.

[56] M. Geissler, C. Oikonomopoulos-Zachos, T. Ould, and M. Arnold, "MIMO Performance Optimisation of Car Antennas", in *6th European Conference on Antennas and Propagation (EUCAP)*, 2012, pp. 2750–2753. DOI: 10.1109/EuCAP.2012.6206423.

[57] E. Ohlmer, G. Fettweis, and D. Plettemeier, "MIMO System Design and Field Tests for Terminals with Confined Space - Impact on Automotive Communication", in *5th European Conference on Antennas and Propagation (EUCAP)*, 2011, pp. 2886–2890, ISBN: 978-88-8202-074-3.

[58] J. Nuckelt, H. Hoffmann, M. Schack, and T. Kürner, "Linear Diversity Combining Techniques Employed in Car-to-X Communication Systems",

in *IEEE 73rd Vehicular Technology Conference (VTC Spring)*, 2011. DOI: 10.1109/VETECS.2011.5956232.

[59] C. Oikonomopoulos-Zachos, T. Ould, and M. Arnold, "Outdoor Channel Characterization of MIMO-LTE Antenna Configurations through Measurements", in *IEEE 75th Vehicular Technology Conference (VTC Spring)*, 2012. DOI: 10.1109/VETECS.2012.6240252.

[60] M. Shemshaki, T. Zemen, and C. F. Mecklenbräuker, "Antenna Selection Diversity for IEEE 802.11p", in *39th Annual Conference of the IEEE Industrial Electronics Society (IECON)*, 2013, pp. 6876–6879. DOI: 10.1109/IECON.2013.6700271.

[61] L. Ekiz, A. Thiel, O. Klemp, and C. F. Mecklenbräuker, "MIMO performance evaluation of automotive qualified LTE antennas", in *European Conference on Antennas and Propagation (EuCAP)*, 2013, pp. 1412–1416.

[62] J. H. Schaffner, A Bekaryan, H. J. Song, T Talty, D Carper, E Yasan, and A Duzdar, "A drive test measurement approach to characterize on-vehicle 2x2 LTE-MIMO antennas", in *IEEE-APS Topical Conference on Antennas and Propagation in Wireless Communications (APWC)*, 2014, pp. 85–88. DOI: 10.1109/APWC.2014.6905524.

[63] L. Ekiz, A. Posselt, O. Klemp, and C. F. Mecklenbräuker, "System Level Assessment of Vehicular MIMO Antennas in 4G LTE Live Networks", in *IEEE 80th Vehicular Technology Conference (VTC2014-Fall)*, 2014. DOI: 10.1109/VTCFall.2014.6966198.

[64] J. H. Schaffner, H. J. Song, A. Bekaryan, T. Talty, D. Carper, and E. Yasan, "Scanner Based Drive Test LTE Capacity Measurements with MIMO Antennas Placed Inside the Vehicle", in *IEEE International Conference on Microwaves, Communications, Antennas and Electronic Systems (COMCAS)*, Tel Aviv, Israel, 2015. DOI: 10.1109/COMCAS.2015.7360365.

[65] S. Fikar, W. Walzik, and A. L. Scholtz, "Vehicular Multi/Broadband MIMO Antenna for Terrestrial Communication", in *IEEE Antennas and Propagation Society International Symposium*, 2008. DOI: 10.1109/APS.2010.5561239.

[66] L. Reichardt, C. Sturm, and T. Zwick, "Performance Evaluation of SISO, SIMO and MIMO Antenna Systems for Car-to-Car Communications in Urban Environments", in *9th International Conference on Intelligent Transport Systems Telecommunications (ITST)*, 2009, pp. 51–56. DOI: 10.1109/ITST.2009.5399385.

[67] A. Thiel, O. Klemp, A. Paier, L. Bernadó, J. Karedal, and A. Kwoczek, "In-Situ Vehicular Antenna Integration and Design Aspects for Vehicle-to-Vehicle Communications", in *European Conference on Antennas and Propagation (EuCAP)*, 2010.

[68] L. Reichardt, J. Pontes, G. Jereczek, and T. Zwick, "Capacity Maximizing MIMO Antenna Design for Car-to-Car Communication", in *International*

Workshop on Antenna Technology (iWAT), 2011, pp. 243–246. DOI: 10.1109/IWAT.2011.5752319.

[69] H. J. Song, A. Bekaryan, J. H. Schaffner, T. Talty, D. Carper, and A. Duzdar, "Evaluation of Vehicle-level MIMO Antennas : Capacity , Total Embedded Efficiency , and Envelope Correlation", in *IEEE-APS Topical Conference on Antennas and Propagation in Wireless Communications (APWC)*, 2014, pp. 89–92. DOI: 10.1109/APWC.2014.6905525.

[70] F. Alexa, B. Bardeanu, and D. Vatau, "MIMO Antenna System for LTE", in *36th International Conference on Telecommunications and Signal Processing (TSP)*, 2013, pp. 294–298. DOI: 10.1109/TSP.2013.6613939.

[71] A. Friedrich, B. Geck, O. Klemp, and H. Kellermann, "On the Design of a 3D LTE Antenna for Automotive Applications based on MID Technology", in *European Microwave Conference (EuMC)*, 2013, pp. 640–643, ISBN: 9782874870316.

[72] A. Thiel, L. Ekiz, O. Klemp, and M. Schultz, "Automotive Grade MIMO Antenna Setup and Performance Evaluation for LTE-Communications", in *International Workshop on Antenna Technology (iWAT)*, 2013, pp. 171–174. DOI: 10.1109/IWAT.2013.6518325.

[73] N. Guan, H. Tayama, M. Ueyama, Y. Yoshijima, and H. Chiba, "A Roof Automobile Module for LTE-MIMO Antennas", in *IEEE-APS Topical Conference on Antennas and Propagation in Wireless Communications (APWC)*, 2015, pp. 387–391. DOI: 10.1109/APWC.2015.7300160.

[74] O.-Y. Kwon, R. Song, Y.-Z. Ma, and B.-S. Kim, "Integrated MIMO Antennas for LTE and V2V applications", in *URSI Asia-Pacific Radio Science Conference (URSI AP-RASC)*, 2016, pp. 1057–1060. DOI: 10.1109/URSIAP-RASC.2016.7601146.

[75] T. Kopacz, A. Narbudowicz, D. Heberling, and M. J. Ammann, "Evaluation of Automotive MIMO Antennas for V2V Communication in Urban Intersection Scenarios", in *European Conference on Antennas and Propagation (EuCAP)*, 2017. DOI: 10.23919/EuCAP.2017.7928476.

[76] N. Saponjic, F. Klefenz, F. Bongard, D. Llorens, A. Boulle, X. Aubry, A. Butler, F. Tiezzi, and S. Vaccaro, "Product concepts for land mobile satellite communication terminals in Ku-/Ka-band", in *European Conference on Antennas and Propagation (EUCAP)*, 2017, pp. 1525–1529. DOI: 10.23919/EuCAP.2017.7928753.

[77] J. D. Boerman and J. T. Bernhard, "Performance Study of Pattern Reconfigurable Antennas in MIMO Communication Systems", *IEEE Transactions on Antennas and Propagation*, vol. 56, no. 1, pp. 231–236, 2008. DOI: 10.1109/TAP.2007.913141.

[78] J. Kowalewski, T. Mahler, L. Reichardt, and T. Zwick, "Shape Memory Alloy (SMA) -Based Pattern-Reconfigurable Antenna", *IEEE Antennas and Wireless Propagation Letters*, vol. 12, pp. 1598–1601, 2013. DOI: 10.1109/LAWP.2013.2293593.

[79] J. Kowalewski, T. Mahler, C. Heine, and T. Zwick, "Compact Pattern Reconfigurable LTE Antenna", in *International Workshop on Antenna Technology (iWAT)*, 2014, pp. 72–75. DOI: 10.1109/IWAT.2014.6958599.

[80] T. Mahler, J. Kowalewski, T. Schipper, and T. Zwick, "A Pattern Reconfigurable Automotive LTE Antenna employing Synthesized Radiation Patterns", in *IEEE MTT-S International Conference on Microwaves for Intelligent Mobility (ICMIM)*, 2015. DOI: 10.1109/ICMIM.2015.7117937.

[81] J. Kowalewski, T. Mahler, J. Mayer, and T. Zwick, "A Miniaturized Pattern Reconfigurable Antenna for Automotive Applications", in *European Conference on Antennas and Propagation (EuCAP)*, 2016. DOI: 10.1109/EuCAP.2016.7481207.

[82] J. Kowalewski, J. Mayer, T. Mahler, and T. Zwick, "A Compact Pattern Reconfigurable Antenna Utilizing Multiple Monopoles", in *International Workshop on Antenna Technology (iWAT)*, 2016. DOI: 10.1109/IWAT.2016.7434783.

[83] J. Kowalewski, L. Keller-Bauer, T. Mahler, J. Mayer, and T. Zwick, "Realization of a Compact Antenna with Reconfigurable Pattern for Multiple Antenna Systems", in *European Conference on Antennas and Propagation (EuCAP)*, Paris, 2017.

[84] T. Mahler, J. Kowalewski, T. Schipper, and T. Zwick, "Channel capacity determination of a pattern reconfigurable automotive roof-top LTE antenna", in *Asia-Pacific Microwave Conference*, 2014, pp. 974–976.

[85] D. Sievenpiper, H. J. Song, H. P. Hsu, G. Tangonan, R. Y. Loo, and J. Schaffner, "MEMS-Based Switched Diversity Antenna at 2.3 GHz for Automotive Applications", in *5th International Symposium on Wireless Personal Multimedia Communications (WPMC)*, 2002, pp. 762–765. DOI: 10.1109/WPMC.2002.1088278.

[86] T. Smits, S. Suckrow, J. Christ, and M. Geissler, "Active intelligent antenna system for car2car", in *International Workshop on Antenna Technology (iWAT)*, 2013, pp. 67–70. DOI: 10.1109/IWAT.2013.6518300.

[87] M. Geissler, K. Schwarwies, and J. Christ, "Intelligent Antenna Systems for Cars", in *German Microwave Conference (GeMiC)*, 2014.

[88] D.-T. Phan-Huy, M. Sternad, T. Svensson, W. Zirwas, B. Villeforceix, F. Karim, and S.-E. El-Ayoubi, "5G on Board: How Many Antennas Do We Need on Connected Cars?", in *IEEE Globecom Workshops (GC Wkshps)*, 2016, ISBN: 9781509024827. DOI: 10.1109/GLOCOMW.2016.7848799.

[89] R. L. Jesch, "Measured Vehicular Antenna Performance", *IEEE Transactions on Vehicular Technology*, vol. 34, no. 2, pp. 97–107, 1985. DOI: 10.1109/T-VT.1985.24042.

[90] Y. Kim and E. Walton, "Effect of body gaps on conformal automotive antennas", *Electronics Letters*, vol. 40, no. 19, pp. 1161–1162, 2017. DOI: 10.1049/el:20045721.

[91] A. Bekaryan, H. J. Song, H.-P. Hsu, and R. W. Wiese, "Parametric Study of Roof Geometry and Roof Rack Crossbar Effects on the Performance of Multi-band Vehicle Antennas", in *IEEE Vehicular Technology Conference Fall (VTC)*, 2009, ISBN: 9781424425150. DOI: 10.1109/VETECF.2009.5379064.

[92] M. S. L. Mocker, S. Liu, V. A. Fuertes, H. Tazi, and T. F. Eibert, "Influence of the Vehicle Environment on the Radiation Characteristics of Vehicle Roof Antennas", in *German Microwave Conference*, 2015, pp. 374–377. DOI: 10.1109/GEMIC.2015.7107831.

[93] R. J. Marhefka, B. A. Baertlein, M. Rao, and K. Prakah-Asante, "Modeling the Performance of Automotive Bumper Mounted Antennas", in *IEEE Antennas and Propagation Society International Symposium*, 2002, pp. 316–319. DOI: 10.1109/APS.2002.1018218.

[94] L. Ekiz, T. Patelczyk, O. Klemp, and C. F. Mecklenbräuker, "Compensation of Vehicle-Specific Antenna Radome Effects at 5 . 9 GHz", in *Annual Conference of the IEEE Industrial Electronics Society (IECON)*, 2013, pp. 6880–6884. DOI: 10.1109/IECON.2013.6700272.

[95] A. Kwoczek, Z. Raida, J. Lačík, M. Pokorný, J. Puskely, and P. Vágner, "Influence of Car Panorama Glass Roofs on Car2Car Communication (Poster)", in *IEEE Vehicular Networking Conference (VNC)*, 2011, pp. 246–251. DOI: 10.1109/VNC.2011.6117107.

[96] J. Kowalewski, T. Mahler, L. Reichardt, and T. Zwick, "Investigation of the Influence of Panoramic Roof on Mobile Telephony Antennas", in *8th European Conference on Antennas and Propagation (EuCAP)*, 2014, pp. 1062–1066. DOI: 10.1109/EuCAP.2014.6901951.

[97] M. B. Diez, P. Plitt, W. Pascher, and S. Lindenmeier, "Antenna placement and wave propagation for Car-To-Car communication", in *European Microwave Conference (EuMC)*, 2015, pp. 207–210. DOI: 10.1109/EuMC.2015.7345736.

[98] M. B. Diez, W. Pascher, and S. Lindenmeier, "Electromagnetic Characterization of Automotive Sunroofs for Car-to-X Applications", in *46th European Microwave Conference (EuMC)*, 2016, pp. 1323–1326. DOI: 10.1109/EuMC.2016.7824595.

[99] B. D. Pell, E. Sulic, W. S. T. Rowe, K. Ghorbani, and S. John, "Experimental Study of the Effect of Modern Automotive Paints on Vehicular Antennas", *IEEE Transactions on Antennas and Propagation*, vol. 59, no. 2, pp. 434–442, 2011. DOI: 10.1109/TAP.2010.2096182.

[100] A. Posselt, A. Friedrich, L. Ekiz, O. Klemp, and B. Geck, "System-level assessment of volumetric 3D vehicular MIMO antenna based on measurement", in *International Conference on Connected Vehicles and Expo (ICCVE)*, 2015, pp. 222–226. DOI: 10.1109/ICCVE.2014.7297545.

[101] Q. H. Dao, A. Friedrich, and B. Geck, "Characterization of electromagnetic properties of MID Materials for high frequency applications up to 67 GHz",

Advances Materials Research, vol. 1038, pp. 63–68, 2014. DOI: 10.4028/www.scientific.net/AMR.1038.63.

[102] S.-I. Matsuzawa and T. Watanabe, "Influence of resin cover on antenna gain for automotive millimeter wave radar", in *International Symposium on Antennas and Propagation (ISAP)*, 2016, pp. 704–705.

[103] L. Low, R. Langley, and J. Batchelor, "Modelling and performance of conformal automotive antennas", *IET Microwaves, Antennas & Propagation*, vol. 1, no. 5, pp. 973 –979, 2006. DOI: 10.1049/iet-map:20070050.

[104] S. Savia, R. Langley, A. Walbeoff, H. I. Europe, and K. Me, "Automotive antenna simulation", in *Second European Conference on Antennas and Propagation (EuCAP)*, 2007. DOI: 10.1049/ic.2007.0878.

[105] H. Zhang, J. Rigelsford, L. Low, and R. Langley, "Field distributions within a rectangular cavity with vehicle-like features", in *Loughborough Antennas and Propagation Conference (LAPC)*, 2008, pp. 205–208. DOI: 10.1109/LAPC.2008.4516902.

[106] H. Zhang, L. Low, J. Rigelsford, and R. Langley, "Effects of Vehicle Furnishings on Performance of Aperture Mounted Multi-Band Conformal Automotive Antenna", in *3rd European Conference on Antennas and Propagation*, 2009, pp. 2694–2697, ISBN: 9783000245732.

[107] L. Low, A. R. Ruddle, J. M. Rigelsford, and R. J. Langley, "Computed Impact of Human Occupants on Field Distributions Within a Passenger Vehicle", in *6th European Conference on Antennas and Propagation (EUCAP) Computed*, 2012, pp. 1214–1217. DOI: 10.1109/EuCAP.2012.6205898.

[108] R. El-Makhour, M. Gatsinzi-Ibambe, X. Bunlon, and P. Boutier, "Overview of Radiofrequency Simulation for Automotive Antennas at Renault", in *European Conference on Antennas and Propagation (EuCAP)*, 2015.

[109] *145-2013 - IEEE Standard for Definitions of Terms for Antennas*, 2014. DOI: 10.1109/IEEESTD.2014.6758443.

[110] R Tian, B. K. Lau, and Z Ying, "Multiplexing Efficiency of MIMO Antennas", *IEEE Antennas and Wireless Propagation Letters*, vol. 10, pp. 183–186, 2011, ISSN: 1536-1225. DOI: 10.1109/LAWP.2011.2125773.

[111] E. C. Neira, "Antenna Evaluation for Vehicular Applications in Multipath Environment", Licentiate Thesis, Chalmers, 2017.

[112] L. Y. Ekiz, "Vehicular Service Delivery via Hybrid Access and Antennas", Dissertation, Technische Universität Wien, 2014.

[113] L. Reichardt, T. Mahler, Y. L. Sit, and T. Zwick, "Using a Synthesis Methodology for the Design of Automotive Antenna Systems", in *European Conference on Antennas and Propagation (EuCAP)*, 2013, pp. 1600–1604, ISBN: 9788890701832.

[114] L. Reichardt, Y. L. Sit, T. Mahler, T. Schipper, and T. Zwick, "Synthesis Based Antenna Design for Car-to-Car Communication", in *IEEE Antennas and Propagation Society International Symposium (APSURSI)*, 2013, pp. 2079–2080. DOI: 10.1109/APS.2013.6711698.

[115] L. Reichardt, "Methodik für den Entwurf von kapazitätsoptimierten Mehrantennensystemen am Fahrzeug", Dissertation, Karlsruhe Institute of Technology, 2013, ISBN: 978-3-7315-0047-6.

[116] R. K. Sharma, W. Kotterman, M. H. Landmann, C. Schirmer, C. Schneider, F. Wollenschläger, G. D. Galdo, M. A. Hein, and R. S. Thomä, "Over-the-Air Testing of Cognitive Radio Nodes in a Virtual Electromagnetic Environment", *International Journal of Antennas and Propagation*, vol. 2013, no. Article ID 945283, p. 16, 2013. DOI: 10.1155/2013/945283.

[117] R. K. Sharma, C. Schneider, W. Kotterman, G. Sommerkorn, P. Große, F. Wollenschläger, G. D. Galdo, M. A. Hein, and R. S. Thoma, "Over-The-Air Testing of Car-to-Car and Car-to-Infrastructure Communication in a Virtual Electromagnetic Environment", in *39th Annual Conference of the IEEE Industrial Electronics Society (IECON)*, 2017, pp. 6897–6902. DOI: 10.1109/IECON.2013.6700275.

[118] R. K. Sharma, C Schneider, W Kotterman, G Sommerkorn, P Große, F Wollenschläger, G. D. Galdo, M. A. Hein, and R. S. Thomä, "Virtual electromagnetic environment for over-the-air testing of car-to-car and car-to-infrastructure communication", in *XXXIth URSI General Assembly and Scientific Symposium (URSI GASS)*, 2014, pp. 1–4. DOI: 10.1109/URSIGASS.2014.6929561.

[119] C Schirmer, M Lorenz, W. A. T. Kotterman, R Perthold, M. H. Landmann, and G. D. Galdo, "MIMO over-the-air testing for electrically large objects in non-anechoic environments", in *European Conference on Antennas and Propagation (EuCAP)*, 2016, pp. 1–6. DOI: 10.1109/EuCAP.2016.7481106.

[120] C Schirmer, A Rügamer, W. A. T. Kotterman, M. H. Landmann, and G. D. Galdo, "Evaluation of array antenna systems for GNSS applications using wave-field synthesis in an OTA laboratory", in *European Conference on Antennas and Propagation (EUCAP)*, 2017, pp. 3370–3374. DOI: 10.23919/EuCAP.2017.7928727.

[121] D. Löschenbrand, "Antenna Characterization in the Near-Field", Master's Thesis, Technische Universität Wien, 2016.

[122] E. Industries, "Rohacell Dielectric Properties", Darmstadt, Germany, Tech. Rep., 2011.

[123] T. Suenaga, H. Ikeda, M. Aya, S. Koyama, N. Mikami, and H. Miyuki, "Carbon Fiber Reinforced Concrete", *U.S. Patent Nr. 4627998*, 1986.

[124] F. Teodorescu, H. Teodorescu, G. Stanca, D. Condurache, and R. S. Craciunoiu, "On the Recycling of Carbon Fibers Reinforced Polymer Matrix Composites", in *4th IASME/WSEAS International Conference on Energy, Environment, Ecosystems and Sustainable Development (EEESD'08)*, 2008, pp. 294–297, ISBN: 9789606766718.

[125] H. C. Kim and S. K. See, "Electrical properties of unidirectional carbon-epoxy composites in wide frequency band", *Journal of Physics D: Applied Physics*, vol. 23, no. 7, p. 916, 1990.

[126] T. A. Ezquerra, M. T. Connor, S. Roy, M. Kulescza, J. Fernandes-Nascimento, and F. J. Baltá-Calleja, "Alternating-current electrical properties of graphite, carbon-black and carbon-fiber polymeric composites", *Composites Science and Technology*, vol. 61, no. 6, pp. 903–909, 2001. DOI: 10.1016/S0266-3538(00)00176-7.

[127] S. E. Lee, K. S. Oh, and C. G. Kim, "Electromagnetic characteristics of frequency selective fabric composites", *Electronics Letters*, vol. 42, no. 8, pp. 439–441, 2006. DOI: 10.1049/el:20060822.

[128] A Galehdar, K. J. Nicholson, W. S. T. Rowe, and K Ghorbani, "The conductivity of unidirectional and quasi isotropic carbon fiber composites", in *The 40th European Microwave Conference*, 2010, pp. 882–885.

[129] A. Galehdar, K. J. Nicholson, P. J. Callus, W. S. T. Rowe, S. John, C. H. Wang, and K. Ghorbani, "The strong diamagnetic behaviour of unidirectional carbon fiber reinforced polymer laminates", *Journal of Applied Physics*, vol. 112, no. 11, p. 113 921, 2012.

[130] A. M. Nicolson and G. F. Ross, "Measurement of the Intrinsic Properties of Materials by Time-Domain Techniques", *IEEE Transactions on Instrumentation and Measurement*, vol. 19, no. 4, pp. 377–382, 1970. DOI: 10.1109/TIM.1970.4313932.

[131] W. B. Weir, "Automatic Measurement of Complex Dielectric Constant and Permeability at Microwave Frequencies", *Proceedings of the IEEE*, vol. 62, no. 1, pp. 33–36, 1974. DOI: 10.1109/PROC.1974.9382.

[132] T. Doan, A. Walters, and C. Leat, "Characterisation of electromagnetic properties of carbon fibre composite materials", in *Electromagnetic Compatibility Symposium Adelaide*, 2009, pp. 87–91.

[133] A. Galehdar, P. J. Callus, and K. Ghorbani, "A Novel Method of Conductivity Measurements for Carbon-Fiber Monopole Antenna", *IEEE Transactions on Antennas and Propagation*, vol. 59, no. 6, pp. 2120–2126, 2011. DOI: 10.1109/TAP.2011.2143676.

[134] C. L. Holloway, M. S. Sarto, and M. Johansson, "Analyzing carbon-fiber composite materials with equivalent-Layer models", *IEEE Transactions on Electromagnetic Compatibility*, vol. 47, no. 4, pp. 833–844, 2005. DOI: 10.1109/TEMC.2005.854101.

[135] G. Wasselynck, D. Trichet, B. Ramdane, and J. Fouldagar, "Interaction Between Electromagnetic Field and CFRP Materials: A New Multiscale Homogenization Approach", *IEEE Transactions on Magnetics*, vol. 46, no. 8, pp. 3277–3280, 2010. DOI: 10.1109/TMAG.2010.2045359.

[136] J. Fouladgar, G. Wasselynck, and D. Trichet, "Shielding and Reflecting Effectiveness of Carbon Fiber Reinforced Polymer (CFRP) Composites", in *International Symposium on Electromagnetic Theory*, 2013, pp. 104–107, ISBN: 9784885522772.

[137] "Commission Decision on the harmonised use of radio spectrum in the 5 875-5 905 MHz frequency band for safety-related applications of Intelligent Transport Systems (ITS)", *Official Journal of the European Union*, 2008.

[138] A. N. Vicente, G. M. Dip, and C. Junqueira, "The Step by Step Development of NRW Method", in *2011 SBMO/IEEE MTT-S International Microwave and Optoelectronics Conference (IMOC 2011)*, 2011, pp. 738–742. DOI: 10.1109/IMOC.2011.6169318.

[139] D. K. Ghodgaonkar, V. V. Varadan, and V. K. Varadan, "Free-space measurement of complex permittivity and complex permeability of magnetic materials at microwave frequencies", *IEEE Transactions on Instrumentation and Measurement*, vol. 39, no. 2, pp. 387–394, 1990. DOI: 10.1109/19.52520.

[140] O. Luukkonen, S. I. Maslovski, and S. A. Tretyakov, "A Stepwise Nicolson-Ross-Weir-Based Material Parameter Extraction Method", *IEEE Antennas and Wireless Propagation Letters*, vol. 10, pp. 1295–1298, 2011. DOI: 10.1109/LAWP.2011.2175897.

[141] A. Galehdar, W. S. T. Rowe, K. Ghorbani, P. J. Callus, S. John, and C. H. Wang, "The effect of ply orientation on the performance of antennas in or on carbon fiber composites", *Progress In Electromagnetics Research*, vol. 116, pp. 123–136, 2011.

[142] B. W. Anderson, "The impact of carbon fibre composites on a military aircraft establishment", *Journal of Physics D: Applied Physics*, vol. 20, no. 3, pp. 311–314, 1987.

[143] F. S. Stringer, "Electromagnetic Effects of (Carbon) Composite Materials Upon Avionics Systems", DTIC Document, Tech. Rep., 1980.

[144] K. M. Keen, "Gain-loss measurements on a carbon-fibre composite reflector antenna", *Electronics Letters*, vol. 11, no. 11, pp. 234–235, 1975.

[145] ——, "Surface efficiency measurements on a high-modulus carbon fibre composite reflector antenna at L-and S-band frequencies", *Electronics Letters*, vol. 12, no. 7, pp. 160–161, 1976.

[146] V. Hombach and E. Kühn, "Complete Dual-Offset Reflector Antenna Analysis Including Near-Field, Paint-Layer and CFRP-Structure Effects", *IEEE Transactions on Antennas and Propagation*, vol. 37, no. 9, pp. 1093–1101, 1989. DOI: 10.1109/8.35788.

[147] E. K. Pfeiffer, O. Reichmann, A. Ihle, S. Linke, C. Tschepe, N. Nathrath, M. Santos, A. Grillenbeck, J. Santiago-Prowald, P. Rinous, and L. Rolo, "Compact and Stable Earth Deck Multi-Beam Ka- Band Antenna Structure and Dual Gridded Reflector", in *5th European Conference on Antennas and Propagation (EUCAP)*, 2011, pp. 3345–3353, ISBN: 9788882020743.

[148] C. G. M. van 't Klooster, V. V. Parshin, and S. E. Myasnikova, "Reflectivity of Antenna Reflectors: Measurements at Frequencies between 110 and 200 GHz", in *IEEE Antennas and Propagation Society International Symposium*, 2003, pp. 528–531. DOI: 10.1109/APS.2003.1219902.

[149] S. E. Myasnikova, V. V. Parshin, K. van't Klooster, and G. Valsecchi, "Reflectivity of antenna and mirrors reflectors at 110 and 200 GHz", in *4th International Conference on Antenna Theory and Techniques (ICATT)*, 2003, pp. 624–627. DOI: 10.1109/ICATT.2003.1238819.

[150] M. Leipold, H. Runge, and C. Sickinger, "Large SAR membrane antennas with lightweight deployable booms", in *28th ESA Antenna Workshop on Space Antenna Systems and Technologies (ESA/ESTEC)*, Noordwijk, The Netherlands, 2005.

[151] N. Yonemoto, A. Kohmura, and S. Futatsumori, "76 GHz Millimeter-Wave Radar System for Helicopter Obstacle Detection", in *12th International Radar Symposium (IRS)*, 2011, pp. 161–166, ISBN: 9783927535282.

[152] S. Futatsumori, K. Morioka, A. Kohmura, M. Shioji, and N. Yonemoto, "Fundamental Applicability Evaluation of Carbon Fiber Reinforced Plast Materials Utilized in Millimeter-Wave Antennas", in *IEEE Conference on Antenna Measurements Applications (CAMA)*, 2014. DOI: 10.1109/CAMA.2014.7003398.

[153] ——, "Evaluation of Fan Beam Carbon Fiber Reinforce Plastics Offset Parabolic Reflector Antenna for W-band Millimeter-Wave Radar Systems", in *International Symposium on Antennas and Propagation Conference Proceedings (ISAP)*, 2015, pp. 307–308. DOI: 10.1109/ISANP.2014.7026653.

[154] G. Lacy, "Development of a 15 Metre Diameter High Performance, Low Cost Radio Antenna for the Square Kilometre Array", in *International Conference on Composite Materials*, Copenhagen, 2015.

[155] E. J. Riley, E. H. Lenzing, and R. M. Narayanan, "Characterization of radar cross section of carbon fiber composite materials", in *Proc. SPIE 9461, Radar Sensor Technology XIX; and Active and Passive Signatures VI*, International Society for Optics and Photonics, 2015, p. 946 103. DOI: 10.1117/12.2176750.

[156] A. Mehdipour, C. W. Trueman, A. R. Sebak, and S. V. Hoa, "Carbon-fiber composite T-match folded bow-tie antenna for RFID applications", in *2009 IEEE Antennas and Propagation Society International Symposium*, 2009, pp. 1–4. DOI: 10.1109/APS.2009.5171640.

[157] L. Manac'h, X. Castel, and M. Himdi, "Microwave Performance of a Carbon Composite Antenna", in *European Microwave Conference*, 2013, pp. 770–773.

[158] S. M. Asif, A. Iftikhar, J. M. Parrow, B. D. Braaten, and M. S. Khan, "On Using the Electrical Characteristics of Carbon Microfibers for Designing a Monopole Antenna", in *IEEE International Symposium on Antennas and Propagation (APSURSI)*, 2016, pp. 1881–1882. DOI: 10.1109/APS.2016.7696647.

[159] C. A. Balanis and D. Decarlo, "Monopole Antenna Patterns on Finite Size Composite Ground Planes", *IEEE Transactions on Antennas and Propagation*, vol. 30, no. 4, pp. 764–768, 1982. DOI: 10.1109/TAP.1982.1142842.

[160] T. J. Seidel, A. Gelehdar, W. S. T. Rowe, S. John, P. J. Callus, and K. Ghorbani, "The anisotropic conductivity of unidirectional carbon fibre reinforced polymer laminates and its effect on microstrip antennas", in *Asia-Pacific Microwave Conference (APMC)*, 2010, pp. 1470–1473.

[161] R. R. de Assis and I. Bianchi, "Analysis of microstrip antennas on carbon fiber composite material", *Journal of Microwaves, Optoelectronics and Electromagnetic Applications*, vol. 11, no. 1, pp. 154–161, 2012.

[162] A. Mehdipour, T. A. Denidni, A.-R. Sebak, C. W. Trueman, I. D. Rosca, and S. V. Hoa, "Mechanically reconfigurable antennas using an anisotropic carbon-fibre composite ground", *IET Microwaves, Antennas Propagation*, vol. 7, no. 13, pp. 1055–1063, 2013. DOI: 10.1049/iet-map.2013.0115.

[163] J. W. Sabat, "Structural Response of the Slotted Waveguide Antenna Stiffened Structure Components Under Compression", Master's Thesis, Air Force Institute of Technology, 2010.

[164] D. Gray, K. Nicholson, K. Ghorbani, and P. Callus, "Carbon fibre reinforced plastic slotted waveguide antenna", in *Asia-Pacific Microwave Conference*, 2010, pp. 307–310.

[165] P. J. Callus and K. J. Nicholson, "Standard Operating Procedure - Manufacture of Carbon Fibre Reinforced Plastic Waveguides and Slotted Waveguide Antennas, Version 1.0", DTIC Document, Tech. Rep., 2011.

[166] K. J. Nicholson, W. S. T. Rowe, P. J. Callus, and K. Ghorbani, "Split-Ring Resonator Loading for the Slotted Waveguide Antenna Stiffened Structure", *IEEE Antennas and Wireless Propagation Letters*, vol. 10, pp. 1524–1527, 2011. DOI: 10.1109/LAWP.2011.2181474.

[167] A. Galehdar, P. J. Callus, W. S. T. Rowe, C. H. Wang, S. John, and K. Ghorbani, "Capacitively Fed Cavity-Backed Slot Antenna in Carbon-Fiber Composite Panels", *IEEE Antennas and Wireless Propagation Letters*, vol. 11, pp. 1028–1031, 2012. DOI: 10.1109/LAWP.2012.2214197.

[168] A. Bojovschi, N. Shariati, and K. Ghorbani, "Analysis of a carbon fibre reinforced polymer slotted waveguide array fed by a loop type end launcher", in *Asia-Pacific Microwave Conference Proceedings (APMC)*, 2017, pp. 476–478. DOI: 10.1109/APMC.2013.6694836.

[169] K. J. Nicholson, W. S. T. Rowe, P. J. Callus, K. Ghorbani, and T. Itoh, "Coaxial Right/Left-Handed Transmission Line for Electronic Beam Steering in the Slotted Waveguide Antenna Stiffened Structure", *IEEE Transactions on Microwave Theory and Techniques*, vol. 62, no. 4, pp. 773–778, 2014. DOI: 10.1109/TMTT.2014.2308480.

[170] A. Heilmann, *Antennen, Band 1.* Mannheim: Bibliographisches Institut, 1970, pp. 108–111.

[171] Y. Dai, T. Talty, and L. Lanctot, "GPS Antenna Selection and Placement for Optimum Automotive Performance", in *IEEE Antennas and Propagation Society International Symposium*, 2001, pp. 132–135. DOI: 10.1109/APS.2001.958810.

[172] C. C. Squires and T. J. Willink, "The Impact of Vehicular Antenna Placement on Polarization Diversity", in *IEEE 70th Vehicular Technology Conference (VTC Fall)*, 2017. DOI: 10.1109/VETECF.2009.5379017.

[173] N. Adhikari and S. Noghanian, "Capacity Measurement of Multiple Antenna Systems for Car to Car Communication", in *IEEE Antennas and Propagation Society International Symposium (APSURSI)*, 2017, pp. 603–604. DOI: 10.1109/APS.2014.6904632.

[174] L. Reichardt, T. Fugen, and T. Zwick, "Influence of antennas placement on car to car communications channel", *2009 3rd European Conference on Antennas and Propagation*, pp. 630–634, 2009.

[175] T. Mahler, L. Reichardt, C. Heine, M. Pauli, and T. Zwick, "Channel based design of systems with multiple antennas", *Progress In Electromagnetics Research B*, vol. 64, pp. 63–81, 2015.

[176] E. Zöchmann, K. Guan, and M. Rupp, "Two-Ray Models in mmWave Communications", in *IEEE International Workshop on Signal Processing Advances in Wireless Communications (SPAWC 2017)*, 2017, pp. 1–5.

[177] H. Dörrie and U. Militz, "Vehicular slot antenna system", *U.S. Patent No. 5,177,494*, 1993.

[178] J. M. Janky and G. T. Janky, "Concealed mobile communications system", *U.S. Patent No. 5,918,183*, 1999.

[179] R. J. Langley and J. C. Batchelor, "Hidden antennas for vehicles", *Electronics & Communication Engineering Journal*, vol. 14, no. 6, pp. 253–262, 2002. DOI: 10.1049/ecej:20020601.

[180] R. D. Zerod, G. F. Tannery IV, and M.-R. S. Movahhed, "Concealed antenna system with remote variable gain RF amplifier", *U.S. Patent No. 5,428,830*, 1995.

[181] J. H. Schaffner, H. J. Song, A. Bekaryan, H. P. Hsu, M. Wisnewski, and J. Graham, "The Impact of Vehicle Structural Components on Radiation Patterns of a Window Glass Embedded FM Antenna", *IEEE Transactions on Antennas and Propagation*, vol. 59, no. 10, pp. 3536–3543, 2011. DOI: 10.1109/TAP.2011.2163778.

[182] A. Böge, J. Kotschor, and S. Lindenmeier, "Adaptive Switchable FM/DAB Windscreen Antenna Matched with a High-Impedance Amplifier", in *10th European Conference on Antennas and Propagation (EuCAP)*, 2016. DOI: 10.1109/EuCAP.2016.7481991.

[183] L. Low, R. Langley, R. Breden, and P. Callaghan, "Automotive Antenna Performance and Simulation", in *First European Conference on Antennas and Propagation (EuCAP)*, 2006. DOI: 10.1109/EUCAP.2006.4584932.

[184] ——, "Hidden Automotive Antenna Performance and Simulation", *IEEE Transactions on Antennas and Propagation*, vol. 54, no. 12, pp. 3707–3712, 2006. DOI: 10.1109/TAP.2006.886546.

[185] M. Brzeska, R. Quintero, E. Martínez, L. Tantiñá, R. Riesco, C. Cisneros, and D. Puy, "New Generation of In-Mirror Integrated Antennas", in *3rd Eu-*

ropean Conference on Antennas and Propagation (EuCAP), 2009, pp. 2704–2707, ISBN: 9783000245732.

[186] J. De Mingo, C. Roncal, and P. L. Carro, "3-D Conformal Spiral Antenna on Elliptical Cylinder Surfaces for Automotive Applications", *IEEE Antennas and Wireless Propagation Letters*, vol. 11, pp. 148–151, 2012. DOI: 10.1109/LAWP.2012.2184254.

[187] H. Yamagishi, M. Tokunaga, and Y. Nishiura, "Vehicle antenna", *U.S. Patent No. 6,011,518*, 2000.

[188] R. R. Turnbull, "Automotive Rearview Mirror Assembly Including a Helical Antenna With a Non-Circular Cross-Section", *U.S. Patent No. 6,431,712 B1*, 2002.

[189] E. Condo Neira, J. Carlsson, K. Karlsson, and E. G. Ström, "Combined LTE and IEEE 802.11p Antenna for Vehicular Applications", in *9th European Conference on Antennas and Propagation (EuCAP 2015)*, Lisbon, Portugal, 2015, ISBN: 9788890701856.

[190] N. Koch, "Vehicular Spoiler Antenna for High Data Rate WLAN", in *Loughborough Antennas and Propagation Conference (LAPC)*, 2015. DOI: 10.1109/LAPC.2015.7366024.

[191] L. Marougi, "Incorporation of Antenna Into Vehicle Door Pillar", *U.S. Patent No. 6,072,436*, 2000.

[192] D. Manteuffel, "Characteristic Mode based antenna design - A straight forward approach to small form factor antenna integration", in *European Conference on Antennas and Propagation (EuCAP)*, 2015.

[193] J. Kammerer and S. Lindenmeier, "Invisible antenna embedded in the roof of a car with high efficiency for reception of Satellite Digital Audio Radio Services (SDARS)", in *European Conference on Antennas and Propagation (EuCAP)*, 2013, pp. 1609–1611.

[194] J. Kammerer and S. Lindenmeier, "Invisible Antenna Combination Embedded in the Roof of a Car with High Efficiency for Reception of SDARS - and GPS - Signals", in *IEEE Antennas and Propagation Society International Symposium (APSURSI)*, 2013, pp. 2075 –2076. DOI: 10.1109/APS.2013.6711696.

[195] L. Rufail and J. J. Laurin, "Aircraft Cavity-Backed Nonprotruding Wideband Antenna", *IEEE Antennas and Wireless Propagation Letters*, vol. 11, pp. 1108–1111, 2017. DOI: 10.1109/LAWP.2012.2217727.

[196] N. Guan, H. Tayama, M. Ueyama, Y. Yamaguchi, and H. Chiba, "An Invisible Vehicle Roof Antenna", in *IEEE-APS Topical Conference on Antennas and Propagation in Wireless Communications (APWC)*, 2016, pp. 51–54. DOI: 10.1109/APWC.2016.7738116.

[197] "Fahrzeug mit mindestens einer verdeckt innerhalb der Karosserie eingebauten Antenne", *Gebrauchsmusterschrift DE 200 02 426 U 1*, 2000.

[198] S. Takamoto and J. Matsumura, "In-Vehicle Antenna Device", *Japanese Patent No. JP 2012232679 A*, 2012.

[199] M. S. Sharawi, D. N. Aloi, and O. A. Rawashdeh, "Design and Implementation of Embedded Printed Antenna Arrays in Small UAV Wing Structures", *IEEE Transactions on Antennas and Propagation*, vol. 58, no. 8, pp. 2531–2538, 2010. DOI: 10.1109/TAP.2010.2050440.

[200] D. Gray, K. Sakakibara, and Y. Zhu, "Narrow-wall confined slotted waveguide structural antennas for small multi-rotor UAV", in *International Symposium on Antennas Propagation*, 2013, pp. 1192–1195, ISBN: 9787564142797.

[201] C. Heuer and S. Lindenmeier, "Antenna diversity system for the mobile reception of satellite digital radio", in *European Conference on Antennas and Propagation (EuCAP)*, 2009, pp. 2473–2476.

[202] J. Kammerer, "Kompakte Ringantennen für satellitengestützte und terrestrische Übertragungsdienste im Fahrzeug", Dissertation, Universität der Bundeswehr München, 2014.

[203] L. Marantis, A. Paraskevopoulos, D. Rongas, A. Kanatas, C. Oikonomopoulos-Zachos, and S. Voell, "A printed monopole ESPAR antenna for Truck-to-Truck communications", in *International Workshop on Antenna Technology: Small Antennas, Innovative Structures, and Applications (iWAT)*, 2017, pp. 239–242. DOI: 10.1109/IWAT.2017.7915368.

[204] E. Gschwendtner and W. Wiesbeck, "Ultra-Broadband Car Antennas for Communications and Navigation Applications", *IEEE Transactions on Antennas and Propagation*, vol. 51, no. 8, pp. 2020–2027, 2003. DOI: 10.1109/TAP.2003.815341.

[205] G. V. Trentini, "Partially reflecting sheet arrays", *IRE Transactions on Antennas and Propagation*, vol. 4, no. 4, pp. 666–671, 1956. DOI: 10.1109/TAP.1956.1144455.

[206] E. Estrat, "A Tablet MIMO Antenna with a Wave-Trap Slot for LTE / WiMAX Applications", in *Proceedings of the International Symposium on Antennas & Propagation (ISAP)*, 2013, pp. 1307 –1310.

[207] A. Nassar, S. Senega, and S. Lindenmeier, "A Time Domain Model for Multipath Wave Propagation of Satellite Radio Reception Underneath Dense Foliage", in *European Conference on Antennas and Propagation (EuCAP)*, 2016. DOI: 10.1109/EuCAP.2016.7481200.

[208] C. F. Mecklenbräuker, A. F. Molisch, J Karedal, F Tufvesson, A Paier, L Bernado, T Zemen, O Klemp, and N Czink, "Vehicular Channel Characterization and Its Implications for Wireless System Design and Performance", *Proceedings of the IEEE*, vol. 99, no. 7, pp. 1189–1212, 2011. DOI: 10.1109/JPROC.2010.2101990.

[209] J. Blumenstein, A. Prokes, A. Chandra, T. Mikulasek, R. Marsalek, T. Zemen, and C. F. Mecklenbräuker, "In-Vehicle Channel Measurement, Characterization, and Spatial Consistency Comparison of 30-11 GHz and 55-65 GHz Frequency Bands", *IEEE Transactions on Vehicular Technology*, vol. 66, no. 5, pp. 3526–3537, 2017. DOI: 10.1109/TVT.2016.2600101.

[210] L. Reichardt, J. Maurer, T. Fugen, and T. Zwick, "Virtual Drive: A Complete V2X Communication and Radar System Simulator for Optimization of Multiple Antenna Systems", *Proceedings of the IEEE*, vol. 99, no. 7, pp. 1295–1310, 2011. DOI: 10.1109/JPROC.2011.2124430.

[211] A. Islam, H. N. Hansen, P. T. Tang, M. B. Jørgensen, and S. F. Ørts, "Two-component microinjection moulding for MID fabrication", *Plastics, Rubber and Composites*, vol. 39, no. 7, pp. 300–307, 2017. DOI: 10.1179/174328910X12691245470356.

[212] A. Kilian, J. Weinzierl, and L. P. Schmidt, "Investigation of the hot embossing technology for low-cost antennas printed on polymer substrates", in *European Microwave Conference (EuMC)*, 2008, pp. 1–4. DOI: 10.1109/EUMC.2008.4751371.

[213] N. Heininger, W. John, and H.-J. Boßler, "Manufacturing of Molded Interconnect Devices from Prototyping to Mass Production with Laser Direct Structuring", in *International Congress Molded Interconnect Devices (MID)*, 2004.

[214] J. Franke, *Three-Dimensional Molded Interconnect Devices (3D-MID): Materials, Manufacturing, Assembly and Applications for Injection Molded Circuit Carriers*. Carl Hanser Verlag GmbH Co KG, 2014.

[215] D. Unnikrishnan, D. Kaddour, and S. Tedjini, "Microstrip Transmission Lines and Antennas on Molded Interconnect Devices Materials", in *13th Mediterranean Microwave Symposium (MMS)*, 2013. DOI: 10.1109/MMS.2013.6663072.

[216] D. Kornek, E. Slottke, C. Orlob, and I. Rolfes, "Experimental Investigation of Bent Patch Antennas on MID Substrate", in *European Conference on Antennas and Propagation (EuCAP)*, Barcelona, Spain, 2010.

[217] C. Orlob, Q. H. Dao, and D. Kornek, "Dual-Polarized Log.-Periodic Antenna on a Conical MID Substrate", in *5th European Conference on Antennas and Propagation (EUCAP)*, 2011, pp. 361–364, ISBN: 9788882020743.

[218] C. Orlob, Q. H. Dao, and B. Geck, "Conformal Log.-Periodic Antenna with Integrated Feeding Network for UWB-MIMO Applications", in *7th German Microwave Conference (GeMiC)*, 2012.

[219] F. Sonnerat, R. Pilard, F. Gianesello, D. Gloria, F. L. Pennec, C. Person, A. Cihangir, F. Ferrero, C. Luxey, and P. Brachat, "Wideband LDS antenna using two radiating elements", in *Loughborough Antennas Propagation Conference (LAPC)*, 2012. DOI: 10.1109/LAPC.2012.6403067.

[220] A. Cihangir, F. Ferrero, C. Luxey, G. Jacquemod, and P. Brachat, "A bandwidth-enhanced antenna in LDS technology for LTE700 and GSM 850/900 standards", in *European Conference on Antennas and Propagation (EuCAP)*, 2013, pp. 2786–2789.

[221] A. Friedrich, L. Berkelmann, T. Martinelli, B. Geck, O. Klemp, and I. Kriebitzsch, "An active three-dimensional GPS patch antenna using MID-

technology", in *European Microwave Conference (EuMC)*, 2015, pp. 373–376. DOI: 10.1109/EuMC.2015.7346033.

[222] A. Friedrich, B. Geck, and M. Fengler, "LDS Manufacturing Technology for Next Generation Radio Frequency Applications", in *12th International Congress Molded Interconnect Devices (MID)*, 2017, pp. 1–6. DOI: 10.1109/ICMID.2016.7738939.

[223] M. Mayer, "Radio Frequency Identification with Compressed Sensing", Dissertation, Technische Universität Wien, 2016.

[224] B. R. Elbal, "Measurement Based Evaluation of the Wireless Identification and Sensing Platform", Master's Thesis, Technische Universität Wien, 2015.

[225] L. Ge and K. M. Luk, "Unidirectional Antenna for Cognitive Radio Applications", in *IEEE International Workshop on Electromagnetics (iWEM)*, 2014, pp. 14–15, ISBN: 9781479948154. DOI: 10.1109/iWEM.2014.6963612.

[226] C. Kittiyanpunya and M. Krairiksh, "A four-beam pattern reconfigurable Yagi-Uda antenna", *IEEE Transactions on Antennas and Propagation*, vol. 61, no. 12, pp. 6210–6214, 2013. DOI: 10.1109/TAP.2013.2282914.

[227] T. Zhang, S.-y. Yao, and Y. Wang, "Design of Radiation-Pattern- Reconfigurable Antenna With Four Beams", *IEEE Antennas and Wireless Propagation Letters*, vol. 14, pp. 183–186, 2015. DOI: 10.1109/LAWP.2014.2360098.

[228] B. Leinwetter and R. A. Dürsch, "Antennenanordnung bei Kraftfahrzeugen", *German Patent No. DE4403643C2*, 2003.

[229] L. L. Nagy, "Automobile Roof Antenna Shelf', *U.S. Patent No. 6,118,410*, 2000.

[230] Y. Noria, "Wave transmitting/receiving structure for vehicle antennas", *European Patent Application No. EP1921708A1*, 2008.

[231] S. Kirtzakis, "Antennenanordnung für ein Fahrzeug", *Offenlegungsschrift DE 10 2011 106 829 A1*, 2012.

[232] T. Prangel and S. Raddatz, "Anordnung einer Sende- und/oder Empfangseinheit an einem Karosseriebauteil oder Außenanbauteil eines Kraftwagens", *German Offenlegungsschrift DE102009036727A1*, 2010.